EMU
Journal of
Pharmaceutical
Sciences

ISSN: 2651-3587
Volume 9 / Issue 1

EMUJPharmSci

May 2026

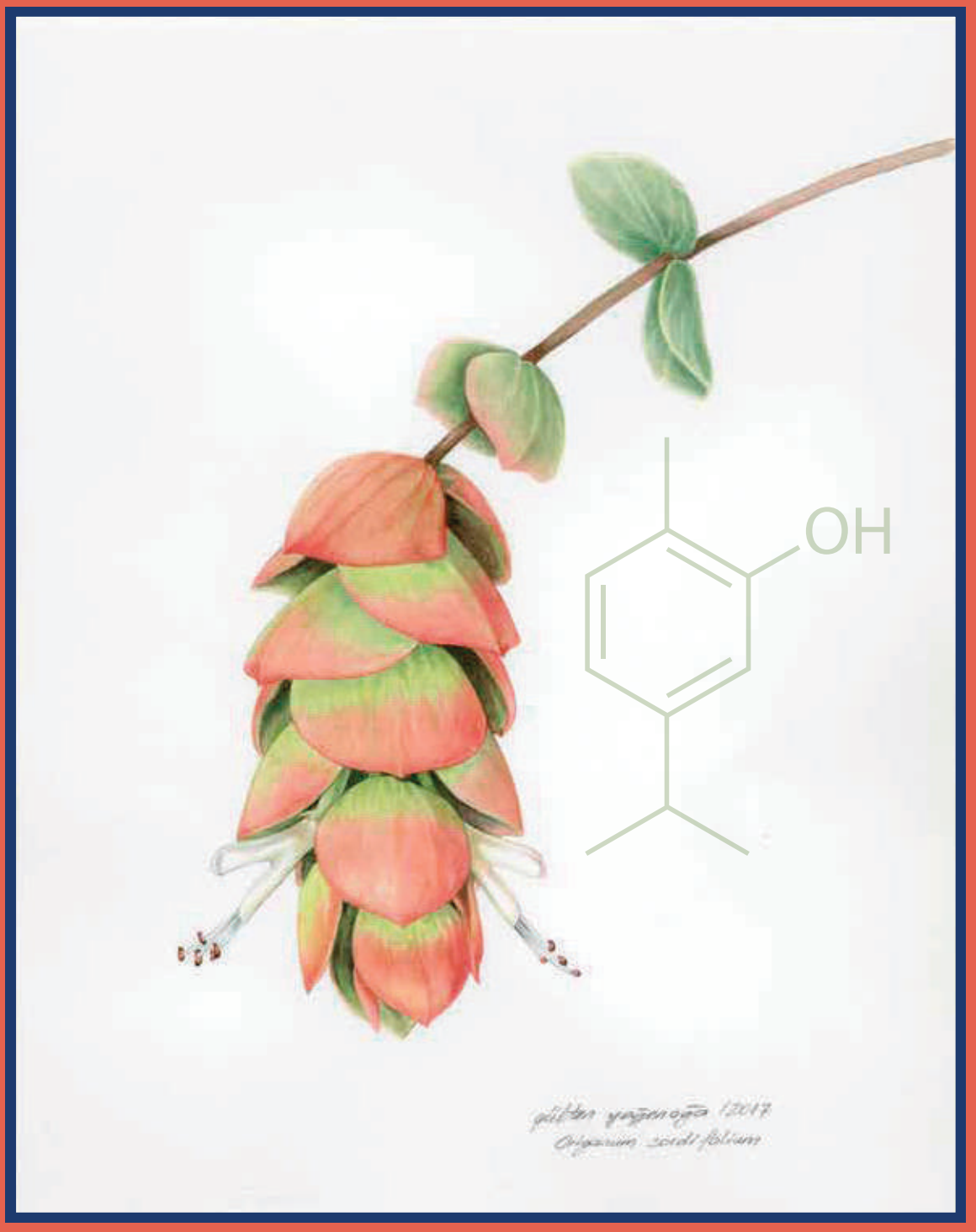

Eastern Mediterranean University Press

EMU Journal of Pharmaceutical Sciences

EMUJPharmSci

EDITORIAL BOARD

Origanum cordifolium* **in cover picture was illustrated by Gülten Yeğenağa

EMU Journal of Pharmaceutical Sciences

EMUJPharmSci

Advisory/Scientific Board

EMU Journal of Pharmaceutical Sciences
EMUJPharmSci

MESSAGE FROM THE EDITOR IN CHIEF

Dear Scientists,

Welcome to the 2026 first issue of EMU Journal of Pharmaceutical Sciences. Starting its journey in 2018, we still have the honor to contribute to science. In an era of rapid scientific transformation and increasingly blurred interdisciplinary boundaries, this issue provides new perspectives in diverse pharmaceutical disciplines.

A new formulation for ketoprofen, benzazole–carboxamide hybrids against breast cancer cells, in silico toxicology analysis of perfluorononanoic acid-induced hepatotoxicity, and microbiological assessment of staphylococcus aureus nasal colonization and antibiotic resistance patterns constitute valuable contributions to their respective fields. Moreover, a review article on medicinal and aromatic plants from ancient civilizations to the modern era is expected to generate curiosity from pharmacognosy perspective.

We would like to thank all the reviewers and members of our editorial board for their meticulous evaluation of the submitted works, and for their contributions to academic integrity and quality. We also extend our gratitude to the researchers who shared their valuable findings with us.

As a member of 'DergiPark' Akademik, an establishment under the Scientific and Technological Research Council of Türkiye (TÜBİTAK), EMU Journal of Pharmaceutical Sciences continues its journey with a transparent peer-review and publication process of scientific studies in diverse fields related to pharmaceutical sciences. The journal will continue to serve and promote global dissemination of pharmaceutical research, providing a platform for scientists worldwide. It is important to note that the journal is free of submission or acceptance fee.

Looking forward to your scientific contributions,

Best wishes,

Prof. Dr. H. Ozan Gülcan

Dean of Faculty of Pharmacy
Editor in Chief
Eastern Mediterranean University
Faculty of Pharmacy
Famagusta, TRNC, via Mersin 10, Türkiye

GUIDE FOR AUTHORS

EMU Journal of Pharmaceutical Sciences (EMUJPharmSci) publishes research on all aspects of pharmacy in the form of original articles, short papers, and reviews.

EMU Journal of Pharmaceutical Sciences is published three times each year. It is an open-access, peer-reviewed journal.

- Contributions to EMU Journal of Pharmaceutical Sciences must be in English.
- All manuscripts are subject to editorial review.
- Manuscripts should not have been previously published or accepted for publication and must not be submitted simultaneously to other journals.
- The manuscripts are published in the order of final acceptance after review and revision.
- If a manuscript is returned to the authors for revision and the revised version is not received by the editor within two months, it will be treated as a new submission.
- If the manuscript is accepted and the proof is returned to the authors, corrected proofs should be sent to the editor within 5 days.

Original Articles: These are limited to 15 manuscript pages, in addition to supplementary materials (schemes, tables, figures, etc.).

Short Papers: Short papers are limited to 5 typewritten pages, with a maximum of 2 supplementary materials (schemes, tables, figures).

Reviews: Reviews are limited to 20 pages, in addition to supplementary materials (schemes, tables, figures, etc.).

- The original manuscript must be arranged as follows: Title page (including the title, authors and correspondence address), abstract, key words, introduction, materials and methods, results and discussion, acknowledgements and references.
- Reviews must be arranged as follows: Title page (including the title, authors, and correspondence address), abstract, introduction, discussion, acknowledgements, and references.

EMU Journal of Pharmaceutical Sciences
EMUJPharmSci

1. General Format

a) All manuscripts can only be submitted electronically via DergiPark.
b) Manuscripts should be 1.5-line spaced and justified.
c) Use 2.5 cm margins and Times New Roman font on A4 paper.
d) Number all pages, starting with the title page.
e) Spell out all acronyms in full at first use.
f) Make sub-headings if necessary.
g) Follow internationally accepted rules and conventions: Use the international system of units (SI).

2. Before main text

A. Title page

a) The first page of the manuscript is a title page containing the following information:
b) The manuscript's full title (*Font: Times New Roman Font Size: 13*). The title must be concise and informative.
c) All authors' full names (*Font: Times New Roman Font Size: 11)*.
d) The affiliation of the author(s) should be linked by superscript numbers, and listed beneath the title.
e) All authors' ORCID ID number (*Font: Times New Roman Font Size: 11)*.
f) Corresponding author (*Font: Times New Roman Font Size: 10)*. E-mail, telephone and fax number (with country and area code) of the corresponding author should be provided.
g) Ethical approval must be provided for studies involving human or animal participants.

B. Abstract

a) The abstract appears on its own page.
b) The abstract should be written in Times New Roman and font size 11.
c) The maximum length of the abstract is 200 words.
d) The abstract should contain the objectives, methods, results and conclusions.
e) 3-6 keywords must be provided in alphabetical order (Font: Times New Roman Font Size: 10). Separate keywords with commas.

3. Main text

A. Introduction

(Font: Times New Roman Font Size: 12)
State the objectives of the work and provide a brief background of the literature related to the topic. The novelty and the aim of the study should be clearly stated.

B. Materials and Methods

(Font: Times New Roman Font Size: 12)
a) Give a brief and clear description of the materials and methods used. Subtitles can be given as appropriate.
b) For plant materials, herbarium name (or acronym), number, name and surname of the person who identified the plant materials should be indicated in this part of the manuscript.
c) Statistical analysis should be provided where appropriate.

EMU Journal of Pharmaceutical Sciences
EMUJPharmSci

C. Results and Discussion

(Font: Times New Roman Font Size: 12)

A combined Results and Discussion section is often appropriate. Results should be concise.

Discussion should explore the significance of the results of the work.

Discussion should not repeat the results.

The main conclusions of the study should be presented.

D. Acknowledgement

(Font: Times New Roman Font Size: 10)

Supporting institutions or individuals should be briefly acknowledged just before the reference list.

E. References

i. Citation in text

(Font: Times New Roman Font Size: 12)

- Please ensure that every reference cited in the text is also present in the reference list (and vice versa).
- Unpublished results and personal communications are not recommended in the reference list.
- References in the text should be cited as: the author(s) surname and the publication date**.**

Examples:

(Sahin, 2000) – one author

(Sahin and Kosar, 2000) – Two authors

(Sahin et al. 2000) – more than two authors

(Celik and Ozhatay 2000 a, b) – More than one paper in the same year by the same author(s)

(Ozhatay and Avci, 2000; Ozhatay et al. 2001; Ozhatay, 2005) – listed by the earliest year first for multiple citations.

ii. Reference style

(Font: Times New Roman Font Size: 10)

- The list of references should be single-spaced.
- List the references in alphabetical order under the "References" section.
- For references up to 5 authors, write the names of all authors.
- For references more than 5 authors, write the names of the first 5 and add et al.
- The title of journal should be abbreviated in italics according to the style used in the National Library of Medicine's Journals in NCBI Databases.
- Volume numbers should be indicated in bold letters.

iii. Examples

Reference to a journal publication:

Ozhatay N, Kultur S, Gurdal B (2017). Check-list of additional taxa to the supplement flora of Türkiye VIII. *Istanbul J Pharm* **47**(1): 31-46.

Ozhatay N, Kultur S, Gurdal B, Ilktac M, Ogmen S, et al. (2019). Check-list of additional taxa to the supplement flora of Türkiye X. *Istanbul J Pharm* **57**(2): 35-46.

Reference to a book:

Strunk W Jr, White EB (1979). The Elements of Style. 3rd ed. New York, NY: Macmillan.

Reference to a chapter in an edited book:

Bonati A (1988). Industry and conservation of medicinal plants. In Akerele O, Heywood V, Synge H (eds). The Conservation of Medicinal Plants p.141-148 Cambridge University Press UK.

Electronic resources:
World Nuclear Association (WNA) (2014). Radioisotopes in Medicine, http://www.world-nuclear.org/info/ Accessed 13.10.2014.

4. After main text

Figures / Tables captions

- Use figures and tables for information better presented visually.
- All the figures and tables must be referred to in the main body of the text.
- Tables and Figures should be numbered consecutively in the order of appearance within the text, referred as “Table 1” and “Figure 1”.
- Descriptive titles should be given at the top of the tables and at the bottom of the figures.
- Figures should be prepared with the highest resolution and should be provided as a separate page following references.

Submission checklist

Check the following submission list before submitting your manuscript:

- Full E-mail address, full postal address, telephone and fax number of the corresponding author.
- All necessary files have been uploaded.
- References are in the correct format for this journal.
- All references mentioned in the Reference list are cited in the text.
- All figure captions.
- All tables (including title, description, footnotes).

For any further information please e-mail: emuj.pharmsci@emu.edu.tr

EMU Journal of Pharmaceutical Sciences
EMUJPharmSci

CONTENTS

Research articles

Reviews

Research Article EMUJPharmSci ISSN 2651-3587 https://dergipark.org.tr/emujpharmsci

EMU Journal of Pharmaceutical Sciences

EMUJPharmSci 2026; **9**(1): 1-17.

DOI: **10.54994/emujpharmsci.1839663**

Formulation and Comprehensive In Vitro Evaluation of Orally Disintegrating Ketoprofen Tablets Prepared by Direct Compression

Tansel Comoglu

[1]Ankara University, Faculty of Pharmacy, Department of Pharmaceutical Technology, Ankara, Türkiye.

Abstract

Orally disintegrating tablets (ODTs) are solid oral dosage forms designed to disintegrate in the oral cavity within one minute without requiring water, offering significant advantages for elderly individuals, children, and patients with swallowing difficulties. The objective of this study was to formulate and evaluate fast disintegrating tablets containing ketoprofen using the direct compression method and to investigate the influence of different excipients on critical in vitro quality control parameters. Two tablet formulations were prepared, each containing 150 mg of ketoprofen as the active pharmaceutical ingredient. Excipients included croscarmellose sodium, sucrose-calcium phosphate co-processed filler, mannitol, microcrystalline cellulose, magnesium stearate, and talc. Tablets were evaluated for diameter, thickness, weight variation, hardness and in vitro disintegration time. Both formulations demonstrated acceptable physical properties, but the formulation containing microcrystalline cellulose and mannitol showed markedly faster in vitro disintegration time (40.5 ± 3.6 seconds) compared with the formulation prepared with sucrose-calcium phosphate (159.5 ± 18.6 seconds). The results indicate that mannitol is a more suitable filler than sucrose-calcium phosphate for fast disintegrating ketoprofen tablet systems and that 150 mg ketoprofen is an adequate dose for this dosage form.

Keywords

Croscarmellose sodium, direct compression, ketoprofen, mannitol, orally disintegrating tablet.

Article History

Submitted:10 December 2025 **Accepted**: 12 February 2026 **Published Online**: May 2026

Reviewer

Invitation Date: 23 December 2025 **Acceptance Date**: 24 December 2025 **Due Date**: 07 January 2026 / 20 January 2026

Article Info

***Corresponding author:** Tansel Çomoğlu **email:** comoglu@pharmacy.ankara.edu.tr

Research Article:

Volume: 9 **Issue: 1** **Pages: 1-17**

DOI: 10.54994/emujpharmsci.1839663

INTRODUCTION

Orally disintegrating tablets (ODTs) are solid unit oral dosage forms that rapidly disintegrate in the oral cavity, usually in less than one minute, producing a drug suspension that can be swallowed without the need for water (Seager, 1998). These dosage forms provide important advantages for patient populations experiencing difficulty in swallowing conventional tablets, such as elderly individuals, children, and individuals with neurological disorders (Chang et al. 2000). They are also advantageous in emergency situations and for individuals with limited access to water (Kuchekar et al. 2003). Furthermore, absorption through the oral mucosa may reduce the impact of hepatic first-pass metabolism and may lead to quicker onset of therapeutic activity (Klancke, 2003).

ODTs are increasingly preferred in pharmaceutical development because they improve patient compliance, offer rapid onset of action, and have strong commercial potential (Habib et al. 2000). They are particularly suitable for drugs used in the management of pain, where fast pharmacological response is desired (Kuchekar et al. 2003).

Ketoprofen is a widely used non-steroidal anti-inflammatory drug belonging to the arylpropionic acid class. It is commonly used for the management of mild or moderate pain, inflammatory conditions such as arthritis, and postoperative discomfort (Famaey, 1997). In the pharmaceutical market, conventional oral dosage forms containing 200 mg ketoprofen are frequently used to achieve adequate systemic drug concentration (Brunton et al. 2017). However, orally disintegrating drug delivery systems have shown that a lower dose may be sufficient due to the faster disintegration and potentially more efficient absorption profile in the oral cavity (Sastry et al. 2000). Therefore, the use of 150 mg ketoprofen in ODT formulations may provide comparable therapeutic efficacy while decreasing the risk of dose-related adverse reactions. This approach reflects a formulation-driven a dose-optimization strategy aimed at improving safety and efficacy.

Direct compression is a simple, cost-effective and widely used method for tablet manufacturing (Jivraj et al. 2000). It is suitable for heat-sensitive or moisture-sensitive drugs and requires excipients with excellent flowability and compressibility. In ODTs manufactured by direct compression, the choice and proportion of excipients are critical in determining the disintegration performance and mechanical strength of the final product (Chang et al. 2000).

Croscarmellose sodium is a crosslinked cellulose derivative commonly used as a superdisintegrant, acting through swelling and wicking mechanisms (Bolhuis and Armstrong, 2006). Mannitol is a water-soluble filler that provides pleasant taste and contributes to rapid disintegration (Shukla et al. 2009). Microcrystalline cellulose improves compressibility and creates porosity in the tablet structure (Bolhuis and Armstrong, 2006). A co-processed sucrose-calcium phosphate excipient (commercially known as Di-Pac) offers compressibility and sweetness but has different solubility characteristics compared with mannitol (Gohel and Jogani, 2005). Magnesium stearate functions as a lubricant, while talc functions as a glidant and anti-adherent excipient (Aulton and Taylor, 2017).

The objective of this study was to develop ketoprofen orally disintegrating tablets by direct compression and to evaluate their in vitro physical and performance characteristics, with particular emphasis on a formulation-driven dose optimization approach. Unlike conventional studies that employ standard ketoprofen doses, this work intentionally investigates a reduced drug load of 150 mg to explore the potential of orally disintegrating systems to maintain therapeutic effectiveness while minimizing dose-related adverse effects. Two distinct excipient systems were systematically compared under identical drug dose and tablet weight conditions in order to isolate the influence of excipient matrix design on mechanical strength, dimensional uniformity and disintegration performance. Through this comparative and mechanistic approach, the study aims to identify a robust, rapidly disintegrating and industrially feasible ketoprofen orally disintegrating tablet formulation suitable for further development.

MATERIALS AND METHODS

Materials

The materials used include ketoprofen as the active pharmaceutical ingredient (Sigma-Aldrich, St. Louis, USA), croscarmellose sodium (Ac-Di-Sol®, FMC BioPolymer, Philadelphia, USA), microcrystalline cellulose (Avicel PH 101®, FMC BioPolymer, Philadelphia, USA), mannitol (Merck, Darmstadt, Germany), sucrose-calcium phosphate co-processed filler (Di-Pac®, Viatrex, New York, USA), magnesium stearate (Merck, Darmstadt, Germany) and talc (Merck, Darmstadt, Germany). All materials were of pharmaceutical grade and were used as supplied.

Tablet formulation

Two formulations (F1 and F2) were designed by keeping ketoprofen content constant at 150 mg per tablet, with total tablet weight of 500 mg.

Table 1: Composition of F1 ODTs.

Component	Role	Quantity (mg)
Ketoprofen	Active ingredient	150
Croscarmellose sodium	Superdisintegrant	80
Sucrose-calcium phosphate	Filler	260
Magnesium stearate	Lubricant	5
Talc	Glidant	5
Total		**500**

Table 2: Composition of F2 ODTs.

Component	Role	Quantity (mg)
Ketoprofen	Active ingredient	150
Croscarmellose sodium	Superdisintegrant	30
Microcrystalline cellulose	Binder/Filler	20
Mannitol	Filler	300
Total		**500**

Tablet preparation

Powders were accurately weighed, blended for 15 minutes to ensure homogeneous distribution of the active pharmaceutical ingredient within the excipient matrix, and the lubricants were subsequently added prior to tableting. The blends were compressed into tablets using a 12-mm flat punch under a compression pressure of 40 bar. The dwell time during compression was adjusted based on the formulation characteristics, in the range of 13 to 15 seconds for F1 and 5 to 7 seconds for F2. Longer dwell time is known to improve particle bonding and mechanical strength in formulations with lower deformation capacity, whereas shorter dwell time is sufficient in systems containing plastically deforming excipients such as microcrystalline cellulose (Hiestand et al. 1983; Sun and Grant, 2001). The processing conditions used in this study are in line with established direct compression practices for ODTs, where blending time, compression force and dwell time collectively determine the final hardness, porosity and disintegration behavior of the dosage form (Jivraj et al. 2000; Aulton and Taylor, 2017).

In vitro characterization of ketoprofen ODTs

The prepared tablets were evaluated using several in vitro quality control tests in order to determine their physical characteristics and performance properties. These tests are essential for assessing the suitability of ODTs, as physical parameters such as hardness, thickness, diameter and weight

uniformity directly influence tablet integrity, packaging compatibility and overall patient acceptability (Aulton and Taylor, 2017). Likewise, disintegration behavior is a critical performance attribute for orally disintegrating dosage forms, since rapid disintegration in the oral cavity is central to their intended therapeutic advantage (Seager, 1998).

All in vitro tests were conducted at room temperature under standard laboratory conditions to minimize environmental variability, as temperature and humidity can affect factors such as tablet moisture content, hardness and disintegration performance (Klancke, 2003). Standardized testing conditions also allow reproducibility and comparability of results across different formulations and studies.

The evaluation methods used in this study included measurements of diameter, thickness, weight variation, hardness and in vitro disintegration time. These parameters were selected based on pharmacopeial recommendations and established guidelines for orally disintegrating tablets, which emphasize the importance of dimensional uniformity, mechanical strength and rapid disintegration to ensure consistent clinical performance (European Pharmacopoeia, 2020; USP, 2022). Detailed descriptions of each test method are provided below, supported by relevant literature concerning the influence of formulation variables on these key quality attributes.

Diameter measurement

The diameter of the tablets was determined using a precision micrometer. A total of 20 tablets from each formulation were randomly selected from the production batch to ensure representative sampling and to avoid systematic bias related to die fill sequence or compression run order (Aulton and Taylor, 2017). Each tablet was placed between the micrometer measuring jaws, and the diameter value in mm was recorded. Measurement of tablet diameter is an important dimensional quality attribute, since uniformity of size reflects consistent die filling, powder flow, and applied compression force during manufacture (Hiestand et al. 1983).

The mean diameter, standard deviation, standard error of the mean and 95% confidence interval values were calculated based on these 20 measurements.

Thickness measurement

The thickness of the tablets was measured using the same precision micrometer used for diameter determination. 20 tablets were selected from each formulation, and the thickness of each tablet was measured in mm by placing the tablet vertically between the micrometer jaws. The results were recorded individually. Thickness determination is an essential dimensional quality attribute in tablet development, as it

reflects the volume of material within the die cavity and the degree of consolidation achieved during the compression cycle (Hiestand *et al*., 1983; Aulton and Taylor, 2017).

Weight variation test

The weight variation test was performed by weighing individual tablets using an analytical balance. 20 tablets from each formulation were randomly selected and weighed separately, and the recorded values were expressed in grams. Weight uniformity represents an important indicator of dosage form consistency, since variation in tablet mass can directly influence the amount of active pharmaceutical ingredient delivered to the patient, particularly in formulations prepared by direct compression where no granulation step is used to compensate for density variations (Aulton and Taylor, 2017; Jivraj et al. 2000). The mean tablet weight, standard deviation, standard error of the mean and 95% confidence interval were calculated.

Hardness test

The mechanical strength of the tablets was determined using a Monsanto tablet hardness tester. 10 tablets from each formulation were selected for the hardness test. Each tablet was placed between the instrument jaws, and pressure was applied until the tablet fractured. The force required to break each tablet was recorded in kilograms. Tablet hardness is a critical physical parameter reflecting the internal bonding strength of compacted particles, which is influenced by compression force, dwell time, and the deformation properties of the excipients used (Hiestand et al. 1983; Sun and Grant, 2001).

***In vitro* disintegration time**

The *in vitro* disintegration time of the tablets was determined using a simple petri dish method to evaluate tablet behavior under simulated oral conditions. 6 tablets from each formulation were randomly selected for the test. All experiments were performed under standard laboratory conditions at room temperature (25 ± 2 °C). A clean glass petri dish was lined with a piece of filter paper, which was uniformly moistened with a small, controlled volume of distilled water at ambient temperature.

Distilled water was used as the test medium without pH adjustment. Simulated gastric fluid or simulated intestinal fluid was not employed, as the aim of the test was to assess the initial disintegration behavior of the tablets upon contact with moisture, corresponding to the conditions encountered in the oral cavity rather than the gastrointestinal environment. Each tablet was placed individually on the moistened filter paper, and the time required for complete disintegration into fine particles was measured using a stopwatch. Complete disintegration was defined as the

point at which no visible solid core remained (Habib et al. 2000; Shukla et al. 2009; European Pharmacopoeia, 2020).

The disintegration time for each tablet was recorded in seconds. For each formulation, the mean disintegration time, standard deviation, standard error of the mean, and 95% confidence interval were calculated to allow quantitative comparison of disintegration performance (Seager, 1998; Chang et al. 2000; Klancke, 2003).

Statistical analysis

All numerical data collected from the physical tests were subjected to a basic statistical evaluation that was carried out separately for each formulation and for each measurement type. For every data set, the arithmetic mean value was calculated in order to represent the central tendency of the results. The mean is the most widely used descriptive parameter in pharmaceutical quality evaluation because it provides a representative estimate of the expected value of a quality attribute within a manufactured batch (Hussain, 1998).

RESULTS AND DISCUSSION

This section presents the experimental findings obtained from the in vitro evaluation of ketoprofen ODT formulations and discusses these findings in relation to formulation variables and expected performance criteria. The results include detailed dimensional measurements (diameter and thickness), weight variation, hardness, and in vitro disintegration time for both formulations that were prepared by direct compression. For each parameter, raw data were collected and subjected to statistical analysis in order to assess the mean values, variability and confidence intervals. The influence of excipient selection and composition on the quality attributes of the tablets is interpreted in the context of ODT design principles.

Diameter measurements

The diameter of the tablets is an important dimension that reflects the uniformity of die filling and the reproducibility of the compression process. For each formulation, 20 tablets were measured using a micrometer and the values were recorded in mm. In F1, individual tablet diameters ranged from 1.6 to 1.7 mm, with a mean diameter of 1.61 mm. In F2, diameters ranged from 1.6 to 1.7 mm, with a mean diameter of 1.605 mm. The individual diameter measurements for both formulations are presented in Table 3.

The descriptive statistical evaluation summarized in Table 4 showed small standard deviations and narrow 95% confidence intervals for both formulations (1.61 ± 0.014 mm for F1 and 1.60 ± 0.009

mm for F2), indicating minimal within-batch variability. Although F2 exhibited a slightly narrower confidence interval, the mean diameter values were very similar, confirming that identical tooling and compression conditions produced tablets of nearly the same size. These results demonstrate satisfactory dimensional uniformity for both formulations, with no expected impact on disintegration behavior or patient acceptability from a manufacturing standpoint.

Table 3: Individual tablet diameter measurements for F1 and F2 (mm).

Tablet number	Formulation 1	Formulation 2	Tablet number	Formulation 1	Formulation 2
1	1.6	1.6	11	1.6	1.6
2	1.6	1.6	12	1.6	1.6
3	1.6	1.6	13	1.6	1.6
4	1.6	1.6	14	1.6	1.6
5	1.6	1.6	15	1.6	1.6
6	1.6	1.6	16	1.7	1.6
7	1.6	1.6	17	1.6	1.6
8	1.6	1.6	18	1.7	1.6
9	1.6	1.6	19	1.6	1.6
10	1.6	1.7	20	1.6	1.7

Table 4: Statistical evaluation of tablet diameter for F1 and F2.

Formulation	Mean diameter (mm)	Standard deviation (mm)	Standard error (mm)	t value	95% confidence interval for mean (mm)
F 1	1.610	0.03	6.7×10^{-3}	2.09	1.61 ± 0.014
F 2	1.605	0.02	4.48×10^{-3}	2.09	1.60 ± 0.009

Thickness measurements

Tablet thickness is influenced by the amount of powder in the die, the applied compression pressure and the mechanical properties of the powder blend. For each formulation, the thickness of 20 tablets was measured using a micrometer and expressed in mm. In F1, individual tablet thickness values ranged from 0.30 to 0.40 mm, with most measurements clustered between 0.36 and 0.38 mm, whereas in F2 the thickness values ranged from 0.36 to 0.38 mm, indicating a narrower distribution. The individual thickness values are presented in Table 5, and the corresponding statistical evaluation is summarized in Table 6. The mean thickness values were similar for both formulations (0.3675 mm for F1 and 0.369 mm for F2); however, F2 exhibited lower variability, as reflected by its smaller standard deviation and narrower 95% confidence interval. This improved thickness reproducibility suggests more uniform compressibility and packing behavior of the powder blend in F2, which may contribute to more consistent tablet porosity and, consequently, more reliable disintegration performance of the fast disintegrating tablets.

Table 5: Thickness measurements for F1 and F2 (mm).

Tablet No	F 1	F 2	Tablet No	F 1	F 2
1	0.36	0.38	11	0.36	0.38
2	0.36	0.36	12	0.40	0.36
3	0.35	0.37	13	0.38	0.36
4	0.37	0.37	14	0.30	0.37
5	0.37	0.38	15	0.39	0.38
6	0.37	0.36	16	0.36	0.36
7	0.40	0.37	17	0.37	0.37
8	0.36	0.38	18	0.37	0.36
9	0.38	0.37	19	0.36	0.36
10	0.37	0.36	20	0.37	0.38

Table 6: Statistical evaluation of tablet thickness for F1 and F2.

Formulation	Mean thickness (mm)	Standard deviation (mm)	Standard error (mm)	t value	95%confidence interval for mean (mm)
F1	0.3675	0.02	4.48×10^{-3}	2.09	0.3675 ± 0.01
F2	0.369	8.5×10^{-3}	1.9×10^{-3}	2.09	0.369 ± 0.003

Weight variation

Weight variation is an indirect indicator of content uniformity and reflects the performance of powder feeding and die filling during the tableting process. For each formulation, 20 tablets were individually weighed using an analytical balance. In F1, individual tablet weights ranged from 0.4952 to 0.5019 g, whereas in F2 the range was 0.4958 to 0.5018 g, with the individual values presented in Table 7. The statistical evaluation summarized in Table 8 showed a mean tablet weight of 0.4985 g for F1 and 0.5005 g for F2, compared with a theoretical target weight of 0.500 g. Although both formulations produced tablets close to the target weight and met typical pharmacopoeial requirements for weight variation, F2 exhibited lower variability, as indicated by its smaller standard deviation and narrower 95% confidence interval. This improved uniformity suggests a more consistent distribution of both excipients and ketoprofen in F2, likely reflecting superior powder flow and die filling behavior of the mannitol and microcrystalline cellulose based blend compared with the sucrose–calcium phosphate based system.

Table 7: Individual tablet weights for F 1 and F2 (g).

Tablet number	Formulation 1	Formulation 2	Tablet number	Formulation 1	Formulation 2
1	0.5016	0.5014	11	0.4958	0.4958
2	0.4954	0.5011	12	0.4957	0.5012
3	0.4959	0.5011	13	0.5013	0.5012
4	0.5012	0.5017	14	0.5017	0.4959
5	0.5014	0.5016	15	0.4955	0.5017
6	0.5018	0.5014	16	0.4956	0.5015
7	0.4952	0.5012	17	0.5019	0.5012
8	0.4953	0.5018	18	0.5016	0.5014

Tablet number	Formulation 1	Formulation 2	Tablet number	Formulation 1	Formulation 2
9	0.5011	0.5013	19	0.4957	0.5013
10	0.5015	0.4959	20	0.4954	0.5012

Table 8: Statistical evaluation of tablet diameter for F1 and F2.

Formulation	Mean diameter (millimeters)	Standard deviation (millimeters)	Standard error (millimeters)	t value	95%percent confidence interval for mean (millimeters)
F 1	1.61	0.03	6.7×10^{-3}	2.09	1.61 ± 0.014
F2	1.605	0.02	4.48×10^{-3}	2.09	1.60 ± 0.009

Hardness

Tablet hardness is a measure of mechanical strength and resistance to breakage during handling and transportation. 10 tablets from each formulation were tested using a Monsanto hardness tester, and the force required to break each tablet was recorded in kg. In F1, individual hardness values ranged from 4.0 to 5.5 kg, whereas in F2 the values ranged from 5.0 to 6.0 kg, with the individual measurements presented in Table 9. The statistical evaluation summarized in Table 10 showed a mean hardness of 4.65 kg for F1 and 5.30 kg for F2. Both formulations produced tablets within a hardness range considered acceptable for fast disintegrating tablets; however, F2 exhibited higher mechanical strength and lower variability, as reflected by its greater mean hardness and narrower 95% confidence interval. These findings indicate that F2 tablets are more robust than those of F1, while maintaining suitability for rapid disintegration, suggesting that the microcrystalline cellulose and mannitol based matrix achieves a favorable balance between mechanical strength and fast disintegrating performance.

Table 9: Individual tablet hardness values for F1 and F2 (kg).

Tablet number	Formulation 1	Formulation 2
1	5.0	5.0
2	4.5	5.0
3	4.5	5.5
4	5.5	5.0
5	5.0	6.0
6	4.5	5.5
7	5.0	5.0
8	4.0	5.0
9	4.5	6.0
10	4.0	5.0

Table 10: Statistical evaluation of tablet hardness for F1 and F2.

Formulation	Mean hardness (kg)	Standard deviation (kg)	Standard error (kg)	t value	95%percent confidence interval for mean (kg)
F1	4.65	0.47	0.1486	2.26	4.65 ± 0.3358
F2	5.30	0.42	0.1328	2.26	5.30 ± 0.2938

In vitro disintegration time

The primary functional requirement for orally disintegrating tablets is rapid disintegration in the oral cavity without the need for water. For each formulation, 6 tablets were tested using a petri dish method under moist conditions simulating the oral environment, and the time required for complete disintegration was recorded in seconds. In F1, individual disintegration times ranged from 138 to 178 s, whereas in F2, disintegration times ranged from 36 to 46 s. The individual disintegration time values for both formulations are presented in Table 11.

The statistical evaluation of disintegration time is summarized in Table 12. The mean in vitro disintegration time was 159.5 s for F1 and 40.5 s for F2. F2 showed markedly faster disintegration and lower variability, as reflected by its smaller standard deviation and narrower 95% confidence interval compared with F1.

Table 11: Individual in vitro disintegration times for F1 and F2 (s).

Tablet number	Formulation 1	Formulation 2
1	148	46
2	168	36
3	138	40
4	173	38
5	152	40
6	178	43

Table 12: Statistical evaluation of in vitro disintegration time for F1 and F2.

Formulation	Mean disintegration time (s)	Standard deviation (s)	Standard error (s)	t value	95%percent confidence interval for mean (s)
F1	159.5	17.8	7.26	2.57	159.5 ± 18.6
F2	40.5	3.5	1.42	2.57	40.5 ± 3.6

These results clearly show that F2 exhibits a much shorter and more reproducible disintegration time than F1. F2 tablets disintegrated in approximately 40 s, fulfilling the general expectation for an ODT dosage form. In contrast, F1 tablets required approximately 160 s to disintegrate, which is considerably longer than the desired range and therefore not acceptable for an ODT.

The superior disintegration performance of F2 is attributable to the combination of croscarmellose sodium, microcrystalline cellulose and mannitol. Mannitol is highly water soluble and creates channels upon dissolution, while microcrystalline cellulose contributes porosity and wicking action. Even though F1 contained a higher amount of croscarmellose sodium, the presence of sucrose-calcium phosphate,

magnesium stearate and talc may have reduced tablet porosity and wettability, thereby slowing disintegration. These findings highlight that the overall matrix structure and excipient interactions are more critical determinants of disintegration time than the amount of superdisintegrant alone.

Comparative evaluation with full statistical interpretation

When considering the physical dimensions, weight variation, hardness and disintegration time together, a clear picture of the performance and reliability of both formulations emerges.

Both formulations showed satisfactory uniformity in diameter and thickness, with F2 having slightly lower variability. Weight variation results demonstrated that tablets of F2 were closer to the theoretical target weight, with narrower confidence intervals, indicating a more consistent filling process and more uniform distribution of ketoprofen and excipients.

Hardness values showed that F2 tablets were mechanically stronger than F1 tablets, while still falling within a suitable range for fast disintegrating tablets. The increased hardness did not lead to increased disintegration time; on the contrary, F2 disintegrated significantly faster. This is a key observation that underlines the importance of an optimized combination of soluble fillers (mannitol), porous binders (microcrystalline cellulose) and efficient superdisintegrants (croscarmellose sodium).

In terms of in vitro disintegration time, the difference between the formulations was pronounced and clinically meaningful. Only F2 can be considered a true orally disintegrating tablet according to commonly accepted criteria. F1, while acceptable in terms of general tablet quality, fails to meet the disintegration requirements for this dosage form and would need reformulation.

Statistical analysis of all parameters showed relatively small standard deviations and tight confidence intervals, which indicate that the experimental results are reliable and that the manufacturing process is reasonably reproducible. The consistent superiority of F2 across multiple quality attributes suggests that it has a better balance of excipient properties and is therefore more suitable for further development as a fast disintegrating ketoprofen tablet.

The development of ODTs requires careful consideration of multiple formulation and process variables. In this study, two different excipient systems were investigated while keeping the therapeutic dose of ketoprofen and the total tablet weight constant. Such a design enables direct comparison of excipient functionality under identical drug loading, thereby

isolating the influence of the excipient matrix on tablet performance (Chang et al. 2000). The results demonstrated that the nature and combination of excipients have a decisive impact on both mechanical properties and disintegration behavior, which is consistent with previous work reporting that the disintegration performance of orally disintegrating tablets is driven by the global behavior of the compacted system rather than individual excipients in isolation (Seager, 1998; Shukla et al. 2009).

A notable aspect of the present work is the choice of a 150 mg ketoprofen dose, rather than the conventional 200 mg dose commonly found in standard oral formulations (Brunton et al. 2017). ODTs are intended to produce rapid onset of action by disintegrating quickly in the oral cavity, allowing the drug to be swallowed as a suspension and potentially facilitating partial absorption through the oral mucosa, bypassing the first-pass metabolism in some cases (Kuchekar et al. 2003; Habib et al. 2000). Evidence from various ODT drug products suggests that faster onset of therapeutic effect may allow a reduction of total dose, provided that sufficient plasma concentrations are still achieved (Sastry et al. 2000). For ketoprofen, which is primarily used for acute pain and inflammatory conditions, such an approach can be clinically valuable because many adverse effects, including gastrointestinal irritation, dizziness and renal burden, are dose-related (Famaey, 1997). Thus, the use of a 150 mg dose in an ODT design represents a formulation-driven dose optimization strategy aiming to balance rapid efficacy with improved safety. Similar dose adjustments have been reported for other analgesics in ODTs (Seager, 1998; Chang et al. 2000).

The comparison of formulations showed that the system containing mannitol and microcrystalline cellulose (F2) provided a favorable combination of mechanical strength and rapid disintegration. Mannitol is a highly water-soluble filler that contributes to the creation of a porous matrix when compressed, increases wettability, and imparts a pleasant cooling sensation and sweetness, enhancing patient acceptability (Gohel and Jogani, 2005). Microcrystalline cellulose acts as a plastically deforming binder, improving compressibility and forming a strong interparticle network during compaction (Bolhuis and Armstrong, 2006). It also enhances capillary action by generating a porous internal structure, which facilitates rapid penetration of saliva into the tablet and promotes superdisintegrant swelling (Jivraj et al. 2000). The synergistic behavior of a soluble excipient with a porous matrix former has been widely recognized as a powerful design strategy for fast

disintegrating tablets (Chang et al. 2000; Shukla et al. 2009), which aligns with the findings of this study.

In contrast, F1 relied on sucrose–calcium phosphate as the main filler, together with magnesium stearate and talc. While sucrose–calcium phosphate (commercially known as Di-Pac) is compressible and imparts sweetness, its solubility and porosity characteristics differ significantly from those of mannitol (Gohel and Jogani, 2005). The presence of magnesium stearate and talc, which are hydrophobic excipients, can hinder wetting of the tablet surface and reduce water penetration, thereby delaying the onset of disintegration (Aulton and Taylor, 2017). This phenomenon has been reported in other studies where excessive hydrophobic lubricant decreased disintegration efficiency despite the presence of superdisintegrants (Seager, 1998). Although F1 contained a higher amount of croscarmellose sodium, its disintegration time was substantially longer. This supports the premise that disintegration performance depends on the overall hydrophilicity, porosity and capillary network of the excipient matrix rather than the absolute quantity of a single superdisintegrant (Sastry et al. 2000; Shukla et al. 2009).

The hardness results highlight a clear distinction between the two tablet systems. As shown in Table 10, the mean hardness value was 4.65 kg for F1 and 5.30 kg for F2. Despite the higher hardness, F2 tablets exhibited markedly faster disintegration than F1. The mean in vitro disintegration time was 159.5 seconds for F1, whereas it was 40.5 seconds for F2, as presented in Table 12.

Thus, although F2 tablets demonstrated greater mechanical strength, they disintegrated approximately four times faster than F1 tablets. This finding indicates that increased hardness did not adversely affect disintegration performance in F2. Similar behavior has been reported for porous tablet matrices containing hydrophilic and plastically deforming excipients, where rapid liquid uptake and capillary action can compensate for higher compaction strength (Hiestand et al. 1983; Bolhuis and Armstrong, 2006; Chang et al. 2000). The combined hardness and disintegration data therefore demonstrate a clear and meaningful difference between F1 and F2 in terms of both mechanical robustness and functional performance (Gohel and Jogani, 2005; Shukla et al. 2009).

From a manufacturing perspective, the improved weight uniformity and lower dimensional variability observed in F2 are also important. These results indicate that the powder blend had better flow properties, which facilitated more consistent die filling during direct compression. Flow uniformity

is essential for scale-up because it reduces batch variability and minimizes the risk of out-of-specification results during industrial production (Jivraj et al. 2000; Aulton and Taylor, 2017). Mannitol and microcrystalline cellulose mixtures are known to demonstrate superior flow and packing behavior compared with sucrose–calcium phosphate when lubricated with hydrophobic agents (Gohel and Jogani, 2005).

Regarding patient acceptability, both the size and the disintegration time are essential determinants of success. Although both formulations have similar dimensions, only F2 delivers the rapid disintegration required to improve the patient experience compared with conventional tablets. Fast disintegration not only enables administration without water but also provides an immediate psychological perception of pain relief, which is especially relevant in acute pain management (Habib et al. 2000). Moreover, taste and mouthfeel are crucial for orally disintegrating dosage forms, and the presence of mannitol is expected to offer favorable sensory attributes (Seager, 1998).

The present study is limited to in vitro evaluations and does not include in vivo pharmacokinetic or pharmacodynamic testing. However, the in vitro results provide a strong foundation for identifying F2 as a suitable candidate for further investigation. Future research should examine the relationship between in vitro disintegration time and in vivo onset of analgesic action. It would also be valuable to perform taste masking and palatability studies to improve patient acceptance, as sensory properties strongly influence patient compliance and overall product success (Kuchekar et al. 2003). Additionally, stability studies under accelerated conditions could provide important insight into long-term product performance.

Overall, the results support the conclusion that rational excipient selection and optimization of excipient ratios can produce ODTs that are both robust and rapidly disintegrating, even when relatively high drug loads, such as 150 mg of ketoprofen, are used. The findings also demonstrate that a formulation-driven dose optimization strategy may enable reduced drug exposure while maintaining therapeutic efficacy, contributing to improved patient safety.

CONCLUSION

This study has demonstrated that direct compression can be successfully used to formulate ketoprofen fast disintegrating tablets when appropriate excipients are

selected and combined in a rational manner. Two formulations were compared, each containing 150 mg of ketoprofen and a total tablet weight of 500 mg, but differing in the type and quantities of excipients.

The key conclusions are as follows: both formulations produced tablets with acceptable diameter, thickness and weight variation, indicating that the manufacturing process was generally robust and reproducible. However, the formulation containing mannitol and microcrystalline cellulose exhibited lower variability in these parameters and was closer to the theoretical tablet weight, which is advantageous for dose accuracy and quality control.

The mannitol and microcrystalline cellulose based formulation showed higher hardness and thus better mechanical strength, which is beneficial for handling, packaging and transportation. Importantly, this increased hardness did not result in slower disintegration. Instead, the same formulation showed rapid in vitro disintegration in approximately 40 seconds, clearly fulfilling the expectations for an ODT. In contrast, the formulation containing sucrose-calcium phosphate, magnesium stearate and talc disintegrated in more than two minutes and therefore failed to meet the basic functional requirement of this dosage form.

The combination of croscarmellose sodium, microcrystalline cellulose and mannitol appears to provide a synergistic effect, creating a porous and hydrophilic tablet matrix that disintegrates quickly while maintaining adequate mechanical strength. The results also suggest that a 150 mg ketoprofen dose, when delivered in an ODT form, may be sufficient to achieve effective therapy, potentially with a lower risk of dose-related adverse effects compared with higher dose conventional tablets.

In conclusion, the formulation containing ketoprofen, croscarmellose sodium, microcrystalline cellulose and mannitol represents a promising ODT system that combines reliable manufacturability, robust mechanical properties and rapid disintegration. This formulation is suitable for further development, including stability testing, taste and palatability evaluation and in vivo performance studies, with the ultimate aim of providing a patient-friendly and effective analgesic dosage form.

ACKNOWLEDGMENTS

The author declare no conflict of interest.

REFERENCES

Aulton ME, Taylor KMG (2017). *Aulton's Pharmaceutics: The Design and Manufacture of Medicines.* 5th ed. Edinburgh, UK: Churchill Livingstone.

Bolhuis GK, Armstrong NA (2006). Excipients for direct compaction—an update. *Pharm Dev Technol* **11**(1): 111–124.

Brunton LL, Hilal-Dandan R, Knollmann BC (2017). *Goodman & Gilman's The Pharmacological Basis of Therapeutics.* 13th ed. New York, NY: McGraw-Hill.

Chang RK, Guo X, Burnside BA, Couch RA (2000). Fast-dissolving tablets. *Pharm Technol* **24**(6): 52–58.

European Pharmacopoeia (2020). *Disintegration of Tablets and Capsules; Uniformity of Mass of Single-Dose Preparations.* Strasbourg, France: Council of Europe.

Famaey JP (1997). Pharmacology of ketoprofen. *Rheumatol Int* **16**(1): 1–10.

Gohel MC, Jogani PD (2005). A review of co-processed directly compressible excipients. *J Pharm Pharm Sci* **8**(1): 76–93.

Habib W, Khankari R, Hontz J (2000). Fast-dissolve drug delivery systems. *Crit Rev Ther Drug Carrier Syst* **17**(1): 61–72.

Hiestand EN, Smith DP, Rees JE (1983). Powder compaction. *Drug Dev Ind Pharm* **9**(2): 219–235.

Hussain AS (1998). Statistical considerations in drug product development. *Pharm Res* **15**(3): 482–486.

ICH (International Council for Harmonisation) (2005). *Q6A Specifications: Test Procedures and Acceptance Criteria for New Drug Substances and New Drug Products.* Geneva, Switzerland: ICH.

Jivraj M, Martini LG, Thomson CM (2000). An overview of the different excipients useful for the direct compression of tablets. *Pharm Sci Technol Today* **3**(2): 58–63.

Klancke J (2003). Dissolution testing of orally disintegrating tablets. *Pharm Technol* **27**(10): 82–90.

Kuchekar BS, Badhan AC, Mahajan HS (2003). Mouth dissolving tablets: A novel drug delivery system. *Pharm Times* **35**(7): 3–10.

Sastry SV, Nyshadham JR, Fix JA (2000). Recent technological advances in oral drug delivery—A review. *Drug Dev Ind Pharm* **26**(9): 1019–1031.

Seager H (1998). Drug-delivery products and the Zydis fast-dissolving dosage form. *J Pharm Pharmacol* **50**(4): 375–382.

Shukla D, Chakraborty S, Singh S, Mishra B (2009). Mouth dissolving tablets I: An overview of formulation technology. *Sci Pharm* **77**(2): 309–326.

Sun CC, Grant DJW (2001). Influence of crystal structure on the tableting properties of sulfamerazine polymorphs. *Pharm Res* **18**(3): 274–280.

United States Pharmacopeia (USP) (2022). *General Chapter <701> Disintegration; <2091> Weight Variation.* Rockville, MD: US Pharmacopeial Convention.

Research Article EMUJPharmSci ISSN 2651-3587 https://dergipark.org.tr/emujpharmsci

EMU Journal of Pharmaceutical Sciences

EMUJPharmSci 2026; 9(1): 18-25.

DOI: 10.54994/emujpharmsci.1838511

Benzazole–Carboxamide Hybrids as Potent Antiproliferative Agents Against Breast Cancer Cells

Ronak Haj Ersan[1], Omer Faruk Col[2,3], Sule Gursoy[4,*]

[1] Cihan University-Duhok, Faculty of Pharmacy, Department of Pharmaceutical Chemistry, Duhok, Iraq.
[2] Gazi University, Faculty of Pharmacy, Department of Pharmaceutical Chemistry, Ankara, Türkiye.
[3] Çöl Pharmacy, Kocasinan, Kayseri, Türkiye.
4 Erzincan Binali Yıldırım University, Faculty of Pharmacy, Department of Biochemistry, Erzincan, Türkiye.

Abstract

Breast cancer remains a leading cause of cancer-related mortality worldwide, and the development of novel small-molecule agents with improved efficacy and selectivity is still urgently needed. Although benzazole and benzamide scaffolds are individually recognized for their diverse pharmacological activities, systematic studies exploring hybrid N-(benzazol-2-yl)-4-substituted benzamide derivatives as antiproliferative agents against breast cancer are limited. In this study, a series of *N*-(benzazol-2-yl)-4-substituted benzamide derivatives was synthesized and fully characterized by ^{1}H NMR, ^{13}C NMR, and IR spectroscopy. The antiproliferative activities of the synthesized compounds were evaluated against the human breast cancer cell line MCF-7 and the normal fibroblast cell line L929 using the MTT assay. The compounds were obtained in good to excellent yields (70–85%). Several derivatives exhibited strong growth-inhibitory effects, with IC_{50} values ranging from 3.11 to 12.39 µM. Among the tested molecules, compounds 6 and 11 demonstrated the most significant cytotoxic effects, and compound 6 emerged as the most promising candidate for further investigation. These findings provide preliminary structure–activity insights and highlight benzazole–benzamide hybrids as promising scaffolds for further anticancer drug development.

Keywords

Antiproliferative activity, benzazole derivatives, breast cancer, synthesis.

Article History

Submitted: 18 December 2025 **Accepted**: 09 March 2026 **Published Online**: May 2026
Reviewer
Invitation Date: 23 December 2025 **Acceptance Date**: 23/24 December 2025 **Due Date**: 07/08 January 2026
Article Info

***Corresponding author:** Sule Gursoy **email:** sule.gursoy@erzincan.edu.tr

Research Article:
Volume: 9 **Issue: 1** **Pages: 18-25**
DOI: 10.54994/emujpharmsci.1838511

INTRODUCTION

Breast cancer remains a major global health concern and is one of the most commonly diagnosed cancers and a leading cause of cancer-related mortality among women worldwide (Banmare and Mude, 2023; Wilkinson and Gathani, 2022). Despite significant advances in screening, molecular classification, and targeted therapies, many patients still face challenges related to treatment failure, systemic toxicity, and the emergence of drug-resistant tumor phenotypes (Yang et al. 2023; Anand et al. 2023; Singh et al. 2023). These limitations underscore the ongoing need for innovative small-molecule agents with improved biological selectivity and tolerability.

Benzazole-based heterocycles constitute an important structural class in medicinal chemistry due to their ability to mimic heteroaromatic motifs found in biological systems and their broad spectrum of pharmacological activities (Irfan et al. 2020). Among these scaffolds, benzoxazole derivatives have attracted particular attention because of their reported antiproliferative, antimicrobial, and anti-inflammatory properties. Moreover, the incorporation of carboxamide functionality is known to modulate physicochemical behavior, facilitate hydrogen-bond interactions with cellular targets, and enhance metabolic stability (Cheong et al. 2018; Szumilak et al. 2021; Singh et al. 2022).

Recent drug design strategies increasingly focus on the development of hybrid molecules capable of interacting with multiple cellular pathways. Compounds combining heterocyclic scaffolds with pharmacophores such as carboxamides have shown promise in overcoming classical resistance mechanisms and achieving enhanced cytotoxic potency against cancer cells (Cheong et al. 2018; Szumilak et al. 2021).

However, despite the recognized pharmacological relevance of benzazole and benzamide motifs, studies specifically investigating *N*-(benzazol-2-yl)-4-substituted benzamide derivatives as antiproliferative agents remain limited. In particular, there is a lack of systematic structure–activity relationship (SAR) evaluations exploring how different heteroatoms within the benzazole core influence cytotoxic activity against breast cancer cells. This gap highlights the need for the rational design and biological assessment of new benzazole–benzamide hybrids with defined structural variations.

Within this context, *N*-(benzazol-2-yl)-4-substituted benzamide derivatives provide a structurally appealing platform for

anticancer agent development. The combination of a benzazole nucleus with a substituted benzamide moiety offers the potential for enhanced binding interactions and improved biological activity. Therefore, the present study was designed to address this gap by synthesizing a focused series of benzazole–benzamide derivatives incorporating different heteroatoms in the benzazole core and evaluating their antiproliferative activity against the MCF-7 breast cancer cell line. The ultimate aim was to identify promising molecular candidates and to generate preliminary insights into their structure–activity relationships for future optimization.

MATERIALS AND METHODS

Materials

2-Aminobenzimidazole, 2-aminobenzothiazole, 2-aminobenzoxazole, benzoyl chloride, 4-chlorobenzoyl chloride, dichloromethane (DCM), tetrahydrofuran (THF), triethylamine (TEA), diisopropylethylamine (DIPEA), n-hexane, ethyl acetate, hydrochloric acid (HCl), sodium bicarbonate ($NaHCO_3$), magnesium sulfate ($MgSO_4$), and other solvents used in this study were purchased from Sigma–Aldrich and Merck and used without further purification. Thin layer chromatography (TLC) analyses were performed on Merck aluminum-backed silica gel plates using ethyl acetate/n-hexane (2:1, v/v) as the mobile phase. ^{1}H-NMR, and ^{13}C-NMR, spectra were recorded at 400, and 100 MHz, respectively, on a Varian-Agilent 400 MHz instrument using Me_4Si as an internal standard. All column chromatography was performed on silica gel (60 mesh, Silycycle).

Synthesis method for *N*-(1*H*-benzazole-2-yl)-4-substitutedbenzamide

Aminobenzazoles (2-aminobenzimidazole, 2-aminobenzothiazole, or 2-aminobenzoxazole) (1.1 mmol) were dissolved in dichloromethane/tetrahydrofuran (15 mL). The solution was cooled to 0 °C, and benzoyl chloride or the corresponding acyl chloride derivatives (phenylacetyl chloride, or 4-chlorobenzoyl chloride) (1.0 mmol) were added dropwise over 10 minutes. The mixture was stirred at the same temperature for 2 hours. Subsequently, a catalytic amount of TEA or DIPEA (~5 drops) was introduced at room temperature. The reaction was then heated under reflux for 12-24 hours using a condenser. After completion, verified by TLC analysis, the reaction was quenched and the solvent was evaporated. The residue was dissolved in dichloromethane (25 mL) and washed successively with 1 N HCl (3 × 20 mL),

saturated $NaHCO_3$ solution (2 × 15 mL), and distilled water (15 mL). The organic layer was separated, dried over anhydrous $MgSO_4$, filtered, and concentrated under reduced pressure. The crude product was purified by column chromatography on silica gel using an appropriate n-hexane/ethyl acetate eluent system. The isolated compounds were finally recrystallized from suitable solvents to afford the pure products. The NMR and IR spectral data confirmed the high purity of the compound (Zoatier et al. 2025a, 2023, 2025b; Gursoy et al. 2024).

Biological activity studies

MTT cell viability assay

The cytotoxic effects of the synthesized compounds were evaluated using the MTT colorimetric assay, which measures mitochondrial metabolic activity as an indicator of cell viability. This assay relies on the ability of viable cells to convert the yellow tetrazolium salt MTT (3-(4,5-dimethylthiazol-2-yl)-2,5-diphenyltetrazolium bromide) into insoluble purple formazan crystals through mitochondrial dehydrogenase activity.

Cells were maintained in RPMI-1640 medium supplemented with 10% fetal bovine serum and penicillin–streptomycin under standard culture conditions (37°C, 5% CO_2, humidified atmosphere). For the assay, cells were seeded into 96-well plates at an approximate density of 1–2.5 × 10^4 cells/mL and allowed to attach for 24 h. Test compounds were dissolved in DMSO and added to the wells at the desired concentrations, with each condition assessed in triplicate.

Following the designated incubation period (24–96 h depending on the experimental design), MTT solution was added to each well and the plates were incubated further to allow the formation of formazan crystals. After incubation, the supernatant was carefully removed and the crystals were solubilized using DMSO. Plates were gently shaken to ensure complete dissolution, and absorbance was recorded at 570 nm using a microplate reader (Burmaoglu et al. 2016; Kuzu et al. 2022a, 2022b; Algul et al. 2021; Ersan et al. 2021). Cell viability was calculated according to the formula below:

$$\%\text{Viability} = \frac{A_{\text{sample}} - A_{\text{blank}}}{A_{\text{control}} - A_{\text{blank}}} \times 100$$

The half-maximal inhibitory concentration (IC_{50}) values were obtained from concentration–response curves. All experiments were performed in three independent replicates.

RESULTS AND DISCUSSION

Chemistry

A convenient synthetic approach was developed for the preparation of benzazole–benzamide derivatives bearing different heteroatoms in the benzazole core. As illustrated in Scheme 1, three distinct aminobenzazole scaffolds—2-aminobenzimidazole (1), 2-aminobenzoxazole (2), and 2-aminobenzothiazole (3)—were selected as key starting materials. These heterocyclic amines were reacted with benzoyl chloride and 4-chloro substituted analogue (4–5) under mild acylation conditions to afford the target amide derivatives (6–11).

Initially, the aminobenzazole derivatives (1–3) (1.1 eq) were dissolved in a DCM/THF mixture, and the corresponding benzoyl chloride or 4-chlorobenzoyl chloride (4–5) (1.0 eq) was added dropwise at 0 °C. After stirring at this temperature for 2 h, a catalytic amount of triethylamine (TEA) or diisopropylethylamine (DIPEA) was introduced to promote amide bond formation. The reaction mixture was then heated under reflux for 24 h to complete the acylation process. Following completion, monitored by TLC, the reaction mixture was subjected to standard aqueous work-up and chromatographic purification to yield the desired N-acylated benzazole derivatives (6–11). The synthesized compounds were obtained in good to excellent yields ranging from 70% to 85%. This strategy proved highly efficient for the preparation of structurally diverse benzazole–benzamide frameworks in good to excellent yields.

The optimized reaction conditions were subsequently applied to expand the compound library using different benzazole cores and acyl chloride partners (Scheme 1). This method significantly simplified the synthetic sequence by enabling direct amidation under mild conditions, providing a practical and general route for the synthesis of the final benzazole–benzamide derivatives.

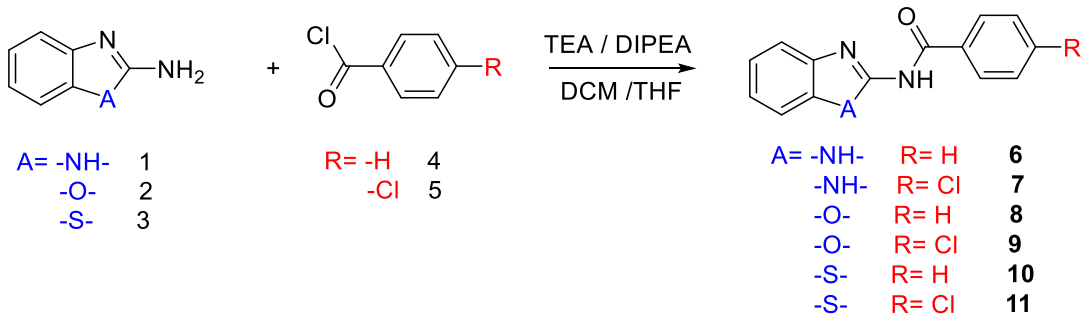

Scheme 1: Synthesis of benzazole-based benzamide derivatives.

Biological activity studies

The cytotoxic effects of the synthesized compounds (6–11) were evaluated against the MCF-7 breast cancer cell line and the normal fibroblast cell line (L929) using the MTT assay. As shown in Table 1, all compounds exhibited notable cytotoxic activity against MCF-7 cells, with IC_{50} values ranging from 3.11 to 12.39 μM. Importantly, these compounds showed higher IC_{50} values in the L929 normal cell line, indicating a degree of selectivity towards cancer cells.

Table 1: IC_{50} values of all compounds in the MCF-7, MDA-MB-231, and MCF-10A cell lines.

Compound No	IC_{50} (μM)		Specificity
	MCF-7	L929	
6	3.67 ± 0.21	8.52 ±0.23	2.32
7	3.87 ±0.12	6.99 ±0.42	1.80
8	3.11 ±0.15	6.49 ±0.31	2.08
9	3.17 ±0.01	5.98 ±0.52	1.88
10	12.39±0.97	26.90±0.97	2.17
11	3.49 ±0.32	6.43 ±0.05	1.84

Among the tested compounds, compound 8 demonstrated the strongest cytotoxic effect on MCF-7 cells, with an IC_{50} value of 3.11 ± 0.15 μM, while maintaining a selectivity index (SI) of 2.08. Compounds 6, 9, and 11 also exhibited potent cytotoxicity with IC_{50} values close to 3.5 μM and SI values ranging between 1.84 and 2.32. Compound 10 showed comparatively lower cytotoxicity with an IC_{50} value of 12.39 ± 0.97 μM but retained good selectivity (SI = 2.17).

These results suggest that the synthesized benzazole–benzamide derivatives possess promising antiproliferative activity against breast cancer cells, with selective toxicity favoring cancer cells over normal fibroblasts. Compounds with higher selectivity indices may serve as lead candidates for further biological evaluation and development.

CONCLUSIONS

In summary, a series of novel *N*-(benzazol-2-yl)-4-substituted benzamide derivatives were successfully synthesized and thoroughly characterized. The optimized synthetic methodology allowed efficient access to structurally diverse benzazole–benzamide frameworks under mild reaction conditions with good to excellent yields. Biological evaluation of these compounds revealed significant antiproliferative activity against the MCF-7 breast cancer cell line, while exhibiting reduced cytotoxicity towards normal fibroblast cells

(L929), indicating promising selectivity profiles.

A preliminary structure–activity relationship (SAR) analysis suggested that both the nature of the heteroatom within the benzazole core and the substituents on the benzamide moiety significantly influence cytotoxic potency and selectivity. In particular, compound 6 exhibited the most potent cytotoxic effect along with a favorable selectivity index, highlighting its potential as a lead candidate for further drug development. Other derivatives showed variable activity, providing insights into how specific structural modifications can modulate biological effects.

Overall, these findings not only demonstrate the anticancer potential of benzazole–benzamide hybrids but also offer guidance for rational design and optimization of future derivatives with enhanced efficacy and selectivity, supporting their continued exploration in anticancer drug discovery.

ACKNOWLEDGMENTS

This study was conducted based on the work of Bayan Zoatier from the Faculty of Pharmacy, Mersin University. The authors do not declare the originality of the test compound and the intermediates used.

REFERENCES

Algul O, Ersan RH, Alagoz MA, Duran N, Burmaoglu S (2021). An efficient synthesis of novel di-heterocyclic benzazole derivatives and evaluation of their antiproliferative activities. *J Biomol Struct Dyn* **39**(18): 6926-6938.

Anand U, Dey A, Chandel AKS, Sanyal R, Mishra A, et al. (2023). Cancer chemotherapy and beyond: Current status, drug candidates, associated risks and progress in targeted therapeutics. *Genes & Diseases* **10**(4): 1367-1401.

Banmare S, Mude G (2023). Awareness regarding breast cancer among the female population in Wardha District. *F1000Research* **12**: 1223.

Burmaoglu S, Algul O, Anıl DA, Gobek A, Duran GG, et al. (2016). Synthesis and anti-proliferative activity of fluoro-substituted chalcones. *Bioorg Med Chem Lett* **26**(13): 3172-3176.

Cheong JE, Zaffagni M, Chung I, Xu Y, Wang Y, et al. (2018). Synthesis and anticancer activity of novel water soluble benzimidazole carbamates. *Eur J Med Chem* **144**(2018): 372-385.

Ersan RH, Alagoz MA, Ertan-Bolelli T, Duran N, Burmaoglu S, et al. (2021). Head-to-head bisbenzazole derivatives as antiproliferative agents: design, synthesis, in vitro activity, and SAR analysis. *Molecular Diversity* **25**(4): 2247-2259.

Gursoy S, Ozturk ES, Zoatier B, Ulger M, Algul O (2024). Synthesis and antitubercular activities of acetamide-substituted benzazole derivatives. *Erzincan University Journal of Science and Technology* **17**(2): 474-487.

Irfan A, Batool F, Zahra Naqvi SA, Islam A, Osman SM, et al. (2020). Benzothiazole derivatives as anticancer agents. *J Enzyme Inhib Med Chem* **35**(1): 265-279.

Kuzu B, Hepokur C, Alagoz MA, Burmaoglu S, Algul O (2022). Synthesis, biological evaluation and in silico studies of some 2-substituted benzoxazole derivatives as potential anticancer agents to breast cancer. *ChemistrySelect* **7**(1): e202103559.

Kuzu B, Hepokur C, Turkmenoglu B, Burmaoglu S, Algul O (2022). Design, synthesis and in vitro antiproliferation activity of some 2-aryl and-heteroaryl benzoxazole derivatives. *Future Med Chem* **14**(14): 1027-1048.

Singh AK, Kumar A, Singh H, Sonawane P, Paliwal H, et al. (2022). Concept of hybrid drugs and recent advancements in anticancer hybrids. *Pharmaceuticals* **15**(9): 1071.

Singh V, Afshan T, Tyagi P, Varadwaj PK, Sahoo AK (2023). Recent development of multi-targeted inhibitors of human topoisomerase II enzyme as potent cancer therapeutics. *Int J Biol Macromol* **226***:* 473-484.

Szumilak M, Anna WO, Andrzej S (2021). "Hybrid drugs—a strategy for overcoming anticancer drug resistance?." *Molecules* **26**(9): 2601.

Wilkinson L, Gathani T (2022). Understanding breast cancer as a global health concern. *Br J Radiol* **95**(1130): 20211033.

Yang F, He Q, Dai X, Zhang X, Song D (2023). The potential role of nanomedicine in the treatment of breast cancer to overcome the obstacles of current therapies. *Front Pharmacol* **14***:* 1143102.

Zoatier B, Gizem Yildiztekin K, Abdullah Alagoz M, Hepokur C, Burmaoglu S, Algul O (2025). Development of Potent Type V MAPK Inhibitors: Design, Synthesis, and Biological Evaluation of Benzothiazole Derivatives Targeting p38α MAPK in Breast Cancer Cells. *Archiv der Pharmazie* **358**(4): e2500011.

Zoatier B, Yildirim M, Alagoz MA, Yetkin D, Turkmenoglu B, et al. (2023). N-(benzazol-2-yl)-2-substituted phenylacetamide derivatives: Design, synthesis and biological evaluation against MCF7 breast cancer cell line. *J Mol Struct* **1285**: 135513.

Zoatier B, Yildiztekin G, Alagoz MA, Hepokur C, Dilek E, et al. (2025). Benzoxazole Derivatives as Dual p38α Mitogen-Activated Protein Kinase and Acetylcholinesterase Inhibitors: Design, Synthesis, and Evaluation for Alzheimer's Disease and Cancer Therapy. *ChemMedChem* **20**(22): e202500669.

Research Article EMUJPharmSci ISSN 2651-3587 https://dergipark.org.tr/emujpharmsci

EMU Journal of Pharmaceutical Sciences

EMUJPharmSci 2026; 9(1): 26-46.

DOI: **10.54994/emujpharmsci.1897731**

Integrated *In Silico* and Network Toxicology Analysis of Perfluorononanoic Acid-Induced Hepatotoxicity in Humans

Fuat Karakus[1*], Burak Kuzu[2]

[1]Van Yüzüncü Yıl University, Faculty of Pharmacy, Department of Pharmaceutical Toxicology, Van, Türkiye.

[2] Van Yüzüncü Yıl University, Faculty of Pharmacy, Department of Pharmaceutical Chemistry, Van, Türkiye.

Abstract

Perfluorononanoic acid (PFNA) is a long-chain perfluorocarboxylic acid that was recently listed as a persistent organic pollutant under the Stockholm Convention. Growing toxicological and epidemiological evidence associates PFNA exposure with multiple adverse health outcomes, including hepatotoxicity; however, the molecular mechanisms underlying PFNA-induced hepatotoxicity in humans remain unclear. In this study, the molecular mechanisms and targets associated with PFNA-induced hepatotoxicity in humans were investigated using *in silico* hepatotoxicity prediction, network toxicology, multi-level bioinformatics approaches, molecular docking, and differential gene expression (DEG) analysis. Through comprehensive database screening, 107 potential targets associated with PFNA-induced hepatotoxicity were identified. Protein-protein interaction network construction and topological analysis using STRING, Cytoscape, and the MCODE algorithm identified six hub targets (SRC, EGFR, ESR1, FN1, MAPK1, and JAK2). Gene-gene interaction analysis revealed enrichment in peptidyl-tyrosine phosphorylation, while Gene Ontology analysis demonstrated significant enrichment in the positive regulation of phosphatidylinositol 3-kinase/protein kinase B signaling. KEGG pathway analysis highlighted pathways associated with proteoglycan-mediated signaling and chemical carcinogenesis-receptor activation. Molecular docking indicated weak binding affinities between PFNA and the identified hub targets. DEG analysis further showed downregulation of SRC, EGFR, and JAK2, whereas ESR1, FN1, and MAPK1 were upregulated. Collectively, these findings suggest that PFNA may perturb key regulatory signaling networks involved in tyrosine kinase activity, PI3K/Akt signaling, and extracellular matrix-associated pathways, which are frequently implicated in carcinogenesis and liver pathophysiology. This study provides mechanistic insights into PFNA-induced hepatotoxicity and establishes a foundation for future experimental validation *in vitro* and *in vivo*.

Keywords

Hepatotoxicity, Long-chain PFCAs, Perfluorononanoic acid, PFAS.

Article History

Submitted: 25 December 2025 **Accepted:** 06 April 2026 **Published Online**: May 2026

Reviewer

Invitation Date: 05/19 March 2026 **Acceptance Date**: 05/19 March 2026 **Due Date**: 20 March/03 April 2026

Article Info

***Corresponding author:** Fuat Karakus **email:** fuatkarakus@yyu.edu.tr

Research Article:

Volume: 9 Issue: 1 Pages: 26-46

DOI: 10.54994/emujpharmsci.1897731

INTRODUCTION

Perfluorononanoic acid (PFNA; $C_9HF_{17}O_2$) is a nine-carbon long-chain perfluorocarboxylic acid (PFCA), belonging to the broader class of synthetic per- and polyfluoroalkyl substances (PFAS), which are characterized by fully fluorinated carbon backbones. PFNA has been primarily used as a processing aid in the emulsion polymerization of polyvinylidene fluoride. It is widely considered that most environmental PFNA originates from historical releases during these manufacturing processes. PFNA has also been detected at trace levels in aqueous film-forming foams used in firefighting (Lohmann et al. 2020; US EPA, 2024).

PFNA and other long-chain PFCAs are highly resistant to hydrolysis, photolysis, and biodegradation. Due to the exceptional stability of the carbon-fluorine bond, long-chain PFCAs, including PFNA, persist in the environment (ATSDR, 2021) and are now ubiquitously detected in air, soil, groundwater, surface waters, and biological tissues of plants, wildlife, and humans worldwide (US EPA, 2024). Global modeling studies indicate that long-chain PFCAs, their salts, and related compounds can undergo long-range environmental transport (Thackray et al. 2020). Consistently, C_9-C_{18} PFCAs have been reported in environmental matrices, wildlife, and human populations in remote regions such as the Arctic and Antarctic, further supporting their capacity for long-range transport (UNEP, 2021, 2023a, 2023b). Owing to their persistence, bioaccumulation potential, adverse health and environmental effects, and long-range transport properties, PFNA and other long-chain PFCAs, along with their salts and related compounds, have been listed in Annex A of the Stockholm Convention under decision SC-12/12 (UNEP 2025).

Human exposure to PFNA may occur through multiple pathways, including inhalation of indoor and outdoor air, ingestion of contaminated drinking water and food, incidental ingestion of household dust, and dermal contact with PFAS-containing products (ATSDR, 2021; US EPA, 2024). Early-life exposure is documented by the detection of PFNA in placental tissue, amniotic fluid, cord blood, and breast milk (ATSDR, 2021; UNEP, 2021, 2023a; US EPA, 2024). Following absorption, PFNA preferentially distributes to the plasma and metabolically active organs, particularly the liver and kidneys (UNEP, 2021, 2023a; US EPA, 2024). In addition, enterohepatic recirculation may enhance hepatic accumulation and prolong biological persistence (Ruggiero et al. 2021; US EPA, 2024).

Epidemiological and experimental studies indicate that PFNA exposure is associated with adverse health effects, particularly hepatotoxicity (Zhang et al. 2018; Costello et al. 2022; UNEP, 2023a; US EPA, 2024). As the central organ for xenobiotic metabolism and detoxification, the liver is especially vulnerable. PFAS-induced hepatotoxicity has primarily been attributed to the activation of peroxisome proliferator-activated receptor alpha (PPARα) and the consequent disruption of PPARα-regulated lipid metabolic pathways (Bjork and Wallace, 2009; Kersten and Stienstra, 2017). Animal studies have consistently demonstrated that exposure to PFNA results in hepatocellular hypertrophy and increased liver weight, which may reflect hepatic lipid accumulation (Costello et al. 2022). Moreover, PFNA has been reported to induce hepatic cholestasis in mice (Zhang et al., 2018). Similarly, *in vitro* studies using human HepaRG cells have shown that PFNA increases intracellular triglyceride accumulation and suppresses cholesterogenic gene expression (Louisse et al. 2020; Sadrabadi et al. 2024). A recent *in vitro* study also suggested that PFNA induces cancer-related pathways, including cell cycle progression, oxidative stress, DNA repair, and inflammation, in hepatocytes within human liver spheroids (Golden-Mason et al. 2025).

Despite these findings, the molecular mechanisms underlying PFNA-induced hepatotoxicity in humans remain unclear. Conventional experimental approaches are often costly and time-consuming. In recent years, computational toxicology has emerged as a powerful means of elucidating interactions between chemicals and biological systems. By integrating multi-omics datasets through computational modeling, this approach enables comprehensive assessment of how toxicants disrupt cellular networks and contribute to disease development. Bioinformatics tools, particularly pathway and network analyses, facilitate the identification of key molecular targets and mechanistic pathways, offering insight into toxicity-related processes. These integrated strategies support biomarker discovery and therapeutic target identification while aligning with non-animal testing approaches and New Approach Methodologies (NAMs) (Karakus & Kuzu, 2024).

In this study, the potential molecular mechanisms of PFNA-induced hepatotoxicity were investigated using an integrated framework combining network toxicology, bioinformatics analyses, and molecular docking. An overview of the study workflow is presented in Figure 1.

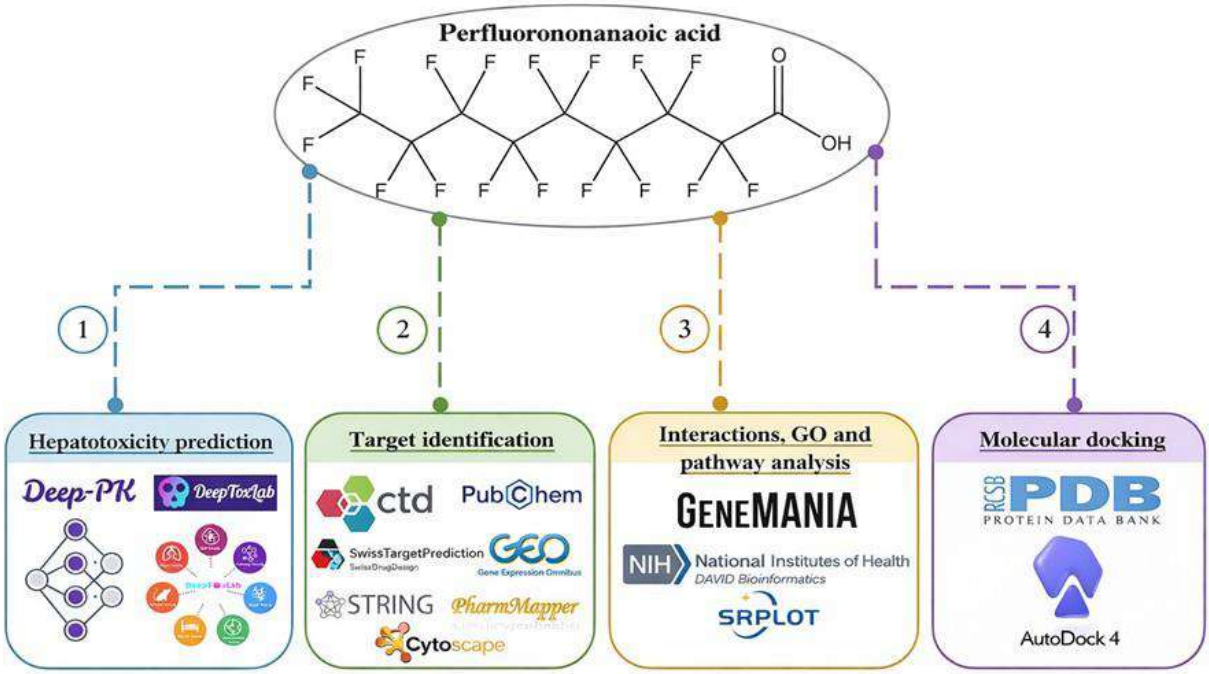

Figure 1: Workflow of the analyses used to predict the hepatotoxicity mechanisms of PFNA.

METHODS

Investigated compound and qualitative hepatotoxicity prediction

In this study, PFNA (CAS No. 375-95-1) was examined, and its Simplified Molecular Input Line Entry System (SMILES) string was obtained from the PubChem database (accessed on December 13, 2025) (Kim et al. 2025). PFNA underwent qualitative *in silico* toxicity assessments using Deep-PK (accessible online at https://biosig.lab.uq.edu.au/deeppk/) (accessed on December 25, 2025) (Myung et al. 2024), and DeepToxLab (available online at https://deeptoxlab.scbdd.com) (accessed on December 25, 2025) (Heid et al. 2024), both of which utilize SMILES strings to evaluate hepatotoxicity potential.

Deep-PK is an advanced deep learning-based platform designed to predict the pharmacokinetic and toxicological properties of chemical compounds, including hepatotoxicity. The results are reported as "toxic" or "safe," along with a predictive confidence score ranging from 0 to 1 (Myung et al. 2024). DeepToxLab employs a Directed Message Passing Neural Network framework and generates a toxicity probability expressed as a percentage ranging from 0 to 100%, with lower values indicating reduced toxic potential. Each prediction is also accompanied by a confidence label (high or low), where high-confidence outputs

(indicated by a blue "H" icon) reflect strong model reliability (Heid et al. 2024).

Curation of PFNA targets

Potential *Homo sapiens*-related targets of PFNA were retrieved from the Comparative Toxicogenomics Database (CTD) v25 (accessed on January 05, 2026) (Davis et al. 2025), PubChem (accessed on January 06, 2026) (Kim et al. 2025), ChEMBL v36 (accessed on January 07, 2026) (Zdrazil et al. 2024), the SwissTargetPrediction platform (accessed on January 07, 2026) (Daina et al. 2019), and the PharmMapper Server (accessed on January 07, 2026) (Wang et al. 2017). All identified targets were integrated, redundant entries were removed, and gene symbols were standardized using the UniProt database (accessed on January 08, 2026) (UniProt Consortium, 2025), yielding a curated PFNA target dataset.

PFNA-associated targets obtained from CTD were based on *in vitro* and *in vivo* experimental evidence as well as literature mining. Targets were retrieved from the "Chemical-Gene Interactions" section of CTD and restricted to *Homo sapiens* (Davis et al. 2025). PubChem was used to retrieve experimentally supported chemical-gene and chemical-protein interactions associated with PFNA, based on curated bioassay data and literature-derived annotations, and restricted to *Homo sapiens* (Kim et al. 2025). ChEMBL was used as a manually curated repository of experimental bioactivity data restricted to *Homo sapiens* (Zdrazil et al. 2024). Targets from SwissTargetPrediction were identified based on a SMILES string search restricted to *Homo sapiens* (Daina et al. 2019). Targets from the PharmMapper server were identified using a pharmacophore mapping approach restricted to *Homo sapiens* and curated by domain experts (Wang et al. 2017).

PFNA-related differentially expressed genes (DEGs) were obtained from the NCBI Gene Expression Omnibus (GEO) database (accessed on January 16, 2026) (Clough et al. 2024) using the search term "perfluorononanoic acid". Among the available datasets, only GSE145239 (Reardon et al. 2021) was associated with *Homo sapiens*. This dataset comprises 24 PFAS compounds, including PFNA, evaluated at multiple concentrations (0.2, 2, 10, 20, 50, and 100 μM) and exposure durations (1 and 10 days) in human liver 3D spheroids using high-throughput transcriptional profiling. DEGs were identified using the thresholds $|\log_2$ fold change (FC)$| > 1$ and an adjusted p-value < 0.05, based on analysis with the GEO2R tool within the GEO database.

Subsequently, a Venn diagram was constructed using the tool (Davis et al. 2025) to visualize overlapping targets between PFNA-associated targets obtained

from databases and DEGs identified from GSE145239. These intersecting targets were considered the final PFNA targets.

Construction of the human hepatotoxicity-related targets

Extensive searches were conducted across the CTD (accessed on January 17, 2026) (Davis et al. 2025), DisGeNET (accessed on January 17, 2026) (Piñero et al. 2020), GeneCards (accessed on January 17, 2026) (Stelzer et al. 2016), and OMIM (accessed on January 17, 2026) (Amberger et al. 2019) databases to identify human hepatotoxicity-related targets. Targets were identified using keywords such as "hepatotoxicity", "liver injury", and "drug-/chemical-induced hepatotoxicity/liver injury". This approach resulted in a refined library of hepatotoxicity-related targets, duplicate entries removed.

Furthermore, a Venn diagram was generated using the MyVenn tool (accessed on January 17, 2026) (Davis et al. 2025) to illustrate overlapping targets between the final PFNA target set and the human hepatotoxicity-related target datasets. The intersecting targets were considered potential targets involved in PFNA-induced hepatotoxicity in humans.

Construction of the protein-protein interaction network and identification of hub targets

Protein–protein interactions (PPIs) of the potential targets involved in PFNA-induced hepatotoxicity were investigated using STRING v12 (accessed on January 18, 2026) (available online at https://string-db.org/) (Szklarczyk et al. 2023). Analysis parameters were stringently defined by restricting the organism to *Homo sapiens* and applying a minimum interaction confidence score of >0.9, which corresponds to the highest confidence level. The false discovery rate (FDR) stringency was set to medium (5%). This strategy ensured a focused analysis of highly reliable protein interactions associated with the targets.

The PPI network generated by STRING was subsequently imported into Cytoscape software (v3.10.4) (Shannon et al. 2003) for visualization and calculation of topological properties of nodes and edges. Within Cytoscape, node significance was evaluated using three centrality algorithms (maximal clique centrality (MCC), maximum neighborhood component (MNC), and degree centrality) implemented via the cytoHubba plugin. In addition, the Molecular Complex Detection (MCODE) algorithm available in Metascape (Zhou et al. 2019) was applied to identify critical hub targets. Because different topological algorithms assess node importance from distinct perspectives, targets shared across all four algorithms were defined as hub targets using the jvenn tool (Bardou et al. 2014) to reduce algorithm-specific bias and

enhance the robustness of hub target selection.

Gene-gene interaction analysis of hub targets

Gene–gene interactions among the identified hub targets were analyzed using the GeneMANIA platform (accessed on January 20, 2026), which integrates extensive functional association datasets to identify genes functionally related to a given set of input genes. These associations include physical interactions, pathways, co-expression, co-localization, and protein domain similarity. The analysis was performed for the target organism *Homo sapiens*, and network weighting was applied using GeneMANIA's automatic weighting option (Warde-Farley et al. 2010).

Gene ontology enrichment and molecular pathway analysis of hub targets

The biological mechanisms underlying PFNA-induced hepatotoxicity associated with the identified hub targets were explored through Gene Ontology (GO) enrichment and Kyoto Encyclopedia of Genes and Genomes (KEGG) pathway analyses. These analyses were conducted using the DAVID Knowledgebase v2025_1 (accessed on January 22, 2026), a widely used bioinformatics platform that provides comprehensive functional annotation of gene lists, including biological processes (BP), cellular components (CC), and molecular functions (MF). DAVID clusters large gene lists into functionally related categories and ranks them according to statistical significance, thereby facilitating the identification of key biological processes and pathways associated with the input genes (Sherman et al. 2022).

In this study, the list of hub target genes was uploaded using the "Step 1: Enter Gene List" option. Subsequently, "OFFICIAL_GENE_SYMBOL" and Homo sapiens were selected under "Step 2: Select Identifier" and "Step 2a: Select Species," respectively. The "Gene List" option was chosen under "Step 3: List Type," and the analysis was submitted in Step 4. The default background gene set provided by DAVID, which consists of genome-wide genes for the selected species, was applied. This background is considered appropriate for analyses with a genome-wide or near genome-wide scope.

Additionally, KEGG pathway enrichment analysis was performed within the DAVID platform to identify significantly enriched molecular pathways related to PFNA-induced hepatotoxicity. Pathways and GO terms with an FDR<0.05 were considered statistically significant. The top 10 enriched terms from both GO and KEGG analyses were visualized using SRplot (Tang et al. 2023).

Molecular docking

Molecular docking analyses were conducted using AutoDock 4.2 (Morris et

al. 2009) to evaluate the binding affinity and interaction profiles between PFNA and its hub target proteins. The chemical structure of PFNA was obtained from PubChem (Kim et al. 2025). The three-dimensional structures of experimentally resolved proteins were retrieved from the RCSB Protein Data Bank (www.rcsb.org).

Crystal co-ligands associated with PFNA were constructed using GaussView 5.0 and subsequently optimized by density functional theory (DFT) calculations with Gaussian 03, employing the B3LYP functional and the 6–31G basis set. Prior to docking, solvent molecules, water, and co-crystallized ligands were removed from the protein structures. Polar hydrogen atoms were added, and Gasteiger and Kollman charges were assigned. Protein Data Bank Identifier (PDB ID) and docking centers for the targets presented in Table 1.

Table 1: Docking coordinates and PDB IDs of target proteins.

Docking coordinates	PDB IDs	References
x:19.972, **y:**31.537, **z:**40.096; **Size**: 40x40x40	1Y57	Cowan-Jacob et al., 2005
x:32.172, **y:**0.056, **z:**27.452; **Size**: 40x40x40	1SJ0	Kim et al., 2004
x:19.093, **y:**35.495, **z:**38.547; **Size**: 40x40x40	1XKK	Wood et al., 2004
x:14.393, **y:**8.684, **z:**5.622; **Size**: 70x70x70	1OWW	Gao et al., 2003
x: -13.614, **y:**13.444, **z:**40.096; **Size**: 40x40x40	2OJG	Aronov et al., 2007
x:14.10, **y:**13.04, **z:**1.51; **Size:** 40x40x40	3IOK	Ledeboer et al., 2009

Docking calculations were carried out using the Lamarckian genetic algorithm with 10 independent runs and a population size of 300. The docking protocol was validated by re-docking the native ligand and comparing the resulting pose with the corresponding crystal structure. The conformation exhibiting the highest binding affinity was selected, and binding energies were recorded. Protein-ligand interactions were visualized and analyzed in both two-dimensional and three-dimensional formats using Discovery Studio Client 4.1.

Validation of hub targets by differential gene expression analysis

Following DEG analysis of GSE145239, PFNA-induced DEGs were identified based on $|\log_2(FC)| > 1$ and an adjusted p-value < 0.05. Downregulated and upregulated hub target genes were visualized using volcano plots generated with GraphPad Prism software (version 8 for Windows; GraphPad Software, San Diego, CA, USA).

RESULTS AND DISCUSSION

PFNA and other long-chain PFCAs, members of the PFAS family, have been listed as persistent organic pollutant due to persistence, bioaccumulation, longe-range transport, and harmful effects on both the environment and humans (US EPA, 2024;

UNEP, 2025). *In vitro*, *in vivo*, and epidemiological evidence indicates that one of the most prominent toxic effects of PFNA is hepatotoxicity (Zhang et al. 2018; Louisse et al. 2020; Costello et al. 2022; UNEP, 2023a; US EPA, 2024). However, the mechanism underlying PFNA-induced hepatotoxicity remains unclear.

In the present study, the mechanism of PFNA-induced hepatotoxicity in humans was investigated using network toxicology, bioinformatics, and molecular modeling (Fig. 1).

Qualitative hepatotoxicity predictions of PFNA

Table 2 summarizes the qualitative *in silico* predictions of hepatotoxicity for PFNA. Deep-PK predicted PFNA to be hepatotoxic with high confidence, and its molecular weight was within the training range. DeepToxLab predicted that PFNA induces drug-induced liver injury (DILI) and human hepatotoxicity with a probability of 97.7%, as well as hepatobiliary disorders with a probability of 100%, all with high confidence. Collectively, these qualitative *in silico* predictions indicate that PFNA exhibits hepatotoxic potential in humans.

Table 2: Qualitative *in silico* prediction of PFNA-induced hepatotoxicity using Deep-PK and DeepToxLab.

PFNA					
Deep-PK			**DeepToxLab**		
Category	Predicted value	Predictive Confidence	Category	Probability (%)	Confidence
Liver Injury I (DILI)	Toxic	0.833	DILI	97.7	High
Liver Injury II	Toxic	0.754	Human hepatotoxicity	97.7	High
			Hepatobiliary disorders	100	High

Acquisition of targets associated with PFNA-induced hepatotoxicity and PPI analysis

In this study, a total of 2269 PFNA targets were obtained from the CTD, PubChem, ChEMBL, SwissTargetPrediction, and PharmMapper. In addition, 610 DEGs associated with PFNA exposure in human liver 3D spheroids were identified from the GSE145239 dataset using the GEO2R analysis tool. Subsequently, the intersection of these two target sets yielded 210 final PFNA-related targets (Fig. 2A). Furthermore, 1688 human hepatotoxicity-related targets were retrieved from the CTD, DisGeNET, GeneCards, and OMIM databases. Using an integrative Venn diagram approach, 107 overlapping targets were identified as potentially relevant to PFNA-induced human hepatotoxicity (Fig. 2B). These potential targets are listed alphabetically in Table S1.

PPI analysis of the 107 potential targets was conducted using the STRING database with a confidence score threshold of 0.9, and the FDR was set at 5% (medium stringency).

This analysis generated an interconnected network comprising 107 nodes and 109 edges, with an average node degree of 2.04 and a PPI enrichment *p*-value of < $1.0x10^{-16}$. Proteins lacking interactions were excluded from the network visualization. In this network, nodes represent proteins, whereas edges denote interactions (Fig. 2C).

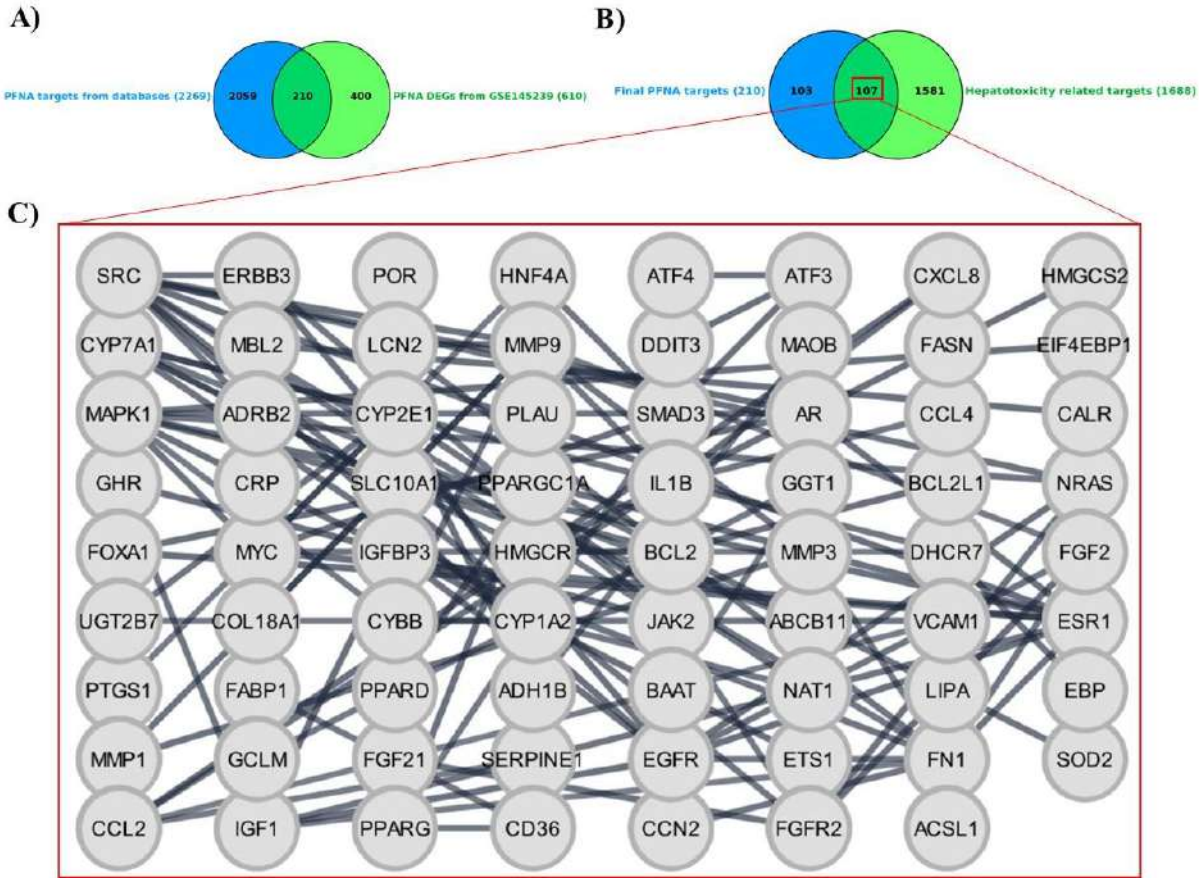

Figure 2: A) Venn diagram of targets and DEGs associated with PFNA. The blue circle represents 2269 PFNA-associated targets obtained from databases, while the green circle represents 610 PFNA-related DEGs obtained from GSE145239 dataset. The overlapping region identifies 210 final PFNA targets. **B)** Venn diagram of final PFNA targets and hepatotoxicity-related targets. The blue circle represents 210 final PFNA-associated targets, while the green circle represents 1688 human hepatotoxicity-related targets. The overlapping region identifies 107 potential targets involved in PFNA-induced hepatotoxicity in humans. **C)** PPI network of the 107 potential targets.

Centrality analysis and identification of hub targets

The PPI network constructed from the 107 potential targets (Fig. 2C) was examined using multiple complementary algorithms to identify highly connected hub candidates. These approaches included the MCODE algorithm implemented in Metascape (Fig. 3A) as well as the MCC (Fig. 3B), MNC (Fig. 3C), and Degree (Fig. 3D) algorithms available in the cytoHubba plugin of Cytoscape. In Metascape, MCODE was employed to detect densely interconnected clusters (modules) within the network, with each cluster represent a separate functional module. In cytoHubba (MCC, MNC, and Degree algorithms), node color intensity

reflected the calculated connectivity, with darker colors indicating higher degree values. Detailed score values of the targets obtained from all algorithms are provided in Table S2.

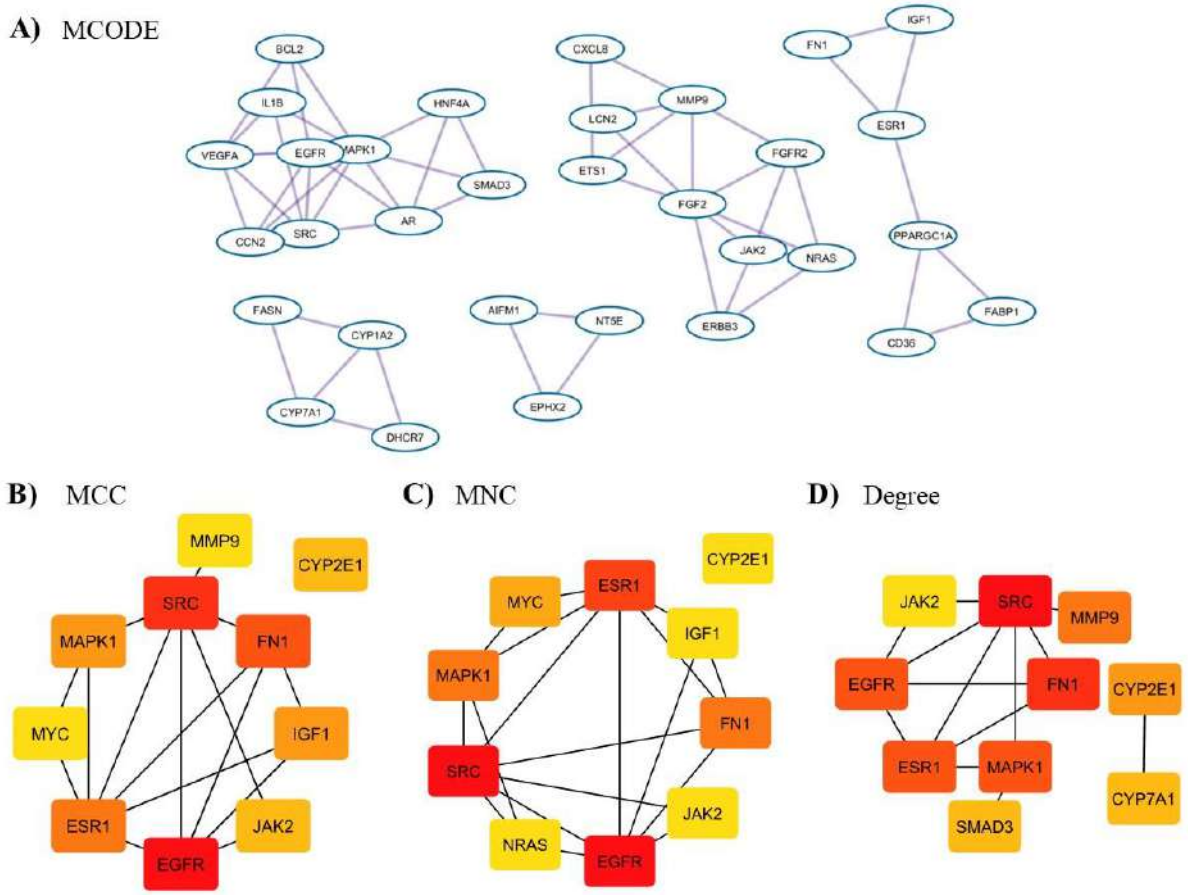

Figure 3: Identification of hub targets using Metascape and the cytoHubba plugin in Cytoscape. **A)** Hub target candidates identified using the MCODE algorithm via Metascape. **B–D)** Hub target candidates identified using the MCC, MNC, and Degree algorithms, respectively. Node color intensity corresponds to the calculated degree, with more intensely colored nodes indicating higher degree values.

Targets consistently identified by all four algorithms (MCODE, MCC, MNC, and Degree) as hubs were selected to reduce algorithm-specific bias and improve robustness, resulting in a subset of six targets closely associated with PFNA-induced hepatotoxicity in humans (Fig. 4A). A corresponding PPI network (Fig. 4B) and the degree distribution of these six targets (Fig. 4C) were subsequently constructed.

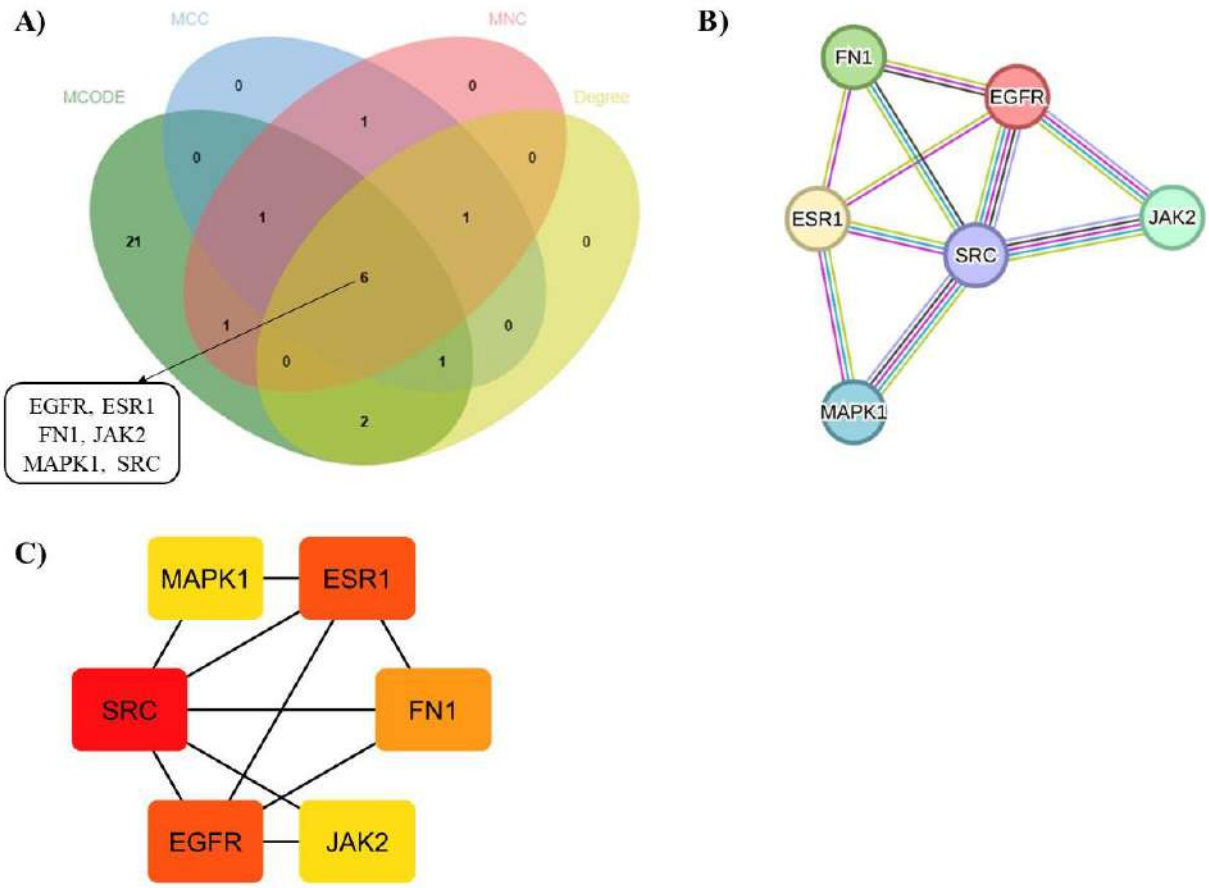

Figure 4: A) Hub targets identified by all four algorithms. **B)** PPI network of the six hub targets constructed using STRING with highest confidence (0.9). **C)** Degree analysis of the six hub targets performed using Cytoscape.

Network analysis of these six hub targets, along with other centrality parameters, is presented in Table 3. Degree indicates the number of direct interactions of a node. Closeness centrality reflects how close a node is to all other nodes in the network. Betweenness centrality represents the extent to which a node lies on the shortest paths between other nodes. The topological coefficient measures the tendency of a node to share interaction partners with other nodes.

Table 3: Degree analysis of six hub targets using Cytoscape.

Hub targets	Degree	Closeness Centrality	Betweenness Centrality	Topological Coefficient
SRC	5	1.00	0.30	0.60
EGFR	4	0.83	0.10	0.70
ESR1	4	0.83	0.10	0.70
FN1	3	0.71	0.00	0.86
MAPK1	2	0.62	0.00	0.90
JAK2	2	0.62	0.00	0.90

Gene-gene interaction network analysis of six hub targets

Following the identification of the six hub targets (Fig. 4, Table 3), their gene-gene interactions were analyzed using

GeneMANIA. The official gene symbols were entered into the GeneMANIA online plugin to construct a comprehensive interaction network. The nodes in the outer ring represent genes associated with the six hub targets located in the inner ring.

The analysis indicated that physical interactions among the hub targets (59.78%) constituted the predominant interaction type among these six genes (Fig. 5A). This finding suggests that these genes may participate in closely coordinated biological processes requiring direct contact. Functional enrichment analysis of the gene-gene interaction network revealed that the six hub targets were primarily associated with "peptidyl-tyrosine phosphorylation". (Fig. 5B) particularly *SRC*, *EGFR*, and *JAK2* (Table S3). Detailed results of the gene-gene interaction network analysis are provided in Table S3.

Peptidyl-tyrosine phosphorylation refers to the addition of a phosphate group to tyrosine residues by protein tyrosine kinases and represents a fundamental regulatory mechanism in cellular signaling (Hunter, 2009). The enrichment of this process, together with the identification of receptor (*EGFR*) and non-receptor (*SRC*, *JAK2*) tyrosine kinases as hub nodes, suggests that PFNA-induced hepatotoxicity may involve dysregulation of tyrosine kinase-mediated signaling cascades.

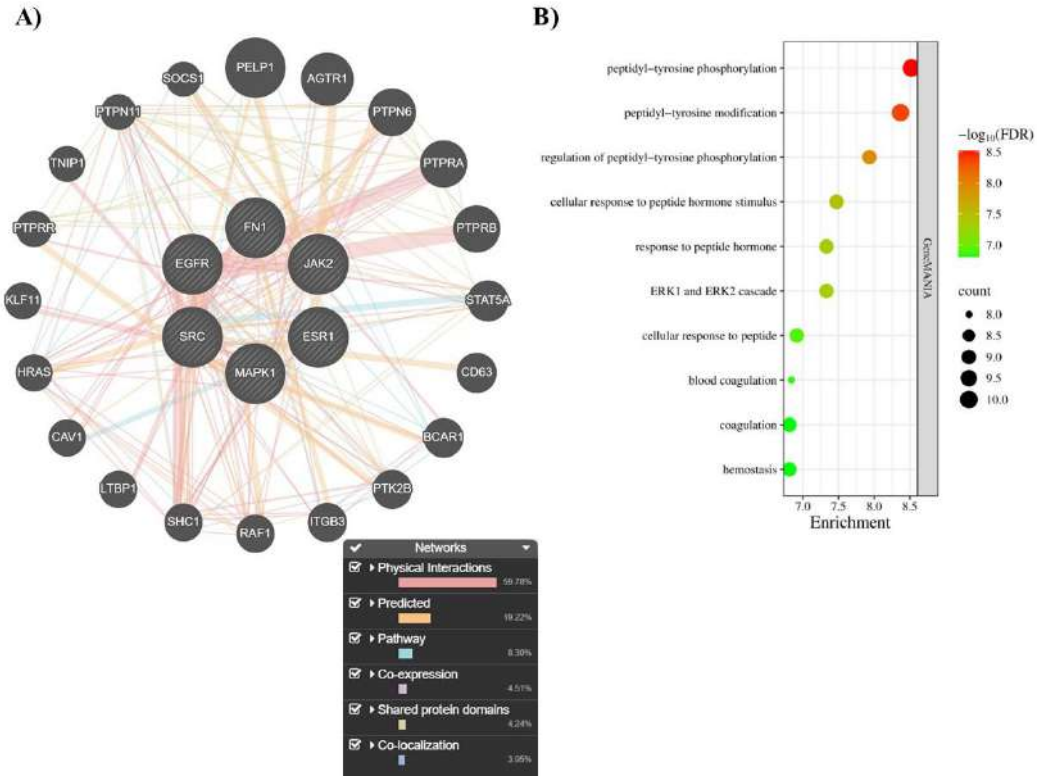

Figure 5: Gene-gene interactions analysis of six hub targets. **A)** The gene-gene interaction network of six hub targets. **B)** Bubble plot showing the top 10 functions associated with the six hub targets. Each bubble represents a function, with its size proportional to the number of enriched targets, while color intensity indicates the significance of enrichment.

GO and pathway analysis of the hub targets

GO enrichment analysis of six hub targets was performed using the DAVID database. The results revealed significant GO terms, defined as those with an FDR<0.05 in DAVID, including 3 biological processes (BPs), 4 cellular components (CCs), and 10 molecular functions (MFs). Prioritization of these GO terms was based on FDR and gene counts, with the most enriched terms visually represented in the enrichment analysis diagrams (Fig. 6). Detailed results of the GO enrichment analysis are provided in Table S4.

GO enrichment analysis provided further mechanistic insights. In the BP category, the hub targets were enriched in "positive regulation of phosphatidylinositol 3-kinase/protein kinase B signal transduction," which is synonymous with positive regulation of the PI3K/Akt signaling pathway (Fig. 6, Table S4). The PI3K/Akt pathway plays a central role in cell survival, proliferation, metabolism, and apoptosis regulation, and its dysregulation has been strongly associated with liver pathology, including hepatocellular carcinoma (Lawrence et al., 2014). Modulation of receptor tyrosine kinases such as EGFR may stimulate PI3K/Akt signaling (He et al., 2021). Therefore, the enrichment of SRC, EGFR, and JAK2 within both tyrosine phosphorylation processes and PI3K/Akt-related signaling suggests a mechanistic axis through which PFNA may modulate hepatocellular survival and stress responses. In CC category, the hub targets were enriched in "focal adhesion," a multiprotein complex that anchors cells to the extracellular matrix and integrates mechanical and biochemical signaling. Disruption of focal adhesion signaling can impair cytoskeletal organization, cell adhesion, and tissue architecture processes that are critical for liver homeostasis. In the MF category, enrichment in "protein kinase activity" further highlights the central role of phosphorylation-dependent signaling in PFNA-associated hepatotoxicity. SRC, EGFR, MAPK1, and JAK2 are well-known mediators of kinase-driven signaling cascades, and aberrant kinase signaling is closely linked to inflammatory responses, fibrosis, and tumorigenesis (Bromann et al., 2004). Collectively, these findings suggest that PFNA may disturb hepatic signaling networks by modulating kinase-associated pathways, particularly those converging on PI3K/Akt and related downstream effectors (Wang and Cole, 2014).

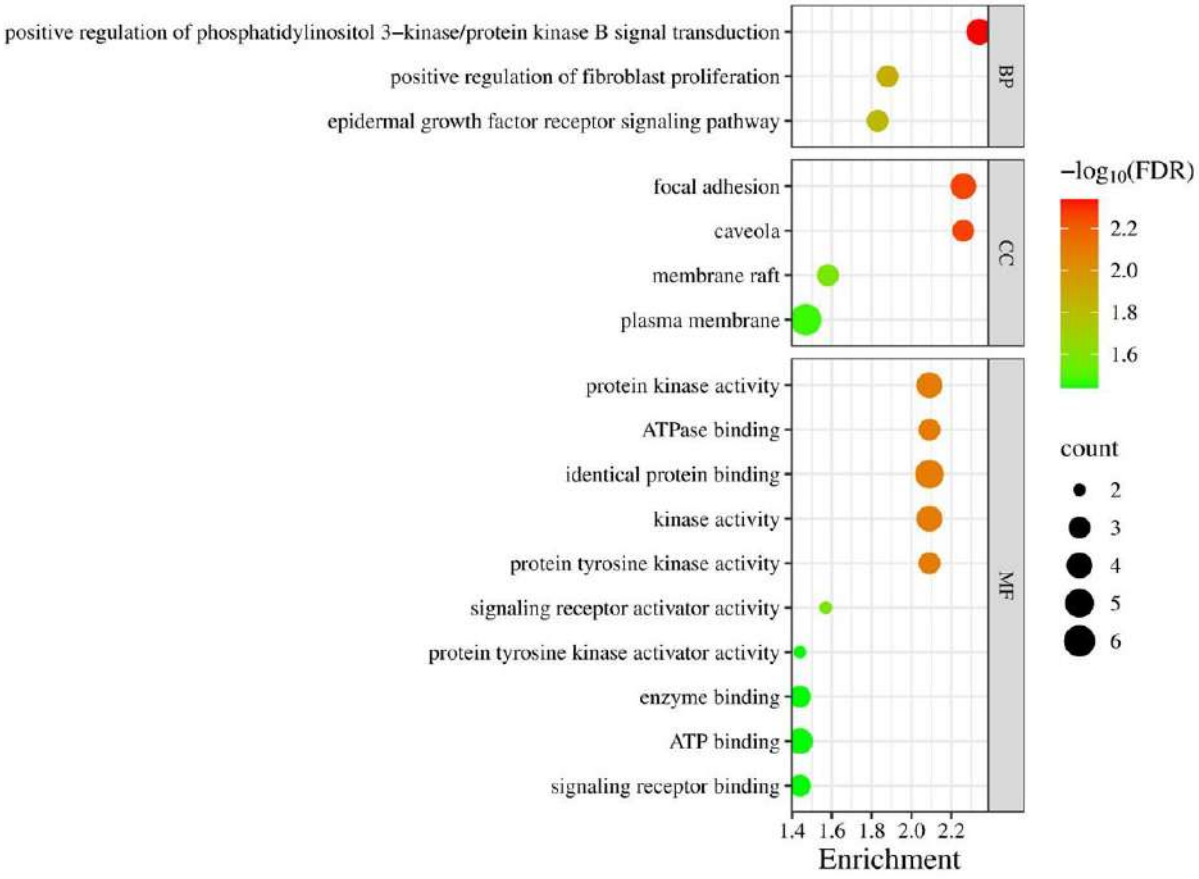

Figure 6: GO term enrichment analysis of the six hub targets. Bubble size represents the gene count for each term, while color intensity corresponds to FDR values, with smaller values indicating greater enrichment significance.

To further investigate the biological relevance of these targets, the six hub genes were subjected to comprehensive pathway enrichment analysis using the DAVID database. This analysis revealed 33 significantly enriched KEGG pathways (FDR<0.05). Detailed pathway terms are provided in Table S5.

KEGG pathway enrichment analysis demonstrated significant involvement of the hub targets in "Proteoglycans in cancer," mainly driven by SRC, EGFR, ESR1, FN1, and MAPK1 (Fig. 7, Table S5).

Proteoglycans are glycoproteins containing covalently attached glycosaminoglycan chains and are major components of the extracellular matrix. In the liver, proteoglycans regulate cell adhesion, growth factor signaling, and tissue remodeling. Alterations in proteoglycan composition or signaling can contribute to chronic liver injury, fibrosis, and carcinogenesis. (Baghy et al., 2016; Theocharis and Karamanos, 2019). Therefore, enrichment of this pathway suggests that PFNA exposure may influence extracellular matrix organization.

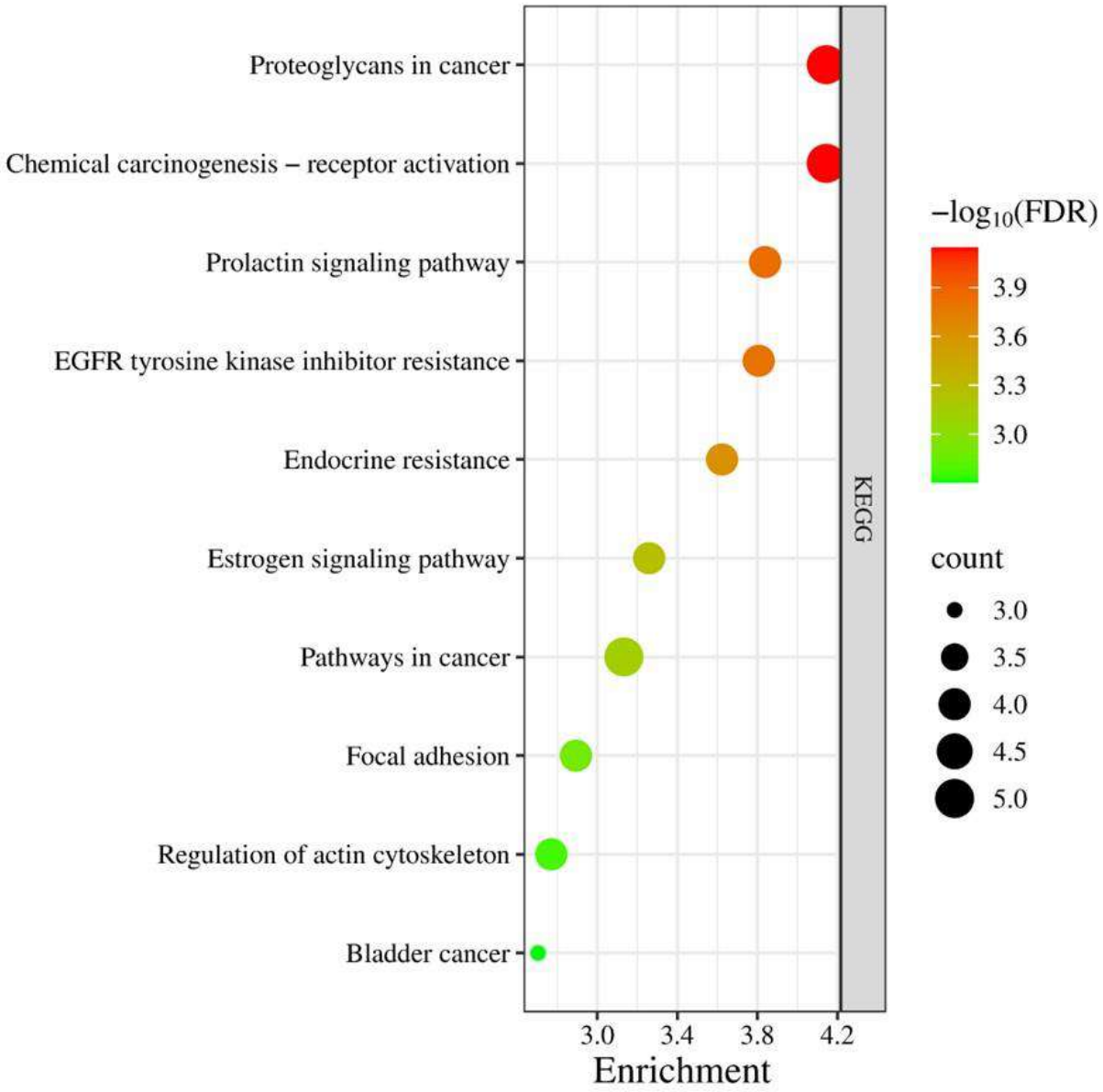

Figure 7: KEGG pathway enrichment analysis of the six hub targets. Bubble size represents the gene count for each pathway, while color intensity corresponds to FDR values, with smaller values indicating greater enrichment significance.

Molecular docking of PFNA against hub targets

A molecular docking analysis was performed to evaluate the binding affinity of PFNA toward six hub targets, including *SRC*, *EGFR*, *ESR1*, *FN1*, *MAPK1*, and *JAK2*. The binding poses and interactions of PFNA with these targets were analyzed using AutoDock 4.2, and the corresponding binding energy values were calculated for each complex. Furthermore, a root mean square deviation (RMSD) value of less than 1.0 Å is generally considered excellent, reflecting high docking accuracy. PFNA exhibited weak binding affinity toward all hub targets, as indicated by its binding energy values (Table 4).

Table 4: Binding energies of PFNA against six hub target proteins.

Targets	Protein name	PDB IDs	PFNA	
			Binding energy (kcal/mol)	RMSD (Å)
SRC	Proto-oncogene tyrosine-protein kinase Src	1Y57	-1.06	0.22
EGFR	Epidermal growth factor receptor	1XKK	-2.56	0.53
ESR1	Estrogen receptor alpha	1SJ0	-2.39	0.22
FN1	Fibronectin	1OWW	-2.21	0.65
MAPK1	Mitogen-activated protein kinase 1	2OJG	-2.87	0.65
JAK2	Tyrosine-protein kinase JAK2	3IOK	-1.97	0.53

Volcano plot highlighting hub targets among PFNA-induced DEGs

In this study, a total of 252 downregulated and 358 upregulated DEGs were identified in PFNA-induced human 3D liver spheroids from the GSE145239 dataset using the GEO2R analysis tool, based on the thresholds of $|\log2\ (FC)| > 1$ and an adjusted p-value < 0.05. Among the six hub targets, *SRC*, *EGFR*, and *JAK2* were significantly downregulated, whereas *ESR1*, *FN1*, and *MAPK1* were upregulated. The volcano plot generated using GraphPad Prism is presented in Figure 8.

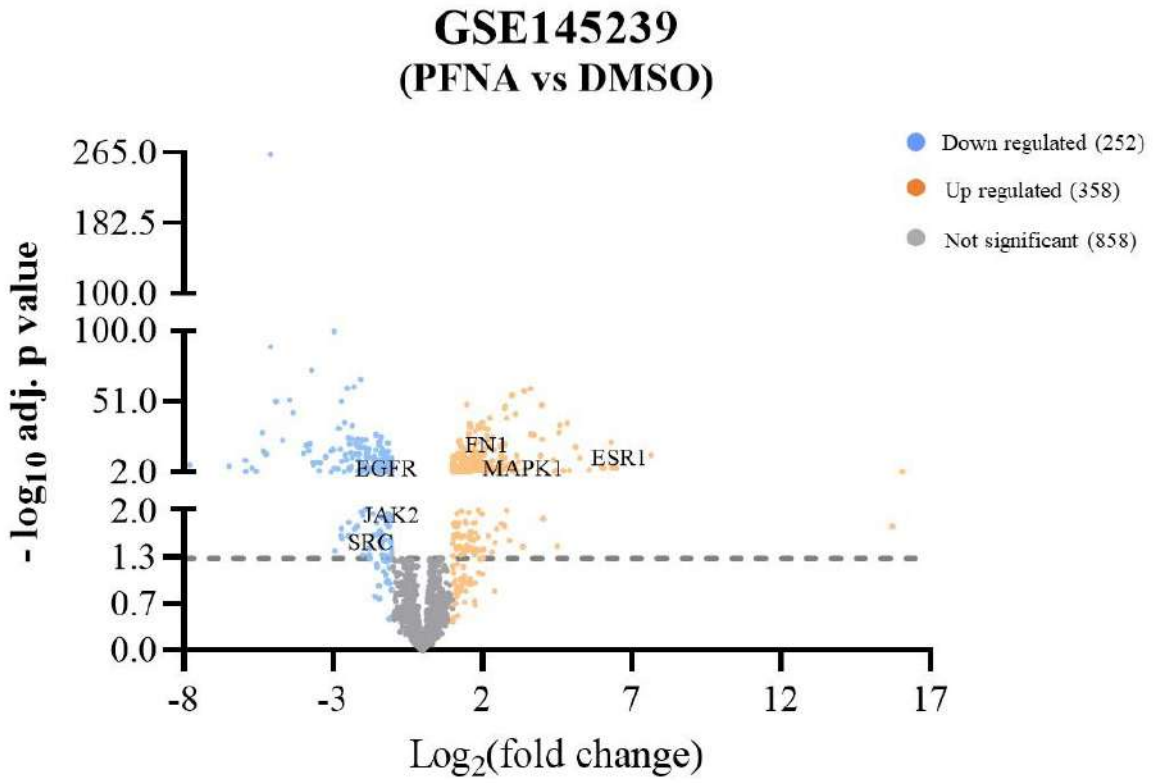

Figure 8: Volcano plot of DEGs and visualization of six hub genes in GSE145239 dataset.

The discrepancy between weak docking affinities and significant transcriptional alterations suggests that PFNA may not act primarily as a direct high-affinity ligand for

these proteins. Instead, PFNA may exert indirect regulatory effects at the transcriptional or upstream signaling level, leading to secondary modulation of hub gene expression.

This study integrated computational toxicology approaches with DEG analysis from transcriptomic data from GSE145239 to predict hepatotoxic mechanisms and identify potential molecular targets. Nevertheless, several limitations should be acknowledged. First, target prediction platforms such as CTD, SwissTargetPrediction, and PubChem rely on existing datasets, which may be incomplete and prone to false-positive associations. Second, the weak docking affinities and transcriptional changes do not fully converge at the protein-interaction level, underscoring the need for experimental validation. Future studies should therefore include *in vitro* and *in vivo* validation experiments, particularly evaluating PFNA-induced alterations in kinase signaling, PI3K/Akt activation status, and proteoglycan-related pathways in human hepatocytes at both gene and protein expression levels.

CONCLUSION

This study employed integrated *in silico* and bioinformatics approaches to investigate the potential hepatotoxic effects of PFNA and its underlying molecular mechanisms in humans. The findings suggest that PFNA exhibits hepatotoxic potential. Network-based analyses identified six key hub targets associated with PFNA-induced liver toxicity. Functional enrichment analyses indicate that PFNA may contribute to hepatotoxicity primarily through modulation of tyrosine kinase-mediated signaling, alterations in the PI3K/Akt pathway, and dysregulation of proteoglycan-related pathways involved in extracellular matrix remodeling and cellular signaling. Overall, these results provide mechanistic insights into PFNA-induced hepatotoxicity and may guide future experimental validation studies.

ACKNOWLEDGMENTS

The authors declare no conflict of interest.

REFERENCES

Amberger JS, Bocchini CA, Scott AF, Hamosh A. (2019). OMIM.org: leveraging knowledge across phenotype-gene relationships. *Nucleic Acids Res* **47**(D1):D1038-D1043.

Aronov AM, Baker C, Bemis GW, Jingrong C, Guanjing C, et al. (2007). Flipped out: structure-guided design of selective pyrazolylpyrrole ERK inhibitors. *J Med Chem* **50**(6):1280-1287.

ATSDR (Agency for Toxic Substances and Disease Registry, US) (2021). Toxicological Profile for Perfluoroalkyls. U.S. Department of Health and Human Services, Public Health Service, Atlanta, GA. Available from: https://www.ncbi.nlm.nih.gov/books/NBK592143/

Baghy K, Tátrai P, Regős E, Kovalszky I. (2016). Proteoglycans in liver cancer. *World J Gastroenterol* **22**(1):379-393.

Bardou P, Mariette J, Escudié F, Djemiel C, Klopp C. (2014). jvenn: an interactive Venn diagram viewer. *BMC bioinformatics* **15**(1), 293.

Bjork JA, Wallace KB. (2009). Structure-activity relationships and human relevance for perfluoroalkyl acid-induced transcriptional activation of peroxisome proliferation in liver cell cultures. *Toxicol Sci* **111**(1):89-99.

Bromann PA, Korkaya H, Courtneidge SA. (2004). The interplay between Src family kinases and receptor tyrosine kinases. *Oncogene* **23**(48):7957-7968.

Clough E, Barrett T, Wilhite SE, Ledoux P, Evangelista C, et al. (2024). NCBI GEO: archive for gene expression and epigenomics data sets: 23-year update. *Nucleic Acids Res* **52**(D1):D138-D144.

Costello E, Rock S, Stratakis N, Eckel SP, Walker DI, et al. (2022). Exposure to per- and polyfluoroalkyl substances and markers of liver injury: a systematic review and meta-analysis. *Environ Health Perspect* **130**(4):46001.

Cowan-Jacob SW, Fendrich G, Manley PW, Jahnke W, Fabbro D, et al. (2005). The crystal structure of a c-Src complex in an active conformation suggests possible steps in c-Src activation. *Structure* **13**(6):861-871.

Daina A, Michielin O, Zoete V. (2019). SwissTargetPrediction: updated data and new features for efficient prediction of protein targets of small molecules. *Nucleic Acids Res* **47**(W1):W357-W364.

Davis AP, Wiegers TC, Sciaky D, Barkalow F, Strong M, et al. (2025). Comparative Toxicogenomics Database's 20th anniversary: update 2025. *Nucleic Acids Res* **53**(D1):D1328-D1334.

Gao M, Craig D, Lequin O, Campbell ID, Vogel V, et al. (2003). Structure and functional significance of mechanically unfolded fibronectin type III1 intermediates. *Proc Natl Acad Sci U S A* **100**(25):14784-14789.

Golden-Mason L, Salomon MP, Matsuba C, Wang Y, Setiawan VW, et al. (2025). Assessing the impact of perfluoroalkyl substances on liver health: a comprehensive study using multi-donor human liver spheroids. *Environ Int* **203**:109763.

He Y, Sun MM, Zhang GG, Yang J, Chen KS, et al. (2021). Targeting PI3K/Akt signal transduction for cancer therapy. *Signal Transduct Target Ther* **6**(1):425.

Heid E, Greenman KP, Chung Y, Li SC, et al. (2024). Chemprop: A Machine Learning Package for Chemical Property Prediction. *J Chem Inf Model* **64**(1):9-17.

Hunter T. (2009). Tyrosine phosphorylation: thirty years and counting. *Curr Opin Cell Biol* **21**(2):140-146.

Karakuş F, Kuzu B. (2024). Predicting the molecular mechanisms of cardiovascular toxicity induced by per- and polyfluoroalkyl substances: an in silico network toxicology perspective. *Toxicol Res* **13**(6):tfae206.

Kersten S, Stienstra R. (2017). The role and regulation of the peroxisome proliferator activated receptor alpha in human liver. *Biochimie* **136**:75-84.

Kim S, Chen J, Cheng T, Gindulyte A, He J, et al. (2025). PubChem 2025 update. *Nucleic Acids Res* **53**(D1):D1516-D1525.

Kim S, Wu JY, Birzin ET, Frisch K, Chan W, et al. (2004). Estrogen receptor ligands. II. Discovery of benzoxathiins as potent, selective estrogen receptor alpha modulators. *J Med Chem* **47**(9):2171-2175.

Lawrence MS, Stojanov P, Mermel CH, Robinson JT, Garraway LA, et al. (2014). Discovery and saturation analysis of cancer genes across 21 tumour types. *Nature* **505**(7484):495-501.

Ledeboer MW, Pierce AC, Duffy JP, Gao H, Messersmith D, et al. (2009). 2-Aminopyrazolo[1,5-a]pyrimidines as potent and selective inhibitors of JAK2. *Bioorg Med Chem Lett* **19**(23):6529-6533.

Lohmann R, Cousins IT, DeWitt JC, Glüge J, Goldenman G, et al. (2020). Are fluoropolymers really of low concern for human and environmental health and separate from other PFAS? *Environ Sci Technol* **54**(20):12820-12828.

Louisse J, Rijkers D, Stoopen G, Janssen A, Staats M, et al. (2020). Perfluorooctanoic acid (PFOA), perfluorooctane sulfonic acid (PFOS), and perfluorononanoic acid (PFNA) increase triglyceride levels and decrease cholesterogenic gene expression in human HepaRG liver cells. *Arch Toxicol* **94**(9):3137-3155.

Morris GM, Huey R, Lindstrom W, Sanner MF, Belew RK, (2009). AutoDock4 and AutoDockTools4: automated docking with selective receptor flexibility. *J Comput Chem* **30**(16):2785-2791.

Myung Y, de Sá AGC, Ascher DB. (2024). Deep-PK: deep learning for small molecule pharmacokinetic and toxicity prediction. *Nucleic Acids Res* **52**(W1):W469-W475.

Piñero J, Ramírez-Anguita JM, Saüch-Pitarch J, Ronzano F, Centeno E, et al. (2020). The DisGeNET knowledge platform for disease genomics: 2019 update. *Nucleic Acids Res* **48**(D1):D845-D855.

Reardon AJF, Rowan-Carroll A, Ferguson SS, Leingartner K, Gagne R, et al. (2021). Potency ranking of per- and polyfluoroalkyl substances using high-throughput transcriptomic analysis of human liver spheroids. *Toxicol Sci* **184**(1):154-169.

Ruggiero MJ, Miller H, Idowu JY, Zitzow JD, Chang SC, et al. (2021). Perfluoroalkyl carboxylic acids interact with the human bile acid transporter NTCP. *Livers* **1**(4):221-229.

Sadrabadi F, Alarcan J, Sprenger H, Braeuning A, Buhrke T. (2024). Impact of perfluoroalkyl substances (PFAS) and PFAS mixtures on lipid metabolism in differentiated HepaRG cells as a model for human hepatocytes. *Arch Toxicol* **98**(2):507-524.
Shannon P, Markiel A, Ozier O, Baliga NS, Wang JT, et al. (2003). Cytoscape: a software environment for integrated models of biomolecular interaction networks. *Genome Res* **13**(11):2498-2504.

Sherman BT, Hao M, Qiu J, Jiao X, Baseler MW, et al. (2022). DAVID: a web server for functional enrichment analysis and functional annotation of gene lists (2021 update). *Nucleic Acids Res* **50**(W1):W216-W221.

Stelzer G, Rosen N, Plaschkes I, Zimmerman S, Twik M, et al. (2016). The GeneCards Suite: from gene data mining to disease genome sequence analyses. *Curr Protoc Bioinformatics* **54**:1.30.1-1.30.33.

Szklarczyk D, Kirsch R, Koutrouli M, Nastou K, Mehryary F, et al. (2023). The STRING database in 2023: protein-protein association networks and functional enrichment analyses for any sequenced genome of interest. *Nucleic Acids Res* **51**(D1):D638-D646.

Tang D, Chen M, Huang X, Zhang G, Zeng L, et al. (2023). SRplot: a free online platform for data visualization and graphing. *PLoS One* **18**(11):e0294236.

Thackray CP, Selin NE, Young CJ. (2020). A global atmospheric chemistry model for the fate and transport of PFCAs and their precursors. *Environ Sci Process Impacts* **22**(2):285-293.

Theocharis AD, Karamanos NK. (2019). Proteoglycans remodeling in cancer: underlying molecular mechanisms. *Matrix Biol* **75-76**:220-259.

UNEP/POPS/COP.12/32/Add.1 (2025) Decisions adopted by the Conference of the Parties to the Stockholm Convention on Persistent Organic Pollutants at its twelfth meeting. Available from: https://chm.pops.int/TheConvention/ConferenceoftheParties/Meetings/COP12/tabid/9744/Default.aspx [Accessed: 13 Oct. 2025]

UNEP/POPS/POPRC.17/7 (2021) Proposal to list long-chain perfluorocarboxylic acids, their salts and related compounds in Annexes A, B and/or C to the Stockholm Convention on Persistent Organic Pollutants. Available from: https://www.pops.int/TheConvention/POPsReviewCommittee/Meetings/POPRC17/Overview/tabid/8900/Default.aspx [Accessed: 14 Oct. 2025]

UNEP/POPS/POPRC.18/11/Add.4 (2023a) Risk profile for long-chain perfluorocarboxylic acids, their salts and related compounds. Available from: https://www.pops.int/TheConvention/POPsReviewCommittee/Meetings/POPRC18/Overview/tabid/9165/Default.aspx [Accessed: 21 Oct. 2025]

UNEP/POPS/POPRC.19/9/Add.2 (2023b) Risk management evaluation for long-chain perfluorocarboxylic acids, their salts and related compounds. Available from: https://www.pops.int/TheConvention/POPsReviewCommittee/Meetings/POPRC19/Overview/tabid/9548/Default.aspx [Accessed: 14 Oct. 2025]

UniProt Consortium (2025). UniProt: the Universal Protein Knowledgebase in 2025. Nucleic acids research, 53(D1), D609–D617.

US EPA (2024) IRIS Toxicological Review of Perfluorononanoic Acid (PFNA) and Related Salts. CASRN 375-95-1. https://assessments.epa.gov/risk/document/&deid%3D355409 [Accessed: 17 Dec. 2025]

Wang X, Shen Y, Wang S, Li S, Zhang W, et al. (2017). PharmMapper 2017 update: a web server for potential drug target identification with a comprehensive target pharmacophore database. *Nucleic Acids Res* **45**(W1):W356-W360.

Wang Z, Cole PA. (2014). Catalytic mechanisms and regulation of protein kinases. *Methods Enzymol* **548**:1-21.

Warde-Farley D, Donaldson SL, Comes O, Zuberi K, Badrawi R, et al. (2010). The GeneMANIA prediction server: biological network integration for gene prioritization and predicting gene function. *Nucleic Acids Res* **38**(Web Server issue):W214-W220.

Wood ER, Truesdale AT, McDonald OB, Yuan D, Hassell A, et al. (2004). A unique structure for epidermal growth factor receptor bound to GW572016 (Lapatinib): relationships among protein conformation, inhibitor off-rate, and receptor activity in tumor cells. *Cancer Res* **64**(18):6652-6659.

Zdrazil B, Felix E, Hunter F, Manners EJ, Blackshaw J, et al. (2024). The ChEMBL Database in 2023: a drug discovery platform spanning multiple bioactivity data types and time periods. *Nucleic Acids Res* **52**(D1):D1180-D1192.

Zhang Y, Zhang Y, Klaassen CD, Cheng X. (2018). Alteration of bile acid and cholesterol biosynthesis and transport by perfluorononanoic acid (PFNA) in mice. *Toxicol Sci* **162**(1):225-233.

Zhou Y, Zhou B, Pache L, Chang M, Khodabakhshi AH, et al. (2019). Metascape provides a biologist-oriented resource for the analysis of systems-level datasets. *Nat Commun* **10**(1):1523.

Research Article EMUJPharmSci ISSN 2651-3587 https://dergipark.org.tr/emujpharmsci

EMU Journal of Pharmaceutical Sciences

EMUJPharmSci 2026; **9**(1): 47-56.

DOI: **10.54994/emujpharmsci.1839816**

Microbiological Assessment of *Staphylococcus aureus* Nasal Colonization and Antibiotic Resistance Patterns According to Nasal Septal Deviation Types

Baris Ali Omer[1], Ekin Ceylanli[1], Dilara Kusi[1], Laden Tepretmez[1], Muharrem Iyican[1], Kadir Cakiral[1,2], Mumtaz Guran[1], Didem Rifki[1,3]

[1]Eastern Mediterranean University, Faculty of Medicine, Famagusta, North Cyprus via Mersin 10, Türkiye.
[2]Eastern Mediterranean University, Faculty of Arts and Sciences, Department of Chemistry, Famagusta, North Cyprus via Mersin 10, Türkiye
[3]Famagusta State Hospital, Department of Head and Neck Surgery, North Cyprus via Mersin 10, Türkiye

Abstract

Nasal septal deviation (NSD) may facilitate bacterial colonization by impairing airflow. The relationship between specific anatomical types (Mladina classification) and *Staphylococcus aureus* colonization, including methicillin-resistant (MRSA) strains remains unclear. This study aims to evaluate the prevalence and antibiotic susceptibility profiles of *Staphylococcus aureus*, within the altered microenvironments created by different Mladina-classified nasal septal deviations (NSD). We further sought to determine if specific clinical comorbidities and environmental exposures serve as independent catalysts for staphylococcal niche colonization.A multicenter prospective observational study was conducted (November 2023–June 2024) in Northern Cyprus. 105 patients with NSD underwent endoscopic examination and were classified using Mladina's system. Nasal swabs were cultured, and antibiotic susceptibility was determined via EUCAST guidelines.MRSA colonization was detected in 21.0% of patients. Although colonization rates varied across Mladina types (7.7%–29.4%), no statistically significant association was found ($p>0.05$). Chronic sinusitis, allergic rhinitis, and smoking showed numerically higher MRSA rates but lacked statistical significance.Mladina's NSD classification does not independently predict MRSA colonization risk. Preoperative screening protocols should incorporate comprehensive risk assessments beyond anatomical classification alone.

Keywords

Mladina classification, MRSA, MSSA, nasal colonization, nasal septal deviation, *Staphylococcus aureus*.

Article History

Submitted: 16 February 2026 **Accepted:** 10 April 2026 **Published Online**: May 2026
Reviewer
Invitation Date: 25 February 2026 **Acceptance Date**: 25 February 2026 **Due Date**: 12 March 2026
Article Info

***Corresponding author:** Kadir Çakıral **email:** kadir.cakiral@emu.edu.tr

Research Article:
Volume: 9 **Issue: 1** **Pages: 47-56**
DOI: 10.54994/emujpharmsci.1839816

INTRODUCTION

Nasal septal deviation (NSD) is one of the most common anatomical anomalies encountered in otorhinolaryngology practice, characterized by displacement of the nasal septum to one side, which often leads to impaired nasal airflow and compromised mucociliary clearance. The disruption of these physiological processes can create an environment conducive to bacterial colonization, contributing to increased susceptibility to nasal infections and inflammatory conditions (Teixeira et al. 2016).

Staphylococcus aureus is a versatile, coagulase-positive pathogen characterized by an expansive arsenal of virulence factors, including surface-bound proteins that facilitate mucosal adhesion and secreted toxins that evade host immune surveillance. In the sinonasal tract, its transition from commensal to pathogen is often mediated by local environmental shifts. Methicillin-resistant *S. aureus* (MRSA) presents a heightened clinical challenge due to the acquisition of the mecA gene, which encodes an alternative penicillin-binding protein (PBP2a) with low affinity for beta-lactam antibiotics. While methicillin-susceptible *S. aureus* (MSSA) remains susceptible to these agents, its role in chronic inflammatory conditions like rhinosinusitis and its potential for biofilm formation within the anatomical crevices of a deviated septum cannot be overlooked (Bessesen et al. 2015; Hulterström et al. 2016). Colonization by *S. aureus*, including methicillin-resistant *S. aureus* (MRSA), is clinically significant due to its association with invasive infections, particularly in hospital settings or among immunocompromised individuals (Chen et al. 2010; Foster, 2017; Titouche et al. 2024).

Mladina classification of nasal septal deviation system categorizes nasal septal deviations based on anatomical characteristics, allowing precise identification of obstruction sites and facilitating targeted surgical interventions (Mladina et al. 2008). Despite its clinical utility, limited research has investigated the relationship between specific types of NSD, as defined by Mladina classification of nasal septal deviation, and bacterial colonization patterns, particularly involving MRSA and MSSA (Hricová et al. 2025).

Furthermore, the influence of lifestyle and environmental factors, such as smoking, occupational exposures, chronic sinusitis, and allergic rhinitis on nasal bacterial colonization remains inadequately defined, with existing studies yielding conflicting results (Manarey et al. 2004; McEachern et al. 2015). Therefore, this study aims to elucidate the relationship between different

anatomical deviations classified by Mladina's system and nasal colonization by *S. aureus*, including MRSA and MSSA, while assessing the potential impact of associated lifestyle and medical risk factors. Understanding these relationships could provide valuable insights for clinical management, potentially influencing preoperative screening protocols and postoperative care strategies.

MATERIALS AND METHODS

Study design and setting

This prospective observational study was conducted over an eight-month period from November 2023 to June 2024. The multicentric design involved collaboration between the Faculty of Medicine at Eastern Mediterranean University and three major healthcare providers in Northern Cyprus: Famagusta State Hospital, Kunter Güven Hospital (Famagusta), and Longbeach Medical Center (Iskele).

Participants

A total of 105 patients presenting with nasal obstruction due to nasal septal deviation (NSD) were enrolled utilizing a consecutive sampling strategy. This specific sample size was not derived from a priori statistical power analysis; rather, it represents the total sequential number of eligible, consenting patients successfully accrued across the participating centers during the predefined eight-month study window. Inclusion criteria encompassed patients aged above 10 years diagnosed with NSD by an otorhinolaryngologist. Exclusion criteria included recent antibiotic use within the past week, ongoing nasal infections, or prior nasal surgeries.

Anatomical assessment protocol

All participants underwent a rigid nasal endoscopic examination or detailed anterior rhinoscopy performed by the attending ENT surgeon. Deviations were categorized according to the Mladina's classification system (Mladina et al. 2008):

- **Type 1:** Simple vertical deviation in the anterior (vestibular) area.
- **Type 2:** Vertical deviation involving the internal nasal valve (Mladina Area 2).
- **Type 3:** Vertical deviation located at the level of the middle turbinate (Mladina Area 3/4).
- **Type 4:** Complex S-shaped or bilateral deviation causing obstruction on both sides.
- **Type 5:** Horizontal spur at the base of the septum (maxillary crest).
- **Type 6:** Horizontal spur with a deep gutter on the contralateral side.
- **Type 7:** Mixed deviation involving multiple areas or combinations of the above.

This functional classification allows for the correlation of specific airflow obstruction patterns with microbiological outcomes.

Data collection

Data was collected using a structured questionnaire administered by the attending ENT surgeon. This questionnaire captured demographic details such as age and gender, as well as lifestyle factors including smoking status and exercise frequency. Additionally, comprehensive medical history information was gathered, encompassing medication use, workplace exposure, healthcare worker status, history of previous surgeries, chronic sinusitis, and allergic rhinitis. Anatomical assessment was performed and documented according to Mladina classification of nasal septal deviation to categorize nasal septal deviation types.

Microbiological analysis

Sample collection

Nasal swabs were collected from both anterior nares using sterile, distinct swabs for each nostril to maximize yield (Acker et al. 2025). The swab was inserted into the nasal vestibule and rotated 3 times against the mucosal surface to ensure adequate biomass collection.

Bacterial identification

Nasal swab samples were obtained from both nostrils of each participant using sterile swabs. Samples were directly inoculated onto Cefoxitin-supplemented and not supplemented Mannitol Salt Agar plates and incubated at 37°C for 72 hours. Mannitol-fermenting colonies with typical morphology were confirmed as *S. aureus* by coagulase test. Post incubation, plates were refrigerated. Later, samples were re-inoculated onto fresh plates to maintain bacterial viability.

Antibiotic susceptibility testing

For antibiotic susceptibility testing disk diffusion method was used. Colonies were suspended in sterile saline to achieve a turbidity equivalent to a 0.5 McFarland standard. The suspension was streaked onto Mueller-Hinton agar plates. Plates were incubated at 37°C for 24 hours. Zones of inhibition were measured in millimeters, and susceptibility was determined based on the European Committee on Antimicrobial Susceptibility Testing (EUCAST) guidelines (EUCAST, 2023).

Statistical analysis

Data were analyzed using Microsoft Excel 2021 and SPSS 22.0 (Statistical Package for the Social Sciences – IBM®). Descriptive statistics were computed for demographic and clinical variables. Associations between MRSA colonization and potential risk factors were assessed using chi-square tests for categorical variables. A p-value of <0.05 was considered statistically significant.

RESULTS

Demographic characteristics

Our cohort of 105 patients exhibited a balanced gender distribution (53.3% female), consistent with established epidemiological patterns for nasal septal deviation (NSD) (Amanian et al. 2024; Bruno et al. 2020; Moshfeghi et al. 2020). Participants ranged from 10 to 100 years old, with a mean age of 41.9 years. The concentration of patients in the 31–50 year age group suggests that individuals primarily seek medical intervention during middle adulthood, likely when symptoms begin to significantly interfere with daily or occupational activities (Amanian et al. 2024; Poorey & Gupta, 2014). Meanwhile, the inclusion of pediatric and geriatric cases highlights the chronic, lifelong nature of this anatomical condition (Kent et al. 1988; Moshfeghi et al. 2020).

Lifestyle and medical history characteristics

The cohort showed a high prevalence of smoking (43.8%) and sedentary lifestyle (76% without regular exercise) (Table 1), both of which are known to impair mucociliary clearance and immune function (Benninger et al. 2003), yet neither translated into a statistically significant increase in MRSA colonization, reinforcing the multifactorial nature of nasal carriage in NSD patients. (Mahmud et al., 2023) Regular medication use was uncommon (17.1%) and recent antibiotic exposure was minimal (1.9%), suggesting that the observed colonization patterns largely reflect intrinsic host and local factors rather than recent pharmacologic selection pressure (Gupta et al. 2013).

Table 1: Frequencies and percentages of risk factors.

	Yes	No
	Frequency (n, %)	**Frequency (n, %)**
Smoking	46, 43.8	59, 56.2
Medication use	18, 17.1	87, 82.9
Workplace Exposure	24, 22.9	81, 77.1
Previous Surgery	21, 20.0	84, 80.0
Previous Nasal Surgery	9, 8.6	96, 91.4
Chronic Sinusitis	38, 36.2	67, 63.8
Recent Antibiotic Use	2, 1.9	103, 98.1
Allergic Rhinitis (AR)	31, 29.5	74, 70.5

Chronic sinonasal conditions were frequent, with chronic sinusitis in 36.2% and allergic rhinitis in 29.5% of participants, and both groups exhibited numerically higher MRSA colonization rates (28.9% and 29.0%, respectively) compared with patients without these conditions, although these trends did not reach statistical significance in this sample (Amanian et al. 2024; Newman et al. 2023). Prior surgery (20.0%) and occupational exposure (22.9%) were

also common but did not show clear associations with colonization, indicating that no single lifestyle or medical history variable emerged as a dominant predictor and that more powered, multivariate studies are needed to clarify how inflammation, host immunity, and environmental factors jointly modulate *S. aureus* carriage in NSD (Abie et al. 2020). Furthermore, while occupational data, including generalized workplace exposure and healthcare worker status, were collected, cross-tabulation revealed no statistically significant variance in MRSA/MSSA positivity across these specific occupational cohorts.

Distribution of nasal septal deviation according to Mladina classification of nasal septal deviation

Nasal septal deviation types were heterogeneously distributed across all seven Mladina categories, with Type 2 being the most frequent (21.9%), followed by Types 3 and 7, while Type 4 was least common (7.6%) (Table 2). This pattern reflects a predominance of deviations affecting the internal nasal valve region and mid-septal area, consistent with the clinical relevance of these sites for airflow obstruction and symptom-driven presentation (Jain & Deshmukh, 2021).

Despite this anatomical diversity, MRSA colonization rates did not differ significantly between Mladina types, with positivity ranging from 7.7% in Type 6 to 29.4% in Type 7 without a statistically meaningful trend ($p>0.05$). These findings indicate that, within this NSD population, the specific Mladina-defined morphology does not appear to be a principal determinant of anterior nasal MRSA carriage, suggesting that factors beyond septal shape and obstruction patterns, such as mucosal inflammation, host immunity, and broader sinonasal architecture—are likely more influential (Mehraj et al. 2016).

Table 2: Types of nasal septal deviation of patients according to Mladina classification of nasal septal deviation.

Type	Frequency (n, %)
Type 1	12, 11.4
Type 2	23, 21.9
Type 3	18, 17.1
Type 4	8, 7.6
Type 5	14, 13.3
Type 6	13, 12.4
Type 7	17, 16.2

DISCUSSION

Microbiological outcomes

In this NSD cohort, MRSA was detected in 21.0% of nasal swab samples, a prevalence that is broadly comparable to reported colonization ranges in general and at-risk populations (e.g., 6–10 % in

community-dwelling adults, up to 25 % in some healthcare or diabetic cohorts) and therefore does not suggest a major excess burden attributable solely to septal deviation (Table 3) (Abbas et al. 2023). Most patients remained MRSA negative (79.0%), indicating that clinically significant deviation of the septum does not inevitably result in colonization despite theoretical concerns about impaired mucociliary clearance (Mehraj et al. 2016). MRSA positivity varied numerically across Mladina types (7.7% to 29.4%), but these differences were not statistically significant, supporting the interpretation that specific septal morphologies are not primary drivers of anterior nasal MRSA carriage in this setting (Shams et al. 2022). Taken together, these findings imply that MRSA colonization in patients with NSD is shaped more by host, microbial, and inflammatory factors than by the anatomical pattern of deviation alone, and that routine risk stratification should not rely exclusively on septal anatomy when considering screening or decolonization strategies (Vanderpool & Rumbaugh, 2023).

Table 3: MRSA Colonization across Mladina classification of nasal septal deviation.

Type	MRSA Positive (n,%)	MRSA Negative (n,%)
Type 1	3, 25.0	9, 75.0
Type 2	4, 17.4	19, 82.6
Type 3	4, 22.2	14, 77.8
Type 4	2, 25.0	6, 75.0
Type 5	3, 21.4	11, 78.6
Type 6	1, 7.7	12, 92.3
Type 7	5, 29.4	12, 70.6

Associations with risk factors

In this cohort, none of the evaluated lifestyle or clinical variables emerged as statistically significant independent risk factors for MRSA colonization, although several showed numerically higher rates (Jayathilaka et al. 2024; Shume et al. 2024). Smoking, for example, was common, but colonization was nearly identical in smokers and non-smokers, suggesting that its known detrimental effects on mucociliary clearance are insufficient on their own to drive carriage in NSD patients (Giri et al. 2021).

Chronic sinusitis and allergic rhinitis were associated with higher MRSA proportions (28.9% and 29.0%, respectively) than in patients without these conditions, but these differences did not reach conventional significance thresholds, likely reflecting limited sample size rather than absence of biological effect. Overall, the pattern supports a multifactorial model in which chronic mucosal inflammation, host immune status, and environmental exposures interact to modulate *S. aureus* colonization risk, underscoring the need for

larger, multivariate studies rather than reliance on single risk indicators.

Limitations

The interpretation of these findings must be contextualized within certain methodological constraints. The cohort size, while sufficient for preliminary observational analysis, lacks the statistical power requisite to detect subtle risk factor associations via multivariate modeling. Additionally, the cross-sectional nature of the microbiological sampling precludes the differentiation between persistent and transient colonization states.

CONCLUSION

In this study of patients with nasal septal deviation, Mladina's anatomical classification did not demonstrate a significant association with nasal MRSA or MSSA colonization. Although certain lifestyle and clinical variables such as chronic sinusitis, allergic rhinitis, and smoking showed numerically higher colonization rates, none emerged as independent predictors. These findings underscore that septal morphology alone is insufficient to estimate colonization risk and highlight the multifactorial nature of *S. aureus* carriage. Future studies with larger samples and multivariate modeling are warranted to clarify the interplay between anatomical deviation, mucosal inflammation, and host factors, and to guide more individualized preoperative screening strategies.

ACKNOWLEDGMENTS

This study conducted as part of the Introduction to Clinical Skills-3 research module within the International Joint Medicine Program at the Faculty of Medicine, Eastern Mediterranean University. The authors would like to thank all hospital personnel who may get involved in the current study. Also, the authors would like to express their gratitude to the trainers who contributed to this study through their feedback and lectures. The authors would like to acknowledge the use of ChatGPT (OpenAI) for assistance in manuscript language editing.

REFERENCES

Abbas MM, Almasri M, Abu-Zant A, Sharef S, Mahajne S, et al. (2023). Prevalence of anterior nares colonization of Palestinian diabetic patients with *Staphylococcus aureus* or methicillin-resistant *Staphylococcus aureus*. *QASCF* **15**(4): 32–41.

Abie S, Tiruneh M, Abebe W (2020). Methicillin-resistant Staphylococcus aureus nasal carriage among janitors working in hospital and non-hospital areas: a comparative cross-sectional study. *Ann Clin Microbiol Antimicrob* **19**(1): 47.

Acker W, Smothers L, Alsoubani M, Campion M, Andujar-Vazquez GM (2025). Evaluating the Appropriateness of MRSA Nasal PCR Screening for De-escalation of MRSA-directed Therapy. *Antimicrobial Stewardship and Healthcare Epidemiology* **5**(Suppl 2):66–7.

Amanian D, Yaghmaei S, Jalilpour M, Taziki MH, Soltaniesmaeili A (2024). Computed Tomography Analysis of the Nasal Septal Deviation and Related Paranasal Sinus Pathologies. *Frontiers in Biomedical Technologies* **11**(4): 622–630.

Bessesen MT, Kotter CV, Wagner BD, Adams JC, Kingery S, et al. (2015). MRSA colonization and the nasal microbiome in adults at high risk of colonization and infection. *Journal of Infection* **71**(6): 649–657.

Bruno G, Stefani A De, Benetazzo C, Cavallin,F, Gracco, A. (2020). Changes in nasal septum morphology after rapid maxillary expansion: a Cone-Beam Computed Tomography study in pre-pubertal patient. *Dental Press Journal of Orthodontics* **25**(5): 51–56.

Chen C, Chang H, Huang Y (2010). Nasal meticillin-resistant Staphylococcus aureus carriage among intensive care unit hospitalised adult patients in a Taiwanese medical centre: one time-point prevalence, molecular characteristics and risk factors for carriage. *Journal of Hospital Infection* **74**(3): 238–244.

EUCAST. (2023). European Committee on Antimicrobial Susceptibility Testing Breakpoint tables for interpretation of MICs and zone diameters European Committee on Antimicrobial Susceptibility Testing Breakpoint tables for interpretation of MICs and zone diameters. The European Committee on Antimicrobial Susceptibility Testing. Breakpoint Tables for Interpretation of MICs and Zone Diameters. Version 13.0, 2023.

Foster TJ (2017). Antibiotic resistance in Staphylococcus aureus. Current status and future prospects. *FEMS Microbiology Reviews* **41**(3): 430–449.

Giri N, Maharjan S, Thapa TB, Pokhrel S, Joshi G, et al. (2021). Nasal Carriage of Methicillin-Resistant Staphylococcus aureus among Healthcare Workers in a Tertiary Care Hospital, Kathmandu, Nepal. *International Journal of Microbiology* **2021**: 1–8.

Gupta K, Martinello RA, Young M, Strymish J, Cho K, et al. (2013). MRSA Nasal Carriage Patterns and the Subsequent Risk of Conversion between Patterns, Infection, and Death. *PLoS ONE* **8**(1): e53674.

Hricová K, Pudová V, Fišerová K, Htoutou Sedláková M, Karpíšková R, et al. (2025). [Molecular biological analysis of methicillin-resistant Staphylococcus aureus (MRSA) isolates of human and animal origin]. *Klinicka Mikrobiologie a Infekcni Lekarstvi* **31**(1): 5–10.

Hulterström AK, Sellin M, Monsen T, Widerström M, Gurram BK, et al. (2016). Bacterial flora and the epidemiology of staphylococcus aureus in the nose among patients with symptomatic nasal septal perforations. *Acta Oto-Laryngologica* **136**(6): 620–625.

Jain S, Deshmukh PT (2021). A Review on Deviated Nasal Septum: Classification, Clinical Features and Management. *Journal of Pharmaceutical Research International* 432–437.

Jayathilaka N, Piyumali M, Weerasinghe TG, Nakkawita D, Senaratne T (2024). Nasal Colonization of Methicillin-Resistant Staphylococcus aureus among Nurses at a Sri Lankan Hospital. *South Asian Journal of Research in Microbiology* **18**(9): 1–9.

Kent SE, Reid AP, Nairn ER, Brain DJ (1988). Neonatal Septal Deviations. *Journal of the Royal Society of Medicine* **81**(3): 132–135.

Mahmud A, Salisu AD, Kolo ES, Hasheem MG, Bello-Muhammad N, et al. (2023). Impact of smoking on nasal mucociliary clearance time in Kano metropolis, Nigeria. *World Journal of Otorhinolaryngology - Head and Neck Surgery* **9**(1): 53–58.

Manarey CRA, Anand VK, Huang C (2004). Incidence of Methicillin-Resistant Staphylococcus aureus Causing Chronic Rhinosinusitis. *The Laryngoscope* **114**(5): 939–941.

McEachern EK, Hwang JH, Sladewski KM, Nicatia S, Dewitz C, et al. (2015). Analysis of the Effects of Cigarette Smoke on Staphylococcal Virulence Phenotypes. *Infection and Immunity* **83**(6): 2443–2452.

Mehraj J, Witte W, Akmatov MK, Layer F, Werner G, et al. (2016). Epidemiology of Staphylococcus aureus Nasal Carriage Patterns in the Community. In *Current Topics in Microbiology and Immunology* (Vol. 398, pp. 55–87). Springer, Cham.

Mladina R, Čujić E, Šubarić M, Vuković K (2008). Nasal septal deformities in ear, nose, and throat patients. *American Journal of Otolaryngology* **29**(2): 75–82.

Moshfeghi M, Abedian B, Ghazizadeh Ahsaie M, Tajdini F (2020). Prevalence of nasal septum deviation using cone-beam computed tomography: A cross-sectional study. *Contemporary Clinical Dentistry* **11**(3): 223.

Newman NI, Mendonça DS, de Silva PG, de B Ribeiro EC, Costa FWG (2023). Prevalence of septation and symmetry of sphenoid sinus and nasal septal deviation in multislice computed tomography. *Brazilian Journal of Case Reports* **3**(Suppl.8): 11.

Poorey VK, Gupta N (2014). Endoscopic and Computed Tomographic Evaluation of Influence of Nasal Septal Deviation on Lateral Wall of Nose and Its Relation to Sinus Diseases. *Indian Journal of Otolaryngology and Head & Neck Surgery* **66**(3): 330–335.

Shams N, Razavi M, Zabihzadeh M, Shokuhifar M, Rakhshan V (2022). Associations between the severity of nasal septal deviation and nasopharynx volume in different ages and sexes: a cone-beam computed tomography study. *Maxillofacial Plastic and Reconstructive Surgery* **44**(1): 13.

Shume T, Urgesa K, Mekonnen S, Ayele F, Tesfa T, et al. (2024). Nasal carriage of MRSA among clinically affiliated undergraduate students at the College of Health and Medical Sciences, Haramaya University, Ethiopia. *Scientific Reports* **14**(1): 29977.

Teixeira J, Certal V, Chang ET, Camacho M (2016). Nasal Septal Deviations: A Systematic Review of Classification Systems. *Plastic Surgery International* **2016**(1): 7089123.

Titouche Y, Akkou M, Djaoui Y, Mechoub D, Fatihi A, et al. (2024). Nasal carriage of Staphylococcus aureus in healthy dairy cows in Algeria: antibiotic resistance, enterotoxin genes and biofilm formation. *BMC Veterinary Research* **20**(1): 247.

Vanderpool EJ, Rumbaugh KP (2023). Host-microbe interactions in chronic rhinosinusitis biofilms and models for investigation. *Biofilm* **6**: 100160.

Review EMUJPharmSci ISSN 2651-3587 https://dergipark.org.tr/emujpharmsci

EMU Journal of Pharmaceutical Sciences

EMUJPharmSci 2026; **9**(1):57-76.

DOI: **10.54994/emujpharmsci.1843372**

The Enduring Legacy of Medicinal and Aromatic Plants from Ancient Civilizations to Modern Era – A Brief Overview

Ilkay Erdogan Orhan[1,2,3], Fatma Sezer Senol Deniz[3,4]

[1]Department of Pharmacognosy, Faculty of Pharmacy, Lokman Hekim University, Ankara, Türkiye.

[2]Turkish Academy of Sciences (TÜBA), Vedat Dalokay Street, No. 112, 06670, Ankara, Türkiye.

[3]Inovabella Biotechnology and R&D Industry and Trade Limited Company, LHUSTEK, Ankara, Türkiye.

[4]Department of Pharmacognosy, Faculty of Pharmacy, Gazi University, Ankara, Türkiye.

Abstract

The historical utilization of medicinal and aromatic plants (MAPs) represents a cornerstone in the development of global medical and pharmaceutical sciences. This paper reviews the ancient wisdom surrounding MAPs, tracing their systematic use from the earliest recorded civilizations to the late pre-modern era. Beginning with the Mesopotamians, where empirical healers (asû) and ritual exorcists (āšipu) integrated botanical therapy with spiritual practice—the narrative expands to Ancient Egypt, highlighting herbal pharmacopoeias documented in the Ebers and Edwin Smith Papyri. The theoretically-grounded systems of Traditional Chinese Medicine and Ayurveda are examined. The analysis further encompasses the Hittite, Greco-Roman, and pre-Columbian South American civilizations, underscoring the systematic and often spiritually-embedded nature of their plant-based therapies. A significant focus is placed on the Islamic Golden Age, where pharmacy emerged as an independent, regulated profession, and scholars such as Al-Razi, Ibn Sina, and Ibn al-Baytar advanced botanical science through critical compilation and cross-cultural synthesis. Finally, the Ottoman synthesis of this inherited knowledge is explored, highlighting its integration of diverse traditions and advanced galenical techniques. The paper concludes that herbal medicine developed as a cumulative global endeavour, supported by exchange routes like the Silk Road, and continues to inform modern pharmacognosy and the ongoing search for novel therapeutics.

Keywords

Ethnopharmacology, history of pharmacy, material medica, medicinal and aromatic plants, traditional medicine, phytotherapy.

Article History

Submitted: 16 December 2026 **Accepted:** 27 April 2026 **Published Online**: May 2026

Reviewer

Invitation Date: 15 January 2026 **Acceptance Date**: 16 January 2026 **Due Date**: 17 January/25 April 2026

Article Info

***Corresponding author:** Ilkay Erdogan Orhan **email:** ilkay.erdoganorhan@lokmanhekim.edu.tr

Review Article:

Volume: 9 **Issue: 1** **Pages: 57-76**

DOI: 10.54994/emujpharmsci.1843372

INTRODUCTION

Mankind has always used medicinal and aromatic plants (MAPs) for various purposes, firstly as food, then for healing. The quest to alleviate suffering and cure disease is a fundamental thread woven throughout the fabric of human history. Long before the advent of modern synthetic chemistry, humanity's primary and most sophisticated resource for healing was the vast and diverse plant kingdom. From the earliest hunter-gatherer societies to the grand empires of antiquity, plants provided not only sustenance but also the basis for a profound and evolving medical wisdom. The systematic use of medicinal and aromatic plants (MAPs) represents humanity's first foray into pharmacology, laying the groundwork for all subsequent medical and pharmaceutical sciences. This ancient knowledge was not a monolithic tradition but a mosaic of distinct, culturally-specific systems, each reflecting the unique environmental, spiritual, and philosophical worldviews of its civilization. These systems, meticulously recorded on clay tablets, papyrus scrolls, and later in encyclopaedic manuscripts, form a priceless inheritance that continues to inform and inspire modern drug discovery and holistic health practices.

Despite their geographic and temporal separation, a remarkable feature of these ancient medicinal traditions is the recurrence of sophisticated, evidence-based principles. Across continents and millennia, one observes the development of complex botanical taxonomies, the refinement of advanced preparation and formulation techniques, and the conceptualization of holistic frameworks linking human health to broader environmental and cosmic balance. This paper aims to trace the historical arc of this wisdom, exploring the use of MAPs from their earliest documented applications in Mesopotamia and Egypt, through their theoretical systematization in the Indian Ayurvedic and Chinese traditions, to their elaboration in the Greco-Roman world. It will further chart their critical preservation, synthesis, and advancement during the Islamic Golden Age, culminating in their institutionalization within the Ottoman Empire. In doing so, this review highlights that the development of herbal medicine was a dynamic, cumulative, and profoundly global endeavour, characterized by continuous intellectual exchange along trade routes like the Silk Road. Understanding this rich history is essential, as it reveals the deep roots of contemporary pharmacognosy and underscores the enduring role of natural products as an

inexhaustible source of novel therapeutic agents.

In contrast to works focusing predominantly on the Classical or Eastern traditions, this review provides significant, integrated coverage of pivotal yet often underrepresented contributions from Hittite, Islamic, and Ottoman medicine, presenting a more balanced and comprehensive global perspective.

To ensure a comprehensive and balanced global perspective, a thorough literature search was conducted across multiple electronic databases, including PubMed, Scopus, Web of Science, and Google Scholar. The search strategy employed keywords and their combinations, such as “medicinal and aromatic plants”, “traditional medicine”, “history of pharmacy”, “ethnopharmacology”, “Materia medica”, and “phytotherapy”. The inclusion criteria focused on peer-reviewed articles, historical manuscripts, and philological or archaeobotanical studies published in English and Turkish that provided systematic data on the evolution of plant-based therapies from ancient civilizations through the Ottoman synthesis. Selection was based on the relevance of the source to the historical arc of pharmacognosy and the development of regulated pharmaceutical practice.

Use of MAPS in ancient Mesopotamia civilization

The ancient civilizations founded in Mesopotamia dates back to the Sumerians, known to have ruled in the 3500s (BC), and then Assyrians and Babylonians founded in 2000s (BC). The antique records of about 250 herbal medicines such as mustard, dates, hemp, and olives are available in those ages as well as mentioning the use of 180 animal-based drugs such as beeswax, honey, oil, blood, and snakes (Asil, 2025). Beyond the role of the individual physician, medical practice in Mesopotamia was formally structured around two distinct specialists: the asû and the āšipu. The asû was an empirical healer who primarily utilized a materia medica of herbal concoctions, poultices, and washes, alongside rudimentary surgical procedures, representing the more tangible origins of pharmacy. In contrast, the āšipu, or exorcist, diagnosed illness as a manifestation of divine wrath or demonic possession and treated patients through incantations and rituals. This duality reflects a world-view where therapy encompassed both the physical and supernatural realms. The detailed pharmacopeias recorded on cuneiform tablets, such as those attributed to figures like Nabu-Leu, largely fall within the domain of the asû, cataloguing practical,

plant-based interventions for specific symptoms.

Information on Mesopotamian medicine was obtained from the texts of the Akkadians, which generally use Sumerian medical knowledge (Karaoz Arihan, 2003). Nabu-Leu, a physician who lived in the period of Assyrians, kept his records in a cuneiform tablet, considered “the oldest pharmacopeia” (Pharmacy History of Kayseri, 2025). In this pharmacopeia, the plants used in drug making in that age are divided into 13 classes according to their effects; the name of the plant is written in three columns as the disease it is used and the way it is prepared and used. This tablet is currently on display at the Berlin Asian Museum. In one of the other two tablets remained to be from the Sumerians, 15 drug recipes with plants were also recorded (Karaoz Arihan, 2003).

The Mesopotamian materia medica was deeply embedded within a cosmological framework where illness was perceived as a tangible manifestation of supernatural discord. Consequently, the preparation and application of plant-based remedies often involved intricate rituals that blended empirical knowledge with symbolic action. Specific plants were selected not only for their observed physiological effects but also for their perceived symbolic affinities with certain deities or celestial bodies. For instance, liquorice root (*Glycyrrhiza glabra* L.), widely used for coughs and digestive ailments, was associated with the goddess Ishtar due to its sweet taste, invoking her restorative powers. Similarly, the use of ḫašû-thorn in preparations likely leveraged its sharp, piercing form in a symbolic act to "break" fever or pain. Furthermore, the efficacy of a prescription was believed to be contingent upon precise, formulaic recitations during its compounding. These incantations, often directed towards healing deities like Gula or Ninurta, served to activate the latent divine potency within the plant material, transforming a simple poultice or decoction into a theurgic instrument. This synthesis of pragmatic herbalism and meticulous ritual underscores a medical philosophy where healing was a deliberate act of restoring order, both within the human body and in the individual's relationship with the divine realm.

Use of MAPS in ancient egyptian civilization

In the Ancient Egyptian civilization ruled in the Nile basin, the medicine was practiced using magic and religious content as well as herbal mixtures, minerals, and various animal parts (Karaoz Arıhan, 2003). The history of papyrus, the most important medical sources in terms of learning about ancient Egyptian medicine, goes to 3000 years back. Some of them are Ebers Papyrus, Edwin Smith Papyrus, Hearts

Papyrus, and Kahun Papyrus. Among them, Ebers Papyrus, which is the most important in terms of history of pharmacy, was named after the ancient Egyptian expert George Maurice Ebers, who made his name known in Cairo in 1873. The sophistication of Egyptian herbal pharmacology is exemplified by specific recipes within the Ebers Papyrus. For instance, a prescription for respiratory distress incorporates the plant likely identified as *Ephedra sinica*, which contains the alkaloid ephedrine, a direct precursor to modern bronchodilators. This indicates a level of empirical efficacy achieved through observation. Furthermore, the Edwin Smith Papyrus, a contemporary surgical treatise, reveals a complementary, rational approach to trauma, employing materia medica such as honey and willow leaves in wound management. Honey's hygroscopic and antibacterial properties, validated by modern science, made it a staple in Egyptian antiseptic dressings, demonstrating an early, functional understanding of microbial prevention. In Ebers Papyrus, 877 prescriptions against 250 diseases and plants used in the preparation of these recipes are mentioned in detail. The Ebers medical papyrus, consisting of 110 pages and 2289 lines, is preserved today in the University of Leipzig, Germany. The prescriptions have been found to contain many plants such as dates, acacia, wormwood, juniper, saffron, resin, onion, flaxseed, anise, aloe, and garlic even known today (Asil, 2025; Karaoz Arihan, 2003). Besides garlic bunches have been found in Egyptian tombs, including the temple of the famous pharaoh Tutankhamen.

Beyond the practical recipes, Egyptian medicine was characterized by a profound, spiritually-informed understanding of plants, deeply intertwined with their cosmology. Plants were not merely therapeutic agents but were often considered sacred gifts from the gods, embodying both physical and magical properties. This duality is evident in the practice of sympathetic magic, where the physical characteristics of a plant suggested its use, a concept known as the Doctrine of Signatures in later traditions. For example, the red sap of the Drakaena tree (Sang-dragon) resembled blood and was thus employed in preparations for circulatory issues and wounds. Similarly, the onion, with its concentric layers, was associated with eternity and was used in mummification as well as medicinally. The efficacy of a remedy was believed to depend as much on its correct ritual preparation including specific incantations to deities like Isis or Thoth—and the auspicious timing of its harvest, as on its material components. This holistic approach, where pharmacological action and divine invocation were inseparable,

created a comprehensive healing system where plants served as the vital link between the corporeal body, the *ka* (spirit), and the pantheon of deities governing health and disease.

Use of MAPS in traditional Chinese medicine (TCM) and Ayurvedic medicine

Considering the use of herbs in treatment throughout history, it is impossible not to mention traditional Chinese medicine (TCM) and Ayurvedic medicine. These two ancient medicines are a systematic practice of medicine, which is said to have thousands of years of their roots. Ancient Indian Civilization, which forms the basis of Ayurvedic medicine, was established in the Indus valley and extends to the present day. Ancient Indian clerics practiced as physician-pharmacists and similarly, approximately 760 plants such as opium, sunflower, shark fin plant, and cassia were used in treatment (Asil, 2025; Pharmacy History of Kayseri, 2025). The first written prescription in TCM is estimated to be written during the Han Dynasty, which ruled in China between BC 200 to AD 200 (Unschuld, 1986). The book on herbal medicines called "Shennong Bencaojing", the oldest pharmacy book ever found, was written by summarizing the information collected by many physicians of the time between the Qin and Han dynasties (221 BC-220 AD). 365 kinds of medicines in this book are still used nowadays. The development of the economy during the Tang dynasty (618-1644 AD) led to the development of TCM and pharmacy. Then, during the Ming Dynasty, "Materia Medica" of Chinese medicine was written by Li Shizhen and published in 1596 after the author died.

The foundational texts of these systems not only catalogued plants but also embedded them within sophisticated theoretical frameworks. In Ayurveda, the Charaka Samhita and Sushruta

Samhita systematically classified plants according to their pharmacological actions (karma), their effects on the three bodily humours or doshas consisting of vata (air & space/ether), pitta (fire & water), and kapha (earth & water), and their taste (rasa), post-digestive effect (vipaka), and potency (virya). This allowed for the precise formulation of complex polyherbal preparations tailored to an individual's constitution and imbalance. Similarly, TCM's Shennong Bencaojing organized its 365 substances into three categories of efficacy and toxicity (superior, middle, and inferior grades) and characterized them by properties such as nature (e.g., hot, cold), flavor, and channel tropism (the meridians they affect). This theoretical depth transformed herbal use from simple empiricism into a comprehensive medical system, where plants like ginger (*Zingiber*

officinale Roscoe, for dispersing cold) or ginseng (*Panax ginseng* C.A.Mey, for replenishing qi) were employed as strategic tools to restore the dynamic balance of yin and yang within the body.

Considering Ayurvedic mecidine, Ayurvedic pharmacology, known as Dravyaguna Shastra, represents one of the world's most elaborate and systematized forms of herbal medicine. It is built upon a profound understanding of the inherent qualities (guna) and energies of plants, which are meticulously matched to the individual's unique constitution (prakriti) and current state of imbalance (vikriti). Central to this is the concept of rasapanchaka, the fivefold assessment of a plant: its taste (rasa), post-digestive effect (vipaka), potency (virya), specific pharmacological action (prabhava), and overall qualities (guna). For instance, the widely used *Tinospora cordifolia* (Willd.) Hook.f. & Thomson (guduchi) is classified as having a bitter and astringent taste (rasa), a pungent post-digestive effect (vipaka), and a hot potency (virya), making it effective for pacifying the kapha and pitta doshas and renowned as a rejuvenating and immunomodulatory agent. This sophisticated classification system enabled the creation of complex, synergistic formulas where multiple herbs were combined not only to enhance efficacy but also to mitigate potential side effects, a principle known as yogavahi. Furthermore, elaborate pharmaceutical processes (bhaishajya kalpana), such as preparing medicated oils (taila), fermented decoctions (asava and arista), and mineral-herb incinerated preparations (bhasma), were developed to extract active principles, enhance bioavailability, and preserve the formulations, showcasing an advanced, pre-modern pharmaceutical science rooted in natural materia medica.

Use of MAPS in ancient Hittite civilization

In the Hittite civilization, which was known to dominate in the 2000s BC in Anatolia, therapy methods used were similar to those of Mesopotamian civilizations aforementioned (Unal, 1980; Unschuld, 1986; Unschuld, 1986; Asil 2025; Pharacy History of Kayseri, 2025). Information about the Hittite medicine has been based on tablets remained from the Hittite archives, located in Hattusa, the capital of the time (Boğazköy, Türkiye). Most medicines were herbal drugs called “wasshi” in the Hittite language. In the prescriptions registered in the Hittite tablets, the plants that grow naturally in Anatolia, *i.e.* mulberry, hawthorn, stilt, barley, almond, wheat, laurel, mustard, poppy, apricot, fir, myrtle, liquorice, saffron, garlic, cedar, cypress, onion, grapes, and olives, in addition to the plants brought from other countries such as ebony,

myrrh, and makkah peleseng, were also recorded.

Complementing the known inventory of medicinal plants used in Hittite Anatolia, recent philological and archaeobotanical studies reveal that Hittite pharmacological practice was also deeply systematic. The surviving cuneiform tablets from Hattusa include not only therapeutic recipes but also structured treatises that categorize ailments and their corresponding treatments according to symptom-based classifications. For example, specific tablets detail treatments for eye diseases, wounds, and gynaecological conditions, utilizing standardized formulations that combine locally sourced herbs such as crushed liquorice root mixed with wine for respiratory complaints with imported resins like myrrh for antiseptic purposes. This systematic approach indicates a sophisticated empirical tradition that integrated local flora with knowledge acquired through trade and diplomatic exchanges with neighbouring Mesopotamian and Egyptian civilizations, positioning Hittite medicine as an active participant in the broader network of ancient Near Eastern medical thought rather than a peripheral derivative.

Use of MAPS in ancient greek-roman civilization

Doubtlessly, ancient Greek civilization had also a great importance in medicine as well as other areas. The medical treatment was applied in the temples called “asclepion”, named after the mythologic God-doctor Asclepius, the son of Apollo, established in the Hellenistic era in Athens, Izmir, and Bergama. In Greek mythology, Asclepius's daughters, Panacea, who was responsible for medicinal plants and his other daughter Hygeia, whose name means health in Greek, were also known as her father's assistants. On the other hand, Empedocles, the ancient Greek physician born on the island of Sicily in 490 BC, was the most important philosopher-physician of his age (Pharmacy History of Kayseri, 2025). He contributed to the knowledge of anatomy and physiology of his period. Believing that the source of health is in nature, Kheiron, an ancient physician benefited from healing waters and plants (Karaoz Arihan, 2003). According to Plinius, Kheiron was considered to be the "first herbalist and pharmacist". The works of Hippocrates, father of doctors, were gathered under the title known as "Corpus Hippocraticum" (Hippocrates Collection), in which he also mentioned use of around 200 plants with especially laxative and emetic effects at the forefront as well as narcotic plants. Medicinal plants used by Hippocrates were fewer in number compared to those in Indian or Egyptian medicines. Some of these were anise, mug wort, centaury, euphorbia, onion, cinnamon, red clover,

peppermint, olive, peony, castor oil plant, sumac, violet, squig, rosemary, and thyme, which are still used in modern phytotherapy. The Hippocratic Corpus established a foundational framework that inextricably linked the medicinal use of plants to a holistic understanding of patient and environment. In works like *Airs, Waters, Places*, health was viewed as a balance influenced by climate, diet, and lifestyle, with herbal remedies serving as tools to correct humoral imbalances. This theoretical system was later expanded and rigidly codified by Galen of Pergamon in the 2nd century AD. Galen introduced a complex classification of drugs, including plants, by their purported “degrees” of potency (e.g., first-degree warming, third-degree drying) based on the Aristotelian qualities of hot, cold, wet, and dry. His elaborate compound formulations, most famously the multi-ingredient theriac, epitomized the principle of “polypharmacy” and dominated Western and Islamic pharmacotherapy for over a millennium. Another of the most important scientists of ancient Greek civilization is Theophrastus, who is called "father of botany". He was born on the island of Lesbos in BC 371. He worked with Aristotle for about 30 years who laid the foundations of natural sciences and morphology (Karaoz Arihan, 2003). It is also known that Theophrastus demonstrated the morphological properties (by illustrating many of them) of about 500 plants and grown medicinal plants in a botanical garden in Athens (Theophrastus, 1998). Only copies of 9 volumes of his great book "Historia Plantarum", consisting of a total of 10 volumes, have survived till today. Some botanical terms that he used such as vessel (canal) or pericarpion (pericarp) are still in use. Theophrastus also managed to separate plants into monocotyledons and dicotyledons. With his contribution, a large medical herb garden was created in Alexandria Medical School (Egypt), which was established in the 3rd century BC, where physicians-pharmacists were also trained (Elsawaby, 2012). The school pioneered to the concept of “polypharmacy”, where the most important antidote “Thériaque de Mithriodaticum” was prepared by this school. This medicine, firstly prepared for Mithridate, the 6th king of Pontus (120-63 BC), is known to consist of 54 kinds of herbal and animal-originated drugs. This solution was later developed by Galen and brought to Ottoman lands through Venice in the 16th century (Griffin, 2004; Totelin, 2004). The first to use of this solution in the treatment by the Ottomans was Merkez Efendi, the first chief physician of the hospital built in 1539 by Sultan Suleyman the Magnificent for his mother Hafza Sultan in Manisa (Türkiye). Pedanios Dioscorides, the ancient Greek scientist, who was accepted as “the first

Pharmacognocist" in history and known to live in the 1st century AD, was born in the Tarsus (Anazarba) region in Anatolia (Tanker et al. 1991; Baytop, 2000; Staub et al. 2016). Dioscorides, besides being a physician, was also engaged in botanical science. Having accompanied the Roman Army of the time, he had the opportunity to examine the plants in various countries and wrote "De Materia Medica", one of the most important books in this field (Scarborough, 2007; Staub et al. 2016). Dioscorides, in his book at De Materia Medica consisting of 5 volumes, handled over 600 herbal, 35 animal and 90 mineral drugs, and introduced many of them with pictures drawn by him. De Materia Medica, the oldest botanical book written in Anatolia, was used as a source book in Europe for 1600 years. In the book "Naturalis Historia" (Natural History), which belongs to Plinius who lived in Rome between 23-79 AD, approximately 1000 drugs were classified in order of their medical effects, while physiology, zoology, and botanical topics have also been covered in the book (Tanker et al. 1991). The famous physician-pharmacist Galen (119-199 AD), who lived during the Roman Empire, is known as "Galen of Pergamon" because of his life spent in Bergama (Karaoz Arihan, 2003). He is well-known for his contributions to anatomy, physiology, and pathology sciences along with his drug preparations, who wrote the description and effects of about 10 herbal and animal drugs used to prepare these prescriptions (Goss and Chodkowski, 1985; Apuzzo, 2000). The reputation of Galen in terms of herbal therapy is the fact that many of his works have been translated into Arabic language centuries later which led to important developments in Arabic medicine (Pormann, 2008; Edriss et al. 2017; Sadeghi et al. 2020).

Use of MAPS in ancient south american civilizations

Ancient South American civilizations developed profound and sophisticated knowledge of medicinal and aromatic plants, deeply embedded within their cosmologies, medical systems, and daily rituals. In the Andean region, the Inca Empire (c. 1400–1533 AD) utilized an extensive pharmacopeia derived from the rich biodiversity of the Andes and Amazon. Key plants included coca leaves (*Erythroxylum coca* Lam.), used as a stimulant, analgesic, and sacred offering in rituals; quina or cinchona bark (*Cinchona officinalis* L.), employed as a febrifuge and later known as the source of quinine for malaria treatment; and muña [*Minthostachys mollis* (Benth.) Griseb.], an aromatic mint used for digestive ailments and in ritual cleansing. The Incas also valued sacha inchi (*Plukenetia volubilis* L.) for its

nutritional and medicinal oils, and yacón [*Smallanthus sonchifolius* (Poepp.) H.Rob.] for metabolic regulation. Healing was often administered by shamans (*paqos* or *curanderos*) who combined herbal remedies with spiritual ceremonies aimed at balancing bodily energies and appeasing mountain spirits (*apus*) and earthly deities (*Pachamama*). In pre-Columbian Amazonia, indigenous tribes such as the Tupi, Guarani, and Shipibo-Conibo developed extensive ethnobotanical knowledge, using plants like ayahuasca [*Banisteriopsis caapi* (Spruce ex Griseb.) Morton combined with *Psychotria viridis* Ruiz & Pav.], a visionary brew employed for healing, divination, and spiritual communication; cat's claw [*Uncaria tomentosa* (Willd. ex Schult.) DC.], used as an anti-inflammatory and immune modulator; and sangre de grado (*Croton lechleri* Müll.Arg.), a latex applied topically for wounds and ulcers. Aromatic resins such as copal and brea [*Cercidium praecox* (Ruiz & Pav.) Hawkins] were burned as incense in purification rites. The Moche and Chimú cultures on the northern coast of Peru (c. 100–1470 AD) depicted medicinal plant use in their ceramics, showing rituals involving wilka [*Anadenanthera colubrina* (Vell.) Brenan], a psychoactive snuff, and jimsonweed (*Datura stramonium* L.), used for its narcotic and diagnostic properties.

In Mesoamerica—though geographically part of North America, its cultural and botanical exchange with South America was significant—the Maya and Aztecs employed aromatic plants such as copal resin [*Protium copal* (Schltdl. & Cham.) Engl.] for ceremonial incense, chanel [*Quararibea funebris* (La Llave) Vischer] in fragrant baths, and zapote [*Pouteria sapota* (Jacq.) H.E.Moore & Stearn] for digestive ailments. The Aztecs compiled their herbal knowledge in codices like the *Libellus de Medicinalibus Indorum Herbis* (1552), which described hundreds of native plants, including tlahçolteōxōchitl (*Psidium guajava* L.) for diarrhea and yauhtli (*Tagetes lucida* Cav.) as a ritual perfume and medicinal tea.

What unified these traditions was a holistic view of health, where plants were considered living beings with spirit and agency. Healing rituals often involved diet, chanting, and the administration of plant medicines in ceremonial contexts, emphasizing balance between the physical, social, and spiritual worlds. This rich heritage not only contributed to later global pharmacopeias such as the introduction of cinchona, coca, and ipecac to European medicine, but also continues to inform

contemporary ethnobotanical research and integrative medicine practices today.

Use of MAPS in Islamic civilization

With the disintegration of the Roman Empire and the translation of many works written in this period into Arabic, Islamic medicine started to develop in the 7th and 8th centuries AD and valuable physicians and pharmacists were trained in the Islamic geography (Masic et al. 2017). The most important stage in which Muslim physicians contributed to medical sciences was observed between 9th-13th centuries AD (Singer et al. 1962). The institutionalization of pharmacy as an independent, regulated profession was a seminal achievement of the Islamic Golden Age. The first documented private pharmacy shops (saydalah) were established in Baghdad under Abbasid rule in the 8th century, operating under state supervision to ensure standards. This formal separation of the roles of physician (tabib) and pharmacist (saydalani) fostered specialized expertise in drug preparation, quality control, and the management of complex compound formulations. This professional structure, along with dedicated market inspections (hisbah), was later adopted and expanded by the Seljuk and Ottoman empires, forming a continuous tradition of pharmaceutical practice in the region. Especially, Huneyn Ibn-i Ishak lived in the 9th century translated many works of Galen into Arabic language. In addition, the works of the Medieval Persian period and medical works such as "Susruta Samhita" and "Charaka Samhita" from the Indian medicine were transferred to the Arabic language in this period. One of the most important physicians of Islamic medicine, Al-Razi (874-932 AD), born in Ray city of Iran wrote many books related to medicine, pharmacy, and deontology. The most important books of Al-Razi are "Al-Tibb al-Mansurias" as well as "El Havi" mostly based on medicine. This work, translated into Latin under the name "Liber Continens", is the largest medical encyclopedia of its period, written on the diagnosis and treatment of diseases. One of the most important works of El-Razi is "Liber de Pestilentia" on smallpox and chickenpox diseases. Al-Dinaveri (828-896 AD) is another Muslim scientist who was born in the city of Dinaver located in the west of Iran today. His contributions to the Arabic botanical science, in particular, are very large including his great book called "Kitab al-Nebat" (The Book of Plants) (Hizmetli, 1991). On the other hand, Al-Biruni, a famous Muslim physician living between 973-1051 AD, studied especially ancient Indian medicine and pharmacy (Tumer et al. 1992). He described the pharmacist in his book "Kitab-ul Al Saydala fi't Tıbb" and mentioned about the use of many herbal drugs in treatment. Al-Biruni,

who is estimated to have written about 180 works, wrote in this book what 3000 plants were useful and how they were used. Besides drugs, his mention about the names of plants in various languages such as Arabic, Persian, Greek, Sanskrit, and Turkish are also very important developments for that period. Born in Andalusia, Ebul Kasim ez-Zehravi (936-1013 AD) is the doctor who used opium for the first time as an anaesthetic in surgery (Kahya, 1992; Aciduman, 2006).

Ibn-i Sina, known as Avicenna in Europe, is doubtlessly the most reputed Muslim physician, who lived between 980-1037 AD. He was born in Afshana town, near Bukhara in today's Uzbekistan. When he died in Hamedan at the age of 57, he left more than 150 works behind, and his works have been translated into Latin and German and shed light on Europe in medicine, chemistry, and philosophy. Westerners considered him as a transmitter of ancient Greek knowledge and philosophy (Aciduman, 2002). The innovations he brought to medicine have been influential in Europe for centuries and works of Ibn-i Sina in European universities have been taught as textbooks. The most famous of his works are “Kitabu's-Shifa” (Book of Recovery) and “Al-Kanun fi't-Tibb” (Law of Medicine), and he also made the greatest contribution to medieval Islamic medicine with his valuable works. 600 years ago, at the top of the 9 main books in the library of the Faculty of Medicine, University of Paris, Al-Kanun of Ibn-i Sina took place. Al-Kanun, consisting of approximately one million words, is the most impressive ancient medical book ever written. Ibn-i Sina is the first physician to use catheters made from various animal skins and talked about silver syringe and intravesical injection.

Ibn-i al-Baytar (1190-1248 AD) is a famous botanist and physician-pharmacist born in Andalusia in the Middle Ages. Ibn al-Baytar's masterpiece “Kitab al-Cami'fi al-Adviyye al-Mufredah” has been an important resource for botanical science for a long time and has a great importance in terms of pharmacy (Huff, 2003). The work includes prescriptions with about 1400 herbs, of which about 300 are completely his own discovery. This work was translated into Latin in 1758 and continued to be used in Europe until the 19th century. It is known that the first pharmacy-like institutions in Anatolia were opened during the Seljuk Empire (Tekiner, 2015). The rigor of Islamic botanical science is exemplified by the methodological advances of scholars like Ibn al-Baytar. In his monumental “Kitab al-Jami’li-Mufradat al-Adwiya wa al-Aghdhiya”, he did not merely compile earlier Greek and Arabic knowledge but engaged in systematic critique and verification. Traveling

extensively from Andalusia across North Africa to the Middle East, he observed, collected, and described plants firsthand, often correcting the identifications of Dioscorides or Galen based on local vernacular names and uses. This emphasis on empirical observation and field research represented a significant evolution from textual reliance toward a more proto-scientific botany.

The transition of this pharmaceutical legacy into Anatolia was institutionalized during the Seljuk Empire (11th–13th centuries). The Seljuks established a network of Darüşşifa (healing houses) in key Anatolian centers such as Konya, Sivas, and Kayseri (e.g., Gevher Nesibe Hospital), which served as the region's first formal medical academies and hospitals. These institutions featured dedicated pharmacy departments where the preparation of macun (electuaries) and şerbet (syrups) was standardized. This Seljuk institutional model directly provided the structural and educational template for the subsequent Ottoman medical system, ensuring the continuity of the Graeco-Arabic botanical tradition on Anatolian soil.

Use of MAPS in Unani (Graeco-Arabic) medicine

A pivotal development in the history of Pharmacognosy was the emergence of Unani medicine. This system represents the direct synthesis of Ancient Greek knowledge within the Islamic world. This intellectual bridge was constructed through the massive translation movement of the 9th century, led by figures such as Hunayn Ibn-i Ishak, who translated the foundational works of Galen and Hippocrates into Arabic (Akhlaq et al. 2021). Unani medicine preserved and refined the Galenic humoral framework, which classified both patients and medicinal plants according to the four Aristotelian qualities: hot, cold, wet, and dry (Itrat, 2020; Alam et al. 2021). This theoretical rigour allowed for a sophisticated "polypharmacy" approach, where complex formulations were designed to restore a patient's specific elemental balance. The pinnacle of this synthesis was achieved by Ibn-i Sina (Avicenna), whose Al-Kanun fi't-Tibb (The Canon of Medicine) systematically integrated Greek logic with Persian and Indian botanical insights, creating a comprehensive medical encyclopaedia that remained the standard text in both the East and West for centuries (Aleem and Khan, 2023). Unlike a purely archival tradition, Unani medicine evolved through empirical verification and field research, as scholars like Ibn al-Baytar corrected ancient Greek botanical identifications based on firsthand observations. This system did not merely serve as a historical placeholder but became a living tradition, transitioning through the Ottoman imperial medical complexes and remaining a practiced and regulated form of

traditional medicine in many parts of the world today.

Unani medicine is not merely a collection of herbal remedies, but a personalized medical system grounded in the concept of 'Mizaj' (temperament) (Kausar et al. 2021). According to this framework, every individual and every medicinal plant possesses a unique temperament—classified as hot, cold, moist, or dry. The primary objective of therapy is to restore humoral equilibrium in alignment with "the Four Humors" (Akhlat) theory (Akhlaq et al. 2021). Furthermore, Unani medicine prioritizes preventive health through the "Asbab-e-Sittah Zaruriyah" (six essential factors), which encompass atmospheric air, nutrition, sleep and wakefulness, physical activity and rest, evacuation and retention, and mental states. From the 13th century onwards, this system became institutionalized in the Indian subcontinent, where it merged with local Ayurvedic insights (Akhtari et al. 2024). Today, it remains a standardized traditional medicine system recognized by the World Health Organization (WHO), representing a continuous bridge between ancient Greek logic and modern regulated practice.

A critical but often overlooked precursor to the Islamic Golden Age was the Academy of Gundeshapur in the Sassanid Persian Empire (Azizi, 2008; Yuan et al. 2016). By the 6th century, this institution had become the world's premier center for medical and botanical transmission (Mishra et al. 2019). It served as a sanctuary for Nestorian and Neo-Platonist scholars who translated Greek medical classics, including the works of Galen and Dioscorides, into Syriac and Persian (Modanlou, 2011). Gundeshapur acted as the bridge, preserving Galenic and Hippocratic medicine, while incorporating Indian pharmacology and Persian clinical techniques. By integrating these Western traditions with Indian Ayurvedic insights and local Persian herbalism, Gundeshapur established a multicultural medical curriculum (Ruben, 2017). This Gundeshapur model of systematic clinical observation and institutionalized pharmacy provided the structural and intellectual foundation for the subsequent Abbasid translation movement in Baghdad. The model developed at Gundeshapur influenced Islamic medicine for centuries and laid the groundwork for hospital systems in Baghdad, Cairo, and Córdoba.

Use of MAPS in Ottoman Empire

Ottoman medicine and pharmacy synthesized its Islamic heritage with pragmatic administration. Major imperial medical complexes (*külliyes*), such as the 16th-century Süleymaniye complex in Istanbul, included dedicated hospitals (*darüşşifa*), medical schools, and often adjacent herb gardens (*nevbethane*). These gardens ensured a fresh, standardized

supply of medicinal plants for both treatment and the education of physician-pharmacists (*hekim*). The role of the Chief Palace Pharmacist (Eczacıbaşı) became crucial, overseeing not only the preparation of medicines for the court but also the regulation of the bustling spice and drug bazaars, maintaining quality in a vast trade network that supplied the empire's needs.

The Ottoman approach to medicinal plants was distinguished by a pragmatic and syncretic methodology that systematically integrated diverse regional knowledge systems. This is exemplified by the extensive use of *Mecmua-i Fevaid* (Compendium of Benefits), practical pharmacopoeias that compiled and standardized formulas from Arab, Persian, Byzantine, and even earlier Seljuk sources, while also incorporating indigenous Anatolian folk remedies and newly introduced plants from the Americas, such as tobacco and maize, which were studied for their therapeutic potential. The integration of New World flora into the Ottomans' medical/pharmacetical books was a systematic process of theoretical assimilation. As species such as tobacco, maize, and cinchona bark reached the Empire, Ottoman physicians did not merely adopt them as folk remedies; they categorized them according to the existing Galenic-Unani humoral framework. By assigning these new plants specific degrees of heat, cold, dryness, or moisture, practitioners could incorporate them into complex polypharmacy formulations. Scholars like Hezarfen Hüseyin Efendi in the 17th century documented these exotic additions, demonstrating how the Ottoman Materia Medica functioned as a living, adaptive system that reconciled global botanical discoveries with classical medical logic. The 17th and 18th centuries saw the Ottoman synthesis, where traditional humoral theory began to meet Western chemical and botanical discoveries. It combined ancient Greek theory, Persian pharmaceutical chemistry, and local Anatolian herbalism. It was anchored in the Darüşşifa and Külliye (social complex) systems. It successfully assimilated global botanical discoveries (New World flora) into its existing theoretical framework for over two centuries.

Furthermore, Ottoman pharmacists developed sophisticated pharmaceutical techniques for processing raw botanicals. These included specialized methods of roasting (*kavurma*), maceration in honey or vinegar (*sirkencübin*), and the preparation of complex electuaries (*ma'cun*) and solid pastilles (*leb*), often containing dozens of ingredients like saffron, cinnamon, and amber, designed for prolonged stability and efficacy. This rigorous, applied science was supported by a thriving commercial ecosystem. The *Kapalıçarşı* (Grand

Bazaar) in Istanbul and similar centers in Cairo and Damascus featured dedicated *attar* (spice and drug seller) districts, where herbs were graded, stored in specialized ceramic jars, and subjected to quality inspections (*hisbe*) to prevent adulteration. This structured integration of global botany, advanced galenical pharmacy, and stringent commerce solidified the Ottoman Empire as a culminating hub in the historical continuum of medicinal plant knowledge, bridging its Islamic past with the emerging material exchanges of the early modern world.

Many translations of "De Materia Medica" of Dioscorides were used as reference books by physicians in Ottoman medicine. It is said that De Materia Medica indirectly affected Ottoman medicine as well as early Islamic medicine. Following the pause in Islamic medicine after the 12th century, the reflection of the scientific medicine and Renaissance understanding that gradually developed in the Western world over the centuries was quite late to Ottomans. However, it is observed that Western medicine has been noticed slowly, even from the manuscripts of the 17th and 18th century in Western medicine. The medical works in Turkish were started to be written during the Ottoman Empire, especially in the 15th century (Akdeniz Sari, 1983). On the other hand, it is observed that Ottomans have a unique understanding of medicine and physician training style. Anatolia maintained its importance in spice and herb transportation during the Ottoman Empire. Roads named as "king's road" or "silk road" have connected Western Anatolian ports and Eastern countries, and sea transportation has always been preferred.

CONCLUSION

In conclusion, ancient civilizations from different parts of the world have always shed a light to modern medicine as their wisdoms were mentioned here only a little bit. At this point, medicinal and aromatic plants have always maintained their importance in therapy for threatening human being. The historical development of herbal knowledge was fundamentally a process of cross-cultural synthesis, facilitated by routes like the Silk Road. This exchange was not merely commercial but profoundly intellectual. For example, Sanskrit medical texts such as the *Sushruta Samhita* were translated into Arabic in Baghdad's *Bayt al-Hikma* (House of Wisdom). Their detailed descriptions of surgical techniques and herbal compounds, including plants like cinnamon and ginger native to the Indian subcontinent, were subsequently analysed, integrated, and expanded upon by Islamic scholars

including Al-Razi and Al-Biruni. This transmission cycle—from India to the Abbasid world and later to Europe—underscores how the wisdom of medicinal plants was a cumulative, global endeavour long before the modern era.

During development of chemistry, medical and pharmaceutical sciences, natural sources have led to discovery of many clinically used drugs of today. Therefore, plants and other natural sources will always keep a great attraction from scientists and will remain as source of novel drugs not discovered, yet.

ACKNOWLEDGMENTS

The authors declare no conflict of interest.

REFERENCES

Aciduman A, Arda B (2006). Abu'l-Kasim Ez-Zehravi, his work on the treatment of Et-Tasrif and hydrocephalus. *Journal of Child Health and Diseases* **49**: 169-173.

Aciduman A (2002). Role of Ibn-i Sina in science history. An approach by Kuhn. *J Ankara Univ Fac Med* **55**: 115-122.

Akdeniz Sari N (1983). Medical education until the establishment of the medicine in the Ottomans. *Studies on Turkish World* **22**: 152.

Akhlaq S, Ara SA, Ahmad B, Fazil M, Akram U, et al. (2021). Interventions of Unani medicine for maintenance of health with special reference to air quality: An evidence-based review. *Rev Environ Health* **38**: 85-96.

Akhtari M, Mojahedi M, Gorji N, Bijani A, Mozaffarpur SA, et al. (2024). Development and validation of self-report Mizaj identification questionnaire based on Persian Medicine for the elders (age over 60). *CASP J INTERN MED* **15**:76-86.

Alam MA, Quamri MA, Sofi G (2021). Historical account of endocrinal disorders in Unani medicine. *J Basic Clin Physiol Pharmacol* **32**: 1013-1019.

Aleem M, Khan MI (2023). Concept of dementia (Nisyān) in Unani system of medicine and scientific validation of an important Unani pharmacopoeial preparation 'Majoon Vaj' for its management: A review. *Journal of Complementary and Integrative Medicine* **21**: 139-153.

Apuzzo ML (2000). The legacy of Galen of Pergamon. *Neurosurgery* **47**: 545.

Asil E (2001). Pharmacy from yesterday to today. *Magazine of Continuing Education (MISED) by Turkish Pharmacists Association* **1**: 4-19.

Azizi MH (2008). Gondishapur School of Medicine: The most important medical center in antiquity. *Archives of Iran Medicine* **11**(1): 116-119.

Baytop T (2000). Dioscorides of Anazarba, Studies on Turkish Pharmacy History, Istanbul.

Goss CM, Chodkowski EG (1985). Whether blood is contained in the arteries of the living animal by Galen of Pergamon: A translation. *The Anatomical Record* **213**: 1-6.

Edriss H, Rosales BN, Nugent C, Conrad C, Nugent K (2017). Islamic medicine in the Middle Ages. *American Journal of Medical Sciences* **354**: 223-229.

Elsawaby MNE (2012). Medicinal and aromatic crops in Egypt: A study in medical geography. *Journal of Educational and Social Research* **2**: 112-124.

Griffin JP. (2004). Venetian treacle and the foundation of medicines regulation. *British Journal of Clinical Pharmacology* **58**: 317-325.

Hizmetli S (1991). History of Islam. Ankara University Faculty of Theology Publications, No. 189, Ankara University Press house, Ankara, 1991.

Huff T (2003). The Rise of Early Modern Science: Islam, China, and the West, Cambridge University Press, Cambridge.

Itrat M. Methods of health promotion and disease prevention in Unani medicine (2020). *Journal of Education in Health Promotion* **9**: 168.

Kahya E (1992). Zehravi. Encyclopedia of Islam by Religious Foundation of Turkey, Vol. 6, Istanbul.

Karaoz Arıhan S (2003). Medicine and herbal treatment in antiquity, Master Thesis, Ankara University, Institute of Social Sciences, Department of Archeology, Ankara.

Kausar F, Yusuf Amin KM, Bashir S, Parvez A, Ahmad P (2021). Concept of 'Ihtiraq' in Unani Medicine - A correlation with oxidative stress, and future prospects. *Journal of Ethnopharmacology* **265**: 113269.

Masic I, Skrbo A, Naser N, Tandir S, Zunic L, et al. (2017). Contribution of Arabic medicine and pharmacy to the development of health care protection in Bosnia and Herzegovina - The first part. *Medical Archives* **71**(5): 364-372.

Mishra SK, Mohammad Khanli H, Akhlaghipour G, Jazi GA, Khosa S (2019). Historical perspective of neurology in Iran. *Iran Journal of Neurology* **18**: 25-32.

Modanlou HD (2011). Historical evidence for the origin of teaching hospital, medical school and the rise of academic medicine. *Journal of Perinatology* **31**(4): 236-239.

Pormann PE (2008). Case notes and clinicians: Galen's "Commentary" on the Hippocratic "Epidemics" in the Arabic tradition. *Arabic Sciences and Philosophy* **18**: 247-284.

Ruben RJ (2017). Otology at the Academy of Gondishapur 200-600 CE. *Otology and Neurotology* **38**(10): 1540-1545.

Sadeghi S, Ghaffari F, Heydarirad G, Alizadeh M (2020). Galen's place in Avicenna's The Canon of Medicine: Respect, confirmation and criticism. *Journal of Integrative Medicine* **18**: 21-25.

Scarborough J (2007). Dioscorides of Anazarbus for moderns - An essay review. *Pharmacy in History* **49**: 76-80.

Singer C, Underwood EA (1962). Short History of Medicine, Oxford University Press, New York and Oxford.

Staub PO, Casu L, Leonti M (2016). Back to the roots: A quantitative survey of herbal drugs in Dioscorides' De Materia Medica (ex Matthioli, 1568). *Phytomedicine* **23**: 1043-1052.

Tanker M, Tanker N (1991). Pharmacognosy, Volume 1, Ankara University Faculty of Pharmacy Publications, No: 60, Ankara University Press house, Ankara.

Tekiner H (2015). One hundred years of the history of pharmacy studies in Turkey. *Pharmazie* **70**: 139–144.

Theophrastus (Translated from ancient Greek language by Sentuna C.) (1998). Characters, Dost Book House Publications, Ankara.

Totelin L (2004). Mithridates' antidote – A pharmacological ghost. *Early Science and Medicine* **9**: 1-19.

Tumer G (1992). Biruni. Encyclopedia of Islam by Religious Foundation of Turkey, Vol. 6, Istanbul.

Unal A (1980). Main lines of Hittite medicine. *Belleten* **44**: 475-480.

Unschuld P (1986). Medicine in China: A History of Pharmaceutics. University of California Press, Berkeley, California.

Unschuld P (1988). Chinese Medicine. Mass Paradigm Publications, Brookline.

Yuan H, Ma Q, Ye L, Piao G (2016). The traditional medicine and modern medicine from natural products. *Molecules* **21**(5): 559.